The Roles of NF-κB, Activin, and Sphingosine-1-Phosphate in Promoting Non-Small Cell Lung Cancer-Initiating Cell Phenotypes

James Jacob Wamsley
Richmond, Virginia

B.S., College of William and Mary, 2006
M.S., University of Virginia, 2008

A Dissertation presented to the Graduate Faculty of the University of Virginia in Candidacy for the Degree of Doctor of Philosophy

Department of Biochemistry, Molecular Biology and Genetics

University of Virginia
December 2013

ABSTRACT

Despite recent advances in personalized therapies, non-small cell lung cancer (NSCLC) remains the most deadly malignancy in the Western world. The frequency of metastases and acquired drug resistance contribute to the high rates of mortality. An evolutionarily conserved cellular program termed the epithelial-to-mesenchymal transition (EMT) promotes metastasis and drug resistance by enriching for a pool of cancer-initiating cells (CICs). The migratory and invasive characteristics of CICs initiate the metastatic cascade. CICs also aid in the final step of metastasis, colonization, through their ability to self-renew and generate progenitor cells that comprise macrometastases. This pool of cells is also highly insensitive to both traditional and targeted treatments, enabling it to regenerate carcinoma cells within the primary tumor that undergo apoptosis due to drug treatment. Work presented in this dissertation illustrates that treatment of three-dimensional (3D) spheroid NSCLC cultures stimulated with tumor necrosis factor (TNF) and transforming growth factor-beta (TGFβ) induces nuclear factor-kappa B (NF-κB) to promote EMT and the subsequent formation of CICs. Furthermore, NF-κB upregulates *Activin*, a TGFβ superfamily member, to sustain the mesenchymal phenotype over a four-day time course. Preliminary data also links the bioactive signaling lipid, sphingosine-1-phosphate (S1P), to EMT within NSCLC. Since successful treatment of NSCLC theoretically requires eradication of this pool of self-renewing cells, soluble factors that promote CIC phenotypes are excellent candidates for targeted therapeutic intervention.

ACKNOWLEDGEMENTS

The path toward my Ph.D. has been a challenging and insightful experience that I could not have completed without assistance and support from a number of individuals. First, I would like to thank my doctoral advisor, Dr. Marty Mayo, for years of advice, support, and assistance, both financial and intellectual. His knowledge and mentorship are primary reasons why I have chosen to pursue a career in science. Additionally, I extend my gratitude to members of my thesis committee, Drs. Stefan Bekiranov, Dan Gioeli, and Kevin Lynch, for insightful feedback throughout my time at the University of Virginia (UVA). Dr. Bekiranov was also instrumental in guiding the bioinformatical side of our three-dimensional cell culture model system.

Within the lab, I have relied on a number of people for various reasons, including technical advice, ideas for experiments, favors, and friendship. I would like to particularly thank David Allison, Sheena Clift, Julia Krupa, Lisa Gray, and Manish Kumar for the multitude of ways that they have helped me. Additional lab members that have supported me include Szymon Szymura, Li Duo, Emily Glidden, Lisa Shock, and Jackie D'Innocenzi. I would also like to thank the department of Biochemistry, Molecular Biology and Genetics for accepting me into the program and giving me the opportunity to study cancer.

When faced with adversity, I have utilized both friends and family for backing and advice. My parents have provided me with unconditional love and outstanding advice throughout graduate school, in addition to being the best role models that any son could ever ask for. I will be forever indebted to them for

everything they have done for me. My brother, Nick, has been a beacon of support and inspiration as well. Our family dog, Paxton, epitomizes the phrase “man’s best friend,” as I cherish every time I get to see him during my visits to Richmond. Other members of my family who have provided a great deal of love and support include my grandparents, my cousins Ryan and Kate Schilling, and all of my aunts and uncles.

I would also like to thank three of my best friends from graduate school from outside the lab, Stephen Hoang, Shaun McCullough, and Clinton Copeland, for years of friendship, memories, and support. Other close friends I would like to acknowledge include Nick Holubowitch, Benning Farmer, and Justin Bell. Without these multiple avenues of support, I would not be the man that I am today, nor would I be on the verge of graduating from UVA and pursuing a career in science.

TABLE OF CONTENTS

LIST OF FIGURES AND TABLES

CHAPTER I: GENERAL INTRODUCTION

Non-Small Cell Lung Cancer

Lung cancer is the most commonly diagnosed cancer in the world, as well as the leading cause of cancer-related mortality in the Western world among both men and women (Aisner & Marshall, 2012; Gottschling et al., 2012). This year, more Americans will die from lung cancer than from breast, colorectal, prostate, and melanoma malignancies combined. The American Cancer Society predicts 228,190 new lung cancer diagnoses in 2013 accompanied by 159,480 lung cancer-related deaths (Siegel et al., 2013). These malignancies can be broadly divided into two types based on histology and response to therapies. Non-small cell lung cancer (NSCLC) comprises approximately 85% of cases, and small-cell lung cancer (SCLC) makes up the remaining 15% (Gottschling et al., 2012).

Non-small cell lung cancer (NSCLC) is composed of three histological subtypes, adenocarcinoma, squamous cell carcinoma, and large cell carcinoma (Gottschling et al., 2012; Raparia et al., 2013). Adenocarcinomas are the most common, comprising between 40 and 50% of NSCLC cases. Moreover, they are the most frequently diagnosed subtype among non-smokers, women, and the Asian population (Aisner & Marshall, 2012). These cancers derive from secretory glandular cells that produce a protective mucus layer. They are typically found in more peripheral areas of the lung. When compared to the two other subtypes, these form more slowly and produce smaller masses, but show an aggressive phenotype by metastasizing at an earlier stage (Gaikwad et al., 2012; Petersen, 2011).

Squamous cell carcinoma accounts for approximately a quarter of NSCLC diagnoses. Originating from the epidermal cells that line the bronchial tubes of the lungs, these tumors often appear in central areas. Their defining characteristics include the presence of intercellular bridges and keratinization (Petersen, 2011). More common in men than women, this subtype displays the strongest link to smoking (Petersen, 2011). Squamous cell used to be the most commonly diagnosed NSCLC subtype, but recently adenocarcinoma has become more prevalent. One popular explanation for this switch is the wide dissemination of filtered cigarettes. Smoke from these is inhaled more deeply, allowing penetration of carcinogens into more peripheral regions of the lung, where adenocarcinomas are more commonly found (Ito et al., 2011).

Large cell lung carcinomas are typically undifferentiated, contributing to their enhanced rates of proliferation and metastasis when compared to the other two subtypes. These tumors are named after the large round morphology of the carcinoma cells, although the tumors tend to be comparatively large as well. Cancers of this subtype can be found anywhere in the lung, but are frequently found in the outer edges. Diagnosis is done on the basis of exclusion when characteristics of the other two subtypes are not identified (Katsenos et al., 2012; Petersen, 2011).

Risk Factors and Prognosis for Non-Small Cell Lung Cancer

The primary risk factor for NSCLC is a history of tobacco smoking, linked to a staggering 80-90% of cases. However, various occupational and

environmental factors can induce genetic abnormalities that initiate lung tumorigenesis. Carcinogens and mutagens such as asbestos, radon, polycyclic aromatic hydrocarbons, arsenic, and nickel, among others, have been linked to NSCLC (Petersen, 2011). Some cases have a viral component as well. For example, the Epstein-Barr virus (EBV) is associated with large cell lymphoepithelial carcinoma (Kasai et al., 1994), a rare variant of large cell carcinoma. Human papillomaviruses (HPV) can also contribute to NSCLC (Klein et al., 2009).

Since risk factors for NSCLC are well known, efforts have been made to screen high-risk patients. For example, one study showed that low dose-CT screening in individuals displaying NSCLC risk factors yielded a 20% reduction in lung cancer-associated mortality (Aberle et al., 2011; Bach et al., 2012). Despite such endeavors, upon diagnosis, over half of patients present with Stage IV (metastatic) disease, presenting a median survival time below 18 months and a five-year survival rate below 5% (Aisner & Marshall, 2012; Gottschling et al., 2012). At this point, the disease is inoperable and patients require systemic treatment, which is only palliative.

Early detection vastly improves a patient's prognosis, as the five year survival rate for localized disease is significantly higher at 52% (Aisner & Marshall, 2012). Treatment for these patients usually consists of surgical resection with curative intent, often followed by adjuvant chemotherapy and radiation therapy, collectively referred to chemoradiotherapy (CRT). Unfortunately, NSCLC is innately insensitive to CRT when compared to other

malignancies, including small cell lung cancer. Moreover, chemotherapy becomes less effective as cancer progresses (Cufer et al., 2013). Resistance to these therapies contributes to the high recurrence rates in NSCLC (Shintani et al., 2011).

For advanced disease, chemotherapy and radiation are utilized as palliative systemic treatment, but as with patients with local disease, the benefits of these treatments are modest at best. A meta-analysis executed in 2008 showed that in patients with advanced NSCLC, chemotherapy in addition to supportive care yields a 23% reduction in risk of death, 1.5 month increase in median survival, and a one-year survival gain of 9%, when compared to supportive care alone (Group, 2008). The well-documented insensitivity of NSCLC to chemotherapy and radiation has focused research efforts on identifying targetable molecular markers that orchestrate disease progression.

Molecular Signatures and Targeted Therapy for NSCLC

NSCLC is a heterogeneous disease whose progression is driven by diverse genetic mutations. Many of these are activating mutations in various oncogenes whose products promote processes essential to tumor growth, such as proliferation, angiogenesis, metastasis, and evasion of apoptosis. Tumors harboring these mutations are thought to be “addicted” to these gene products’ constitutive activity, requiring their persistent hyperactivation for maintenance and growth (Weinstein, 2002). Therefore, these genetic lesions are also referred to as “sensitizing” mutations, as they accurately predict patient sensitivity to

molecular therapies targeting the oncogenic gene products. When applied to identified cohorts, molecularly targeted therapies yield significantly higher response rates in NSCLC than conventional chemotherapy (Aisner & Marshall, 2012; Petersen, 2011).

Mutations in the epidermal growth factor receptor (EGFR) tyrosine kinase domain and gene rearrangements of anaplastic lymphoma kinase (ALK) are the two most thoroughly characterized, targetable molecular alterations in NSCLC. However, the combined frequency of these two mutations is significantly less than 50%, and they are almost exclusively found in adenocarcinomas (Aisner & Marshall, 2012). Unfortunately, research to uncover targetable molecular drivers for squamous cell carcinoma and large cell lung carcinoma lags behind.

Between 10% and 15% of NSCLC harbor activating mutations in the EGFR kinase domain, resulting in ligand-independent activation of EGFR. This constitutive kinase activity hyperactivates downstream pathways that drive tumor cell proliferation, such as Akt, c-Jun N-terminal kinase (JNK), and mitogen-activated protein kinase (MAPK) (Petersen, 2011; Raparia et al., 2013). In NSCLC, EGFR activating mutations are most frequently found in women, never-smokers, and Asians. The two most common mutations are an in-frame deletion in exon 19 and a point mutation in exon 21 (L858R), both within the kinase domain (Aisner & Marshall, 2012; Cufer et al., 2013; D'Addario et al., 2010).

Two tyrosine kinase inhibitors (TKIs) targeting the kinase domain of EGFR have been approved for use in NSCLC, gefitinib and erlotinib. Several phase III trials have shown that in patients whose tumors harbor EGFR sensitizing

mutations, treatment with EGFR-TKIs results in prolonged progression-free survival (PFS), enhanced quality of life, and reduced treatment-induced toxicities, when compared to platinum-based chemotherapy (Maemondo et al., 2010; Mitsudomi et al., 2010; Zhou et al., 2011). Conversely, tumors without these mutations are almost always refractory to EGFR-TKIs. For example, in chemotherapy-naïve, molecularly unselected patients, four large phase III studies demonstrated no added benefit by adding gefitinib or erlotinib to chemotherapy when compared to chemotherapy alone (Gatzemeier et al., 2007; Giaccone et al., 2004; Herbst et al., 2004, 2005). The strong predictive power of EGFR mutations and the success of gefitinib and erlotinib have made screening for EGFR mutations the standard of care in advanced NSCLC, particularly adenocarcinoma.

Despite the dramatic efficacy of these EGFR antagonists, resistance often emerges within twelve months (Sequist et al., 2011). Several mechanisms for this resistance have been confirmed. Approximately half of tumors that develop resistance contain a secondary mutation (T790M) that abrogates TKI binding to the EGFR kinase domain (Sequist et al., 2011). A subset of tumors harboring the T790M mutation concomitantly undergoes gene amplification of *EGFR*, bolstering resistance provided by the secondary mutation. Gene amplification of mesenchymal epithelial transition factor (*MET)* accounts for resistance in another 15% to 20% of patients (Sequist et al., 2011). *MET* encodes hepatocyte growth factor receptor (HGFR), another receptor tyrosine kinase (RTK), that activates downstream pathways that overlap with those induced by EGFR. Although *MET*

amplifications can occasionally be found in patients prior to targeted therapy, they are most often associated with acquired resistance to EGFR-TKIs (Aisner & Marshall, 2012).

Approximately 5% of NSCLC contain a rearrangement in the *ALK* gene. In NSCLC, the majority of these yield an *EML4-ALK* fusion gene encoding a protein with constitutive tyrosine kinase activity (Aisner & Marshall, 2012; Chen et al., 2011; Raparia et al., 2013). This chimeric kinase hyperactivates the Ras-extracellular signal-related kinase (ERK) and phosphatidylinositide 3-kinase (PI3K)-Akt pathways to promote NSCLC progression. Like *EGFR* mutations, these rearrangements are most common in patients with either a nonexistent or a light smoking history. Crizotinib, a selective ALK inhibitor, has been approved for treatment of NSCLC. This drug has been quite successful, demonstrating response rates between 50% and 60% among patients with an *ALK* rearrangement following relapse to first-line chemotherapy (Camidge et al., 2011; Kim et al., 2012).

Kirsten rat sarcoma viral oncogene (*KRAS*), also known as V-Ki-ras2, was one of the first genes found to be mutated in NSCLC. Present in 30% of adenocarcinomas and 5% of squamous cell carcinomas, *KRAS* mutations are strongly associated with smoking (Aisner & Marshall, 2012; Raparia et al., 2013). Although no therapeutic agent targeting *KRAS* has been approved for NSCLC, these mutations still have diagnostic relevance, as it is extremely rare for *KRAS* mutations to occur simultaneously with *EGFR* and *ALK* alterations (Aisner & Marshall, 2012; Petersen, 2011; Raparia et al., 2013). Hence, identification of a

KRAS mutation within a specimen is an excellent predictor for resistance to EGFR and ALK inhibitors (Petersen, 2011).

The epithelial-to-mesenchymal transition is an embryonic dedifferentiation program utilized by cancer cells

NSCLC initiation results from the sequential accumulation of genetic alterations within lung epithelial cells. Identifying intracellular molecular changes that induce NSCLC has been instrumental in developing effective targeted therapies. However, it has become increasingly clear that NSCLC metastasis strongly relies on interactions between the carcinoma cells and various components of the tumor microenvironment.

Ninety percent of cancer-related deaths are caused by metastasis (Valastyan & Weinberg, 2011). The metastatic cascade is a multi-step process that begins within the primary tumor. First, carcinoma cells acquire the ability to invade the basement membrane, the specialized form of extracellular matrix that separates the epithelium from the underlying stroma. Second, cells enter the lumina of the blood or lymphatic vessels (intravasation). These invasive cells utilize the body's blood and lymphatic systems to migrate to a distal site, where they exit the vasculature (extravasation). Colonization, the final step of metastasis, occurs when disseminated tumor cells successfully adapt to and proliferate in their new microenvironment, forming macroscopic metastases (Valastyan & Weinberg, 2011).

A conundrum that has faced tumor biologists for decades is how carcinoma *in situ* acquires the individual characteristics necessary to achieve metastasis. One hypothesis proposes that within an epithelial tumor, cancer cell-tumor microenvironment interactions trigger a subset of cells to undergo a cellular re-programming event termed the epithelial-to-mesenchymal transition (EMT) (Cirri & Chiarugi, 2012; Fuxe & Karlsson, 2012; Gao et al., 2012). This transition confers upon carcinoma cells almost all properties required for metastasis.

EMT is a developmental program that is indispensable for normal physiological processes such as embryogenesis and wound healing (Fuxe & Karlsson, 2012; Gao et al., 2012). Re-activation of EMT has been described in a number of human diseases characterized by a strong inflammatory component, including cancer, asthma, kidney disease, and fibrotic disorders (Fuxe & Karlsson, 2012). Cell junction disassembly, cytoskeletal remodeling, decreased cell structure, and loss of polarization in the epithelial cell characterize the transition. Concomitantly, these cells acquire a mesenchymal phenotype, characterized by resistance to apoptotic cues, upregulation of genes associated with de-differentiation, and increased capacities for migration and invasion (Gao et al., 2012; Thiery et al., 2009).

A number of signals from the tumor microenvironment, particularly cytokines and growth factors, orchestrate EMT. Transforming growth factor beta (TGFβ), a pleiotropic growth factor that controls many cellular processes, is one of the most potent EMT inducers (Floor et al., 2011; Fuxe & Karlsson, 2012;

Heldin et al., 2012; Xu et al., 2009). Tumor necrosis factor (TNF), a pro-inflammatory cytokine, has been shown to synergize with TGFβ to fully activate EMT (Asiedu et al., 2011; Bates & Mercurio, 2003; Câmara & Jarai, 2010; Kawata et al., 2012; Shintani et al., 2013; Takahashi et al., 2010). Hypoxic and anoxic conditions within a tumor can induce the expression of hypoxia-inducible factors (HIFs) that can promote EMT and angiogenesis, both rate-limiting steps for disease progression (Cheng et al., 2011). Other soluble factors capable of inducing EMT in various model systems include Notch, Wnts, epidermal growth factor (EGF), fibroblast growth factor (FGF), and hepatocyte growth factor (HGF) (Thiery et al., 2009).

Genetic studies have identified a set of EMT "master-switch transcription factors" that mediate the massive genetic and epigenetic changes underlying the conversion (Wu et al., 2012). These transcription factors fall into two structural categories: zinc finger proteins (Snail, Slug, and SIP1) and basic helix-loop-helix (bHLH) proteins (Twist and E47). They repress genes encoding caretakers of the epithelial phenotype, including cytokeratins, polarity proteins, and junction proteins such as claudins, occludin, and E-cadherin. Downregulation of E-cadherin, the primary component of adherens junctions, is both one of the most important hallmarks of EMT as well as one of the best studied. Snail, Slug, and SIP1 bind directly to E-boxes in the E-cadherin promoter to repress its transcription (Chua et al., 2007; Bolós et al., 2002; Zhang et al., 2011). Alongside these repressive events, these transcription factors also upregulate proteins governing mesenchymal morphology, including such as vimentin, a

mesenchymal intermediate filament, and N-cadherin, which together collectively promote cellular migration (Fuxe & Karlsson, 2012; Valastyan & Weinberg, 2011). These changes in cellular morphology allow individual carcinoma cells to detach from the tightly bound epithelium, initiating the metastatic cascade.

Following EMT, neoplastic cells also upregulate remodelers of the extracellular matrix (ECM). These mesenchymal cells secrete enzymes that degrade the ECM, particularly matrix metalloproteases (MMPs) (Yu & Stamenkovic, 2000), and others that restructure the ECM following degradation, such as lysyl oxidase (LOX) (Kirschmann et al., 2002). Upon synthesis and activation, MMPs further promote the mesenchymal phenotype. For example, upon localizing to the cell surface by binding the hyaluronan receptor CD44, MMP2 and MMP9 cleave latent TGFβ, resulting in its activation and subsequent promotion of tumor growth and angiogenesis (Yu & Stamenkovic, 2000). Moreover, MMP3 and MMP9 can directly cleave E-cadherin to weaken intercellular interactions, stimulating acquisition of the mesenchymal phenotype (Dahl et al., 2008; Noë et al., 2001). Mesenchymal cells also secrete ECM structural components such as fibronectin, collagen, glycoproteins, hyaluronan, laminins, and proteoglycans that allow ECM restructuring (Fuxe & Karlsson, 2012; Gao et al., 2012; Valastyan & Weinberg, 2011). This newfound ability to actively remodel the underlying basement membrane facilitates motility, enabling carcinoma cells to emigrate from the primary tumor and intravasate into the blood and lymphatic system.

EMT confers stem-like properties in cancer-initiating cells

A large amount of evidence has illustrated the presence of organ-specific stem cells in adult tissues that are capable of self-renewal. These “adult” stem cells maintain a steady population by asymmetric cell division, producing one identical copy of the original stem cell and a second daughter cell with limited progenitor capacity, committed to differentiate and execute tissue-specific functions. The multipotent status of adult stem cells enables them to recapitulate every somatic cell phenotype within a given organ, making them indispensable for maintaining the natural cellular turnover that occurs over the course of a lifetime (Passier & Mummery, 2003). Healthy adult stem cells play critical roles in tissue repair, so they have evolved mechanisms to protect them from lethal damage, including immortality, slow kinetics of division, and resistance to apoptosis (Gottschling et al., 2012).

More recently, researchers have identified stem-like cells within neoplastic tissues, termed “cancer-initiating cells” (CIC), which are capable of recapitulating cellular phenotypes found within the primary tumor. CIC share many characteristics with normal stem cells that contribute to their drug-resistant phenotype, including slow rates of proliferation and innate resistance to apoptosis (Alison et al., 2011). This population of progenitor cells is essential to both primary tumor maintenance and disease progression. For example, CICs maintain homeostasis of the primary tumor by regenerating cells that die due to an immune response or by chemotherapeutic drugs. Furthermore, upon

dissemination, the multipotent status of CICs increases the efficiency of metastatic colonization (Scheel & Weinberg, 2012).

Since successful treatment of cancer would theoretically require complete eradication of this rare fraction of cells, efforts have focused on identifying the mechanisms that create and support CICs. A well-accepted hypothesis in the cancer biology field proposes that EMT enriches for CICs by de-differentiating somatic carcinoma cells, enabling their self-renewal and limitless replication (Scheel & Weinberg, 2011, 2012). Therefore, EMT is believed to contribute to multiple steps of the metastatic cascade, making it doubly perilous for a cancer patient. First, the acquisition of a mesenchymal phenotype permits carcinoma cells to invade the basement membrane and extravasate into the bloodstream. Second, EMT confers cancer-initiating traits to promote dissemination and colonization of distal sites.

The first study to link EMT and CIC formation came from the Weinberg lab. Mani and colleagues showed that upon undergoing EMT, human mammary epithelial cells (HMLEs) express stem cell markers and display phenotypes characteristic of cancer stem cells, such as increased capacity to form soft agar colonies, mammospheres, and tumors. Conversely, stem-like cells isolated from HMLE cultures display EMT markers (Mani et al., 2008). Since this finding, a number of other studies have confirmed that EMT confers stem-like characteristics upon neoplastic cells (Floor et al., 2011; Morel et al., 2008; Scheel et al., 2011).

Similarly to normal human embryonic or organ-specific stem cells, CICs possess a number of unique characteristics that facilitate their isolation from mixed cellular populations. Flow cytometry of stem cell surface antigens, including various “cluster of differentiation” (CD) proteins and ATP-binding cassette (ABC) transporters, has enabled researchers to identify and enrich for CICs. Moreover, these self-renewing cells selectively exclude dyes such as Hoescht 33342 and Rhodamine 123, a phenotype attributed to the upregulation of ABC transporters, particularly ABCG2, also known as breast cancer resistance protein (BRCP) (Alison et al., 2011; Gottschling et al., 2012). Moreover, reduced kinetics of division in CICs yield enhanced retention of DNA and membrane dyes such as PKH or BrDU when compared to non-CICs (Gottschling et al., 2012). Although these methods have been instrumental in identifying potential CIC among mixed populations, the benchmark for confirming their presence is demonstration of multipotency.

The multipotent status of CICs can be demonstrated at both a genotypic and phenotypic level. To maintain multipotency, CICs upregulate the same transcription factors that preserve the pluripotent state of human embryonic stem cells (hESC), including octamer-binding transcription factor (Oct) 3/4, Nanog, SRY (sex-determining region Y)-box 2 (Sox2), c-Myc, and Kruppel-like factor 4 (KLF4) (Takahashi et al., 2007). Upregulation of human *telomerase reverse transcriptase* (*hTERT*) contributes to the characteristic long life span of stem cells. Phenotypically, multipotency is typically verified by two types of assays. The gold standard is the ability for cells to efficiently form tumors under limiting

dilution following xenograft transplantation into immunocompromised mice. *Ex vivo* assays include the ability to form clonogenic populations, referred to as tumorspheres, in non-adherent cell culture (Alison et al., 2011).

CICs were first isolated in acute myeloid leukemia (AML) based on a $CD34^{+}/CD38^{-}$ antigenic phenotype and their tumor-initiating capacity *in vivo* (Lapidot et al., 1994). Since this discovery, prospective CICs have been identified and expanded from a number of solid tumors based on cell surface markers. For example, multiple studies have shown that within breast tumors, a small subset of cells exhibiting a $CD44^{high}/CD24^{low}$ antigenic phenotype is highly enriched for CICs (Mani et al., 2008; Meyer et al., 2009; Morel et al., 2008). Similar side populations since have been isolated from brain (S. K. Singh et al., 2004) ($CD133^{+}$), colon ($CD133^{+}$) (O'Brien et al., 2007), and pancreas ($CD133^{+}/CXCR4^{+}$) (Hermann et al., 2007). In addition to these solid tumors, it has become increasingly clear that CIC play an instrumental role in NSCLC progression as well.

In vitro *evidence for CICs in NSCLC*

Over sixty percent of all NSCLC contain multiple subtypes, contributing to the hypothesis that lung cancer derives from a multipotent stem cell capable of differentiating into these diverse components (Gottschling et al., 2012). Indeed, a number of different laboratories have isolated NSCLC CICs *in vitro* from both primary cells and established cell lines. For example, Eramo et al. identified $CD133^{+}$ subpopulations from several primary human NSCLC tumors that

demonstrated stem-like features, including growth as tumorspheres, the generation of xenografts in mice that were histologically identical to the primary tumor, and expression of Oct3/4 and Nanog (Eramo et al., 2008). A study conducted by Leung and colleagues identified CD44 as an NSCLC CIC surface marker in six of ten cell lines examined. Their work showed that side populations expressing CD44 form spheroid cultures *in vitro* and tumors *in vivo* at a significantly higher rate than $CD44^-$ cells. Moreover, $CD44^+$ cells express genes responsible for self-renewal, including *OCT4, NANOG,* and *SOX2*, that $CD44^-$ cells do not express (Leung et al., 2010a). Moreover, Sung and colleagues utilized flow cytometry for Hoechst 33342 to purify a side population of A549 (NSCLC adenocarcinoma) cells with enhanced clonogenicity, reduced proliferation, and drug resistance (Sung et al., 2008). Additionally, side populations isolated from six NSCLC cell lines based on their ability to exclude Hoechst 33342 demonstrated CIC characteristics, including increased tumorigenicity in mice, resistance to multiple drugs, and upregulation of ABC transporters and *hTERT* (Ho et al., 2007).

EMT drives NSCLC progression by enriching for drug-resistant CICs

Since the groundbreaking study linking EMT and breast CIC formation from the Weinberg lab, researchers have made efforts to demonstrate this connection in other solid tumors. Several studies have shown that EMT confers stem-like properties upon NSCLC cells *in vitro*. TGFβ-treatment of LC31 cells, a primary NSCLC cell line, induced EMT as well as a stem cell-like phenotype,

characterized by upregulation of *OCT4, NANOG, SOX2,* and *CD133*, enhanced formation of tumorspheres, and increased tumorigenicity in nude mice (Tirino et al., 2013). Another study provided support for the role of cancer-associated fibroblasts (CAFs) in promoting a mesenchymal and stem-like phenotype in A549 and H358 cells. Conditioned media from cultured CAFs, highly enriched in TGFβ, induced the expression of classic mesenchymal and stem cell markers as well as enhanced resistance to cisplatin, formation of tumorspheres, and tumors in nude mice (Kim et al., 2013).

Given the association of CICs with drug resistance, researchers have examined whether EMT in NSCLC can act as an additional mechanism of resistance to EGFR and ALK TKIs. The first solid evidence for EMT as a mechanism for TKI resistance came from Yauch et al. These researchers took a pharmacogenomic approach to identify gene signatures that would predict sensitivity to erlotinib in 42 NSCLC cell lines. Interestingly, they found a multigene mRNA expression signature indicative of an EMT that strongly separated erlotinib-sensitive versus erlotinib-insensitive NSCLC cell lines (Yauch et al., 2005). Similarly, Witta et al. demonstrated a strong correlation between 22 NSCLC cell lines between high *CHD1* (E-cadherin) expression, low *ZEB1* expression, and sensitivity to gefitinib. Interestingly, in gefinitib-resistant cell lines, restoring E-cadherin expression was sufficient to induce sensitivity to gefinitib (Witta et al., 2006).

To determine the relative frequencies of the classic TKI resistance mechanisms, including *EGFR* gene amplification, the *EGFR* T790M point

mutation, and *MET* amplification, Sequist and colleagues performed genetic and histological analyses of thirty-seven TKI-resistant NSCLC tumors harboring an activating *EGFR* mutation. Classic mechanisms of resistance were identified in thirty of these patients, but in seven of these patients, none of these alterations were found. Instead, three of these seven tumors displayed markers characteristic of having undergone EMT. Moreover, patients whose tumors harbored previously characterized mechanisms of resistance did not exhibit features of EMT, suggesting that EMT-conferred resistance may occur exclusively from other mechanisms (Sequist et al., 2011).

In addition to TKI resistance, EMT has been shown to confer insensitivity to chemotherapy in NSCLC. Knockdown of *SNAIL* or *TWIST* in A549 cells sensitizes them to cisplatin-induced apoptosis (Zhuo et al., 2008). A strong study by Shintani et al. demonstrated that following TGFβ-induced EMT, A549 cells display reduced sensitivity to both cisplatin and paclitaxel. Resistant sublines created by repeated exposure to cisplatin, paclitaxel, or radiation demonstrated a significant decrease in E-cadherin and increase in N-cadherin. Moreover, this study compared surgically resected specimens following CRT to pre-CRT biopsies in fifty patients whose tumors responded poorly to CRT, and twenty of these exhibited markers indicative of having undergone EMT (Shintani et al., 2011).

Markers of EMT and CICs correlate with poor prognosis in NSCLC patients

To ensure that these laboratory findings have clinical relevance, a number of studies have examined the relationship between EMT and CIC markers and patient prognosis. While not causative, these studies consistently demonstrate associations between elevated mesenchymal and stem cell marker expression, reduced epithelial marker expression, and poor patient prognosis. Taken together, the large number of studies and wide assortment of markers examined inspire confidence that EMT-driven CIC enrichment plays a critical role in NSCLC progression.

For example, levels of TGFβ, the most potent inducer of EMT, correlate with NSCLC stage, angiogenesis, lymph node metastasis, and poor prognosis (Hasegawa et al., 2001). Moreover, tissue microarray analysis (TMA) of 237 lung adenocarcinomas revealed that *SNAIL* levels are associated with decreased overall survival (Yanagawa et al., 2009). In patients with resectable NSCLC, overexpression of Snail or Twist correlates with shorter overall survival, and co-expression of two or more of HIF-1α, Snail, and Twist is a negative prognostic indicator for recurrence-free survival and overall survival (Hung et al., 2009). Shih et al. showed that Slug levels are significantly associated with shorter patient survival and postoperative relapse (Shih et al., 2005). Additionally, TMA analysis of 335 patients with Stage I-IIIA NSCLC showed that high expression of E-cadherin or low expression of vimentin are positive prognostic indicators for disease-free survival (Al-Saad et al., 2008). Using IHC analysis of 331 NSCLC tissues, Kase at al. found that reduced E-cadherin levels significantly correlate with lymph node metastasis and dedifferentiation (Kase et al., 2000).

Importantly, markers of self-renewal and multipotency are also associated with poor prognosis in NSCLC patients. For example, overexpression of ABCG2 and CD133, two NSCLC CIC markers, predicts relapse in patients with stage I NSCLC (Li et al., 2011). Additionally, triple positivity of Oct4, Nanog, and Slug expression is correlated with poor prognosis in NSCLC (Chiou et al., 2010). These prognostic studies provide further support for EMT-driven induction of CIC phenotypes as a critical promoter of NSCLC progression.

The TGFβ Superfamily

The TGFβ superfamily consists of over forty structurally related ligands in humans. In addition to three TGFβs (TGFβ1-3), the superfamily includes Activins, Inhibins, Nodal, bone morphogenic proteins (BMPs), growth and differentiation factors (GDFs), and anti-Müllerian hormone (AMH) (Wakefield & Hill, 2013). These ligands regulate essential physiological processes including embryonic development, cell differentiation, and tissue homeostasis (Oshimori & Fuchs, 2012). Produced as precursors consisting of an amino-terminal prodomain and a carboxy-terminal mature domain, they undergo cleavage by proprotein convertases. Functionally active TGFβ superfamily ligands are either homodimers or heterodimers linked by disulfide bonds (Wakefield & Hill, 2013).

All members of the superfamily share the same fundamental signaling pathway. Each mature ligand signals through both a type I and a type II serine/threonine kinase transmembrane receptor. Dimeric TGFβ superfamily members initiate signaling by binding and activating the type II receptor's kinase

activity. Upon activation, the type II receptor recruits and phosphorylates the type I receptor within its glycine/serine (GS)-rich region, activating its kinase activity and providing a docking site for one of the TGFβ intracellular effector proteins, known as the receptor-regulated SMADs (R-SMADs). TGFβs, Activins, and Nodal all signal through SMAD2 and SMAD3, whereas BMPs and GDFs utilize SMADs 1, 5, and 8 (Horbelt et al., 2012). Upon binding, the R-SMAD is phosphorylated by the type I receptor and subsequently dimerizes with the common mediator SMAD (co-SMAD, SMAD4). This heterodimeric transcription factor then translocates to the nucleus where it activates or represses expression of TGFβ superfamily member target genes. These changes are executed by interaction of the bipartite transcription factor with chromatin modifying enzymes such as histone acetyltransferases (HATs) or histone deacetyltransferases (HDACs) (Wakefield & Hill, 2013).

The best studied member of the superfamily is TGFβ itself. The role of TGFβ in carcinogenesis varies based on cell type, environmental signals, and state of the disease. Early in cancer development, TGFβ acts as a tumor suppressor by arresting cells in phase G1 of the cell cycle. However, later in cancer progression, TGFβ drives disease progression and metastasis by regulating critical pathways such as angiogenesis, inflammation, migration, and invasion. The TGFβ growth arrest program appears to be solely dependent on SMAD signaling, whereas its role in promoting cancer progression in later stages is driven by SMADs as well as non-SMAD pathways, including ERK1/2, JNK, and PI3K-Akt pathways (Wakefield & Hill, 2013).

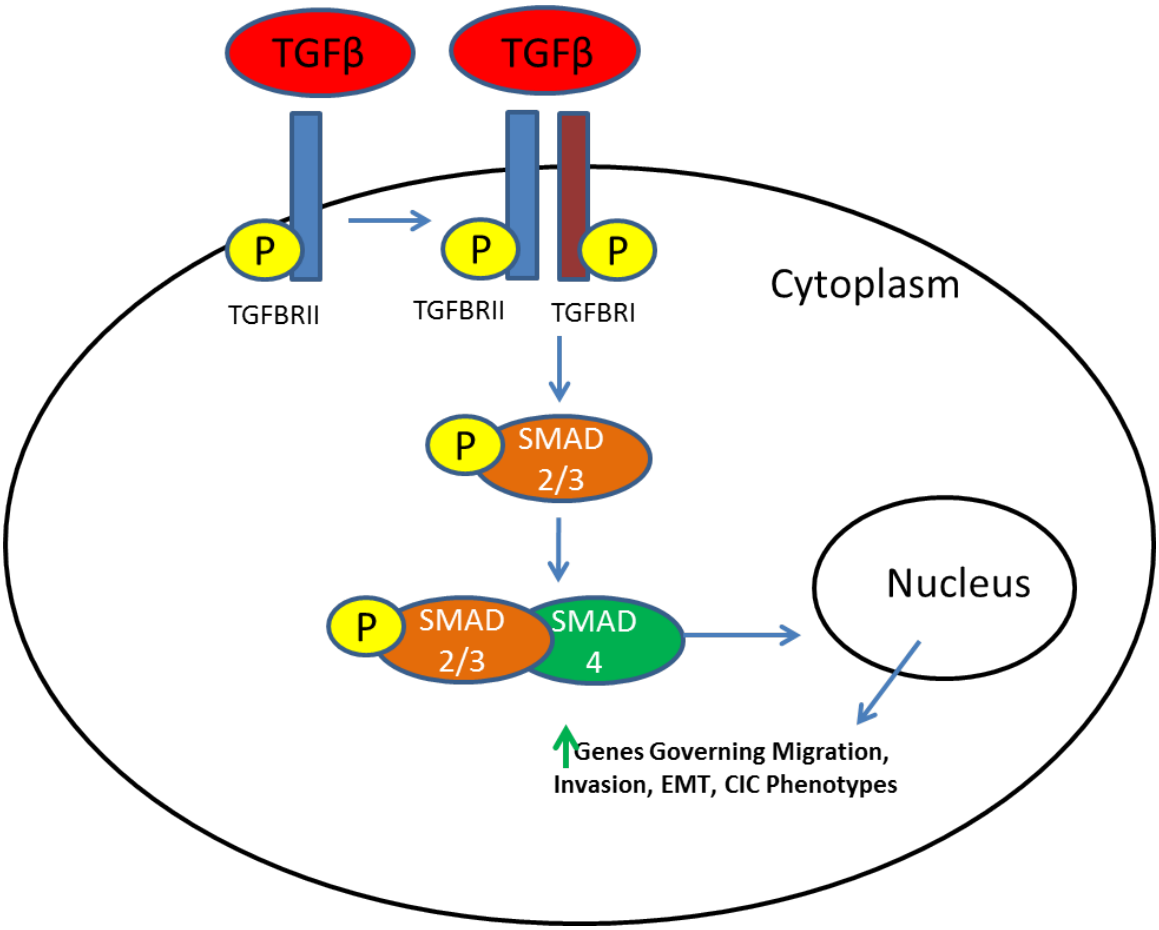
TGFβ
TGFβ
P
P
P
TGFBRII
TGFBRII
TGFBRI
Cytoplasm
P
SMAD
2/3
Nucleus
P
SMAD
2/3
SMAD
4
Genes Governing Migration,
Invasion, EMT, CIC Phenotypes

Figure 1: Canonical TGFβ Signaling. TGFβ (red) initiates the signaling cascade by binding its type II receptor (blue) and activating its kinase activity. Active TGFβRII binds and phosphorylates TGFβRI (blue), stimulating its kinase activity. TGFβRI then phosphorylates one of two regulatory SMADs (R-SMADs), SMAD2 or SMAD3 (orange). Phosphorylated SMAD2/3 then bind the co-SMAD, SMAD4 (green), to form a transcriptionally competent heterodimer that translocates to the nucleus and binds TGFβ target genes to modulate EMT and cancer-initiating cell phenotypes.

NF-κB, a pleiotropic growth factor that drives cancer progression and EMT

NF-κB is a family of proto-oncogenic transcription factors that respond to environmental cues to regulate cell survival, proliferation, angiogenesis, and EMT. Studies in both animal models and cell lines have illustrated the role of NF-κB in driving lung carcinogenesis. One of the best-studied activators of the NF-κB pathway is tumor necrosis factor (TNF), a powerful pro-inflammatory cytokine. A number of other extracellular signals can activate NF-κB, including other cytokines, growth factors, tumor suppressors, and carcinogens. Intracellular cues such as endoreticular stress or DNA damage can also activate NF-κB (Ben-Neriah & Karin, 2011; Min et al., 2008).

In mammals, NF-κB is composed of five Rel family members: RelA/p65, RelB, cRel, p50 and p52. Each contains an N-terminal Rel homology domain (RHD) that mediates DNA binding and dimerization. Only p65, RelB, and c-Rel contain a C-terminal transactivation domain (TAD). Upon heterodimerization with p50 or p52, these TAD-containing subunits bind consensus NF-κB sequences and activate target gene transcription. In the absence of a TAD-containing factor, homodimers of p50 or p52 bind chromatin to suppress transcription (Ben-Neriah & Karin, 2011).

In the canonical NF-κB signaling pathway, transcription is mediated predominately by two dimeric transcription factors: the repressive p50 homodimer and the activating p50:p65 heterodimer. Prior to stimulation, p50 homodimers occupy NF-κB binding sites, tethering core repression complexes comprised of HDAC3 and one of two homologous corepressors, SMRT or

nuclear corepressor (NCoR). These complexes recruit other HDACs to further promote chromatin condensation. In this basal state, a family of inhibitor proteins, IκB, binds p65 and masks its nuclear localization sequence (NLS), sequestering the p50:p65 heterodimer in the cytoplasm (Hayden & Ghosh, 2008). Two events precede transcriptional activation by the p50:p65 transcription factor.

First, upon cellular stimulation, a signaling cascade converges on the IκB kinase (IKK) complex. Two catalytic subunits, IKKα and IKKβ, as well as one regulatory subunit, IKKγ/NEMO (NF-κB essential modulator), comprise the classical IKK complex. Upon activation, the IKK complex phosphorylates IκB, targeting it for poly-ubiquitination by the SCF-type E3 ligase, $E3RS^{IκB/β\text{-}TrCP}$. Ubiquitylation marks IκB for degradation by the 26S proteasome, exposing the NLS on p65. Liberated NF-κB then translocates to the nucleus to activate gene expression by recruiting transcriptional coactivators (Ben-Neriah & Karin, 2011; Hayden & Ghosh, 2008; Min et al., 2008). Our laboratory has shown that posttranslational modifications on p65 must precede full NF-κB transcriptional activity (Allison et al., 2012; Hoberg et al., 2004, 2006; Yeung et al., 2004).

As a pleiotropic transcription factor, NF-κB plays a key role in the expression of genes involved in cancer initiation and progression. Constitutive NF-κB activity is often observed in both solid and hematological malignancies, directly correlating with less differentiated morphology, advanced tumor stage, and poor clinical prognosis (Bassères & Baldwin, 2006; Ben-Neriah & Karin, 2011). High NF-κB expression in NSCLC tumors correlates with increased

plasticity, higher staged tumors, and poor clinical prognoses (W. Chen et al., 2011). A number of oncogenic viruses and oncoproteins activate NF-κB, relying on it for complete cellular transformation (Hayden & Ghosh, 2008).

NF-κB induces and maintains EMT in model systems through two primary mechanisms. First, NF-κB upregulates the EMT master-switch transcription factors, including Snail (Barberà et al., 2004; Julien et al., 2007; Zhang et al., 2011), Twist (Li et al., 2012; Pham et al., 2007), and SIP1 (Chua et al., 2007). Second, NF-κB directly stabilizes Snail by upregulating the COP9 signalosome 2 (CSN2) complex, which blocks Snail polyubiquitination and degradation (Wu & Zhou, 2010; Wu et al., 2009). NF-κB is also required for EMT induced by HIF-1α or hypoxic conditions in pancreatic cancer (Cheng et al., 2011). Importantly, NF-κB has been linked to maintaining the pluripotency of human embryonic stem cells (Takase et al., 2013), as well as the formation and maintenance of breast CICs (Kendellen et al., 2013; Shostak & Chariot, 2011; Yamamoto et al., 2013). Moreover, it also plays a role in maintaining the pluripotency of human embryonic stem cells (Takase et al., 2013). Work presented in this dissertation demonstrates that the induction and maintenance of the mesenchymal and CIC phenotypes in NSCLC requires NF-κB.

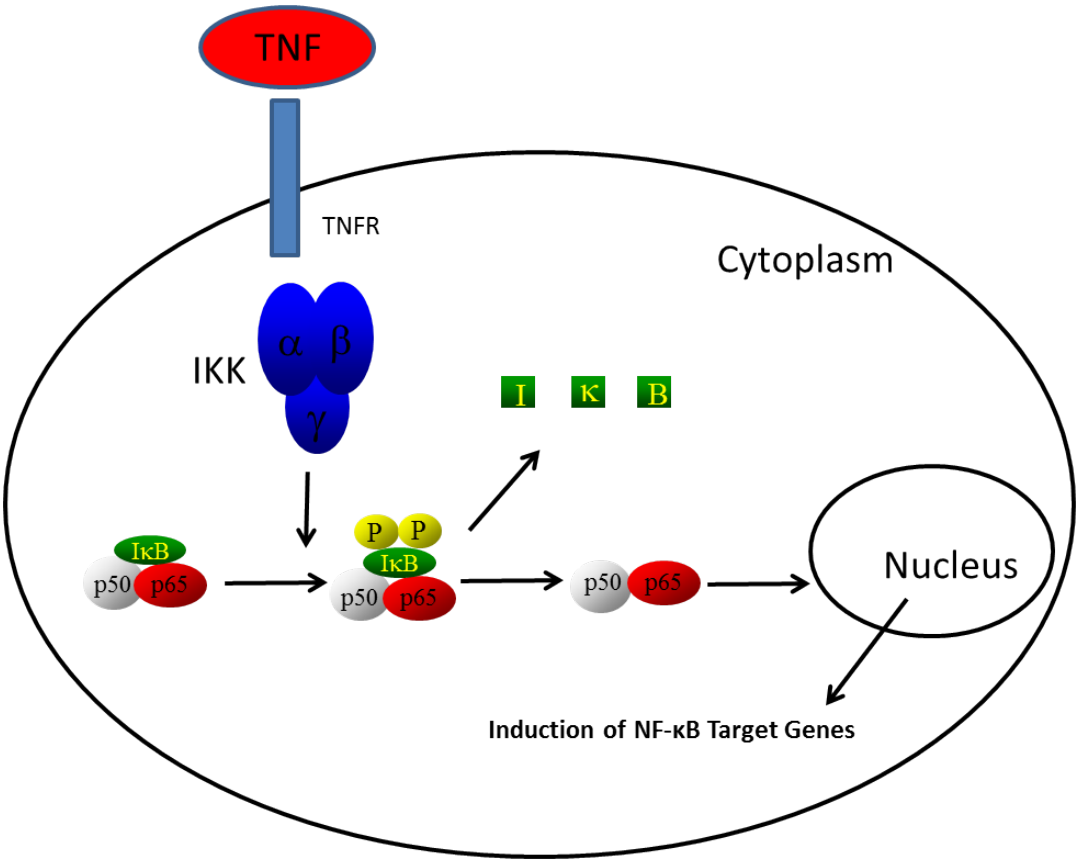
TNF
TNFR
Cytoplasm
IKK
α
β
γ
I
κ
B
IκB
p50
p65
P
P
IκB
p50
p65
p50
p65
Nucleus
Induction of NF-κB Target Genes

Figure 2: TNF activates canonical NF-κB signaling. Prior to stimulation by TNF (red), the heterodimer comprised of p50 (gray) and p65 (red) is sequestered in the cytoplasm by IκB (green). Signaling is initiated when TNF (red) binds its receptor (blue), which activates the IκB kinase (IKK) heterotrimeric complex (dark blue). IKK phosphorylates IκB, marking it for polubiquitination and subsequent degradation by the 26S proteasome. This permits the p50:p65 heterodimer to move to the nucleus and activate NF-κB target genes, synergizing with TGFβ to induce EMT and cancer-initiating cell phenotypes.

CHAPTER 2: MATERIALS AND METHODS

Cell Culture

A549 (NSCLC adenocarcinoma), H358 (NSCLC squamous cell), and H1299 (NSCLC large cell carcinoma) cell lines were obtained from ATCC. A549, as well as stable clonal lines, were grown in DMEM (Corning 10-017) with 10% fetal bovine serum (FBS, Invitrogen 16000044) and 5% Penicillin/Streptomycin (Pen/Strep, Invitrogen 15070-063). H358 and H1299 cells were grown in RPMI 1640 (Corning 10-040) with 10% FBS and 5% Pen/Strep. Cells in this study were grown at 37°C and 5% CO_2.

EMT was induced following stimulation with TNF (Invitrogen PHC3016, 10 ng/mL) and TGFβ (Invitrogen PHG9024, 2 ng/mL). Other cell culture reagents include recombinant Activin (Gibco PHC9564), the Alk4/5/7 inhibitor SB431542 (Sigma S4317), sphingosine-1-phosphate (S1P), and the sphingosine kinase 1 (SK1) inhibitor SKX96091. S1P and SKX96091 were graciously provided by Dr. Kevin Lynch.

Generation of Stable Cell Lines

A549 stable cell lines expressing the super-repressor (SR) IκBα (A549.I) or vector control (A549.V) were created by retroviral delivery of pBABE-Puro (empty vector) or pBABE-Flag-SRIκBα followed by puromycin selection (1.5 μg/mL) (Kumar et al., 2013). A549 cell lines stably expressing control shRNA (A549.C) or shRNA to *INHBA/Activin A* (A549.A) were generated by infection with replication-defective lentivirus (Thermo Scientific SK-011701-00-10) containing either non-targeting shRNA control or one of three shRNA sequences targeting

INHBA/Activin A. Following puromycin (1.5 µg/mL) selection, 3D cultures were created with each pool, left unstimulated or treated with TNF and TGFβ, and Activin A mRNA and protein levels were measured. The shRNA Activin.2 yielded the best knockdown. Following limiting cell dilution, three single clones were isolated and used to create the Activin.2 clonal pool (A549.A). Similar methods were used to generate the non-targeting shRNA control clonal pool (A549.C).

Primary Human NSCLC Cells

Freshly resected NSCLC tumors were washed in PBS, minced with scalpels, and incubated with type IV collagenase (Sigma C5138, 1 mg/mL), type V hyaluronidase (Sigma H6254, 100 µg/mL), and type IV DNase (Sigma D5025, 20 mg/mL) for thirty minutes. Following digestion of the tissue, cells were pelleted, washed, and cultured in RPMI/10% FBS/Pen/Strep on standard tissue culture plates for two days before creating 3D cultures as described below.

Three-Dimensional (3D) Multicellular Spheroid Cultures

Multicellular spheroid cultures were created using a modified hanging droplet method (Kelm et al., 2003). Cells were grown to approximately 80% confluence on standard tissue-culture plates. The cells were subsequently trypsinized, resuspended in DMEM/10% FBS/Pen/Strep, and counted. To create 25,000 cell spheroids, the cell suspension was diluted to 1 x 10^6 cells/mL, and 25 µl of the cell suspension were pipetted onto the underside of a sterile 10 cm Petri dish. Each lid holds approximately fifty droplets. After loading the droplets, the lid was

placed onto a tissue culture plate containing 6 mL of sterile PBS and incubated for 48 hours to facilitate cellular aggregation and spheroid formation. The freshly formed spheroids were then transferred into 10 cm suspension plates containing DMEM/ 2% FBS/Pen/Strep to prevent cell attachment to the dish. Suspension plates were made by adding 8 mL of polyHEMA solution (Sigma-Aldrich P3932, 10 mg/mL) in 95% ethanol to sterile polystyrene Petri dish plates (Fisher Scientific). The plates were then incubated for 24 hours in a sterile environment to allow the ethanol to evaporate. Prior to use, plates were washed with sterile PBS to remove any residual ethanol or other contaminants. Each suspension plate holds up to 100 spheroids.

Conditioned Media and Neutralizing Antibody Experiments

Conditioned media (CM) from 2D and 3D cultures either left untreated or stimulated with TNF and TGFβ were harvested and filtered through a 0.22 μm pore. Supernatants were added fresh, without freezing, to naïve 3D (N3D) cultures for 48 hours. After two days, cultures were pelleted, media removed, cultures were incubated with a second batch of fresh CM, and cells were harvested 48 hours later. For neutralizing antibody experiments, filtered CM were pre-treated with either an Activin A neutralizing antibody (R&D MAB3381, 2, 4 μg/mL) or with an IgG mouse control antibody (Millipore 12-371, 0, 4 μg/mL) for four hours at 37°C with agitation before incubating with N3D cultures.

Microarray Analysis

Monolayer and spheroid cultures were treated with TNF and TGFβ or left unstimulated for 96 hours before harvesting. Total RNA was isolated using the RNeasy Total RNA Minikit (Chemstores 52515), and reverse transcribed using the iScript cDNA Synthesis Kit (Bio-Rad 170-8891BUN). Technical duplicates of the experiment were performed. The resulting cDNA from both experiments were labeled and hybridized to a GeneChip Human Genome U133 Plus 2.0 Array (Affymetrix 900470). The *gcrma* package of the Bioconductor project was used to convert background-adjusted probe intensities to gene expression measures (Wu et al., 2004). Comparison of gene expression profiles between 1) 2D treated vs. untreated and 2) 3D treated vs. untreated was conducted using the Limma package of the Bioconductor project (Smyth, 2004). P-values were adjusted using a 5% false discovery rate (FDR), and a cutoff of $p \leq .05$ was applied.

Quantitative Real-Time Polymerase Chain Reaction (QRT-PCR)

Total RNA was isolated and cDNA was synthesized as described above for microarray analysis. Relative expression of mRNA was evaluated by quantifying cDNA samples with gene-specific primer sets by QRT-PCR using a SYBR Green/Taq Supermix (Bio-Rad 170-8884). Results were normalized to GAPDH. QRT-PCR primers are listed in Table 1.

TABLE 1: QRT-PCR PRIMERS

Gene	Sequence
H. sapiens BIRC3 F	GCAGCAACCTCATTCAGAAA
H. sapiens BIRC3 R	GCAATGTCATCTGTGGGAAG
H. sapiens BMP2 F	CGGTTGGAGAGGGCAGC
H. sapiens BMP2 R	CTTCCAAAGATTCTTCATGGTGG
H. sapiens CDH1 F	TGAGTGTCCCCCGGTATCTTC
H. sapiens CDH1 R	CAGTATCAGCCGCTTTCAGATTTT
H. sapiens CDH2 F	ATCAACCCCATACACCAGCCTG
H. sapiens CDH2 R	GCAGCAACAGTAAGGACAAACATCC
H. sapiens COL22A1 F	ACGAACGCTAGGACAGAGCA
H. sapiens COL22A1 R	GTCTTCCACGTGTCCGACTT
H. sapiens GAPDH F	GAAGGTGAAGGTCGGAGTC
H. sapiens GAPDH R	GAAGATGGTGATGGGATTTC
H. sapiens HMGA2 F	AGTCCCTCTAAAGCAGCTCAAAAG
H. sapiens HMGA2 R	GCCATTTCCTAGGTCTGCCTC
H. sapiens IL8 F	CTCTTGGCAGCCTTCCTG
H. sapiens IL8 R	CTGTGTTGGCGCAGTGTG
H. sapiens INHA F	GTCTCCCAAGCCATCCTTTT
H. sapiens INHA R	AGAGCTATTGGAGGCTGCTG
H. sapiens INHBA F	TCATGCCAACTACTGCGAGG
H. sapiens INHBA R	ACAGTGAGGACCCGGACG
H. sapiens INHBB F	CGCGTTTCCGAAATCATCA
H. sapiens INHBB R	GGACCACAAACAGGTTCTGGTT
H. sapiens INHBC F	GCAGCCCGGGTGAGAGTTGG
H. sapiens INHBC R	ACTGCACCCACAGGCCTC
H. sapiens INHBE F	AGCCCTTCCTAGAGCTTAAG
H. sapiens INHBE R	GCTGCAGCCACAGGCC
H. sapiens KDM6B F	CCCCCATTTCAGCTAACCAAGCCAG
H. sapiens KDM6B R	GGAGCAGCCGGGACCAGCCG
H. sapiens KIT F	AGGATTCCCAGAGCCCACAATAG
H. sapiens KIT R	ACGGTGGCCCAGATGAGTTTAG
H. sapiens KLF4 F	ACCAGGCACTACCGTAAACACA
H. sapiens KLF4 R	GGTCCGACCTGGAAAATGCT
H. sapiens LOX F	CGGCGGAGGAAAACTGTCT
H. sapiens LOX R	TGAGCAGCACCCTGTGATCA
H. sapiens MMP2 F	TCTCCTGACATTGACCTTGGC
H. sapiens MMP2 R	CAAGGTGCTGGCTGAGTAGATC
H. sapiens MMP9 F	TTGACAGCGACAAGAAGTGG
H. sapiens MMP9 R	GCCATTCACGTCGTCCTTAT
H. sapiens MYCN F	CGCAAAAGCCACCTCTCATTA
H. sapiens MYCN R	TCCAGCAGATGCCACATAAGG
H. sapiens NODAL F	AGCATGGTTGTTGAGGTGAC
H. sapiens NODAL R	CCTGCGAGAGGTTGGAGTAG
H. sapiens POU5F1 F	ACCCCTGGTGCCGTGAAGC

H. sapiens POU5F1 R	CAGATGGTCGTTTGGCTGAATACC
H. sapiens SNAI1 F	CACTATGCCGCGCTCTTTC
H. sapiens SNAI1 R	GGTCGTAGGGCTGCTGGAA
H. sapiens SNAI2 F	ATGAGGAATCTGGCTGCTGT
H. sapiens SNAI2 R	CAGGAGAAAATGCCTTTGGA
H. sapiens SOX2 F	GCCCAGGAGAACCCCAAGATG
H. sapiens SOX2 R	GCTCGCAGCCGCTTAGCCTC
H. sapiens SK1 F	AGCTTCCTTGAACCATTATGCTG
H. sapiens SK1 R	AGGTCTTCATTGGTGACCTGCT
H. sapiens SK2 F	CTGTCTGCTCCGAGGACTGC
H. sapiens SK2 R	CAAAGGGATTGACCAATAGAAGC
H. sapiens S1PR1 F	TATCATCGTCCGGCATTACA
H. sapiens S1PR1 R	GAACACCACCGAGGTAGTT
H. sapiens S1PR3 F	GGTGATTGTGGTGAGCGTGTT
H. sapiens S1PR3 F	AGGCCACATCAATGAGGAAGA
H. sapiens TGFB1 F	CAACAATTCCTGGCGATACCT
H. sapiens TGFB1 R	GCTAAGGCGAAAGCCCTCAAT
H. sapiens TWIST1 F	CGGGAGTCCGCAGTCTTA
H. sapiens TWIST1 R	CTTGAGGGTCTGAATCTTGCT
H. sapiens VIM F	CTTCGTGAATACCAAGACCTGC
H. sapiens VIM R	TATCAACCAGAGGGAGTGAATCC
H. sapiens ZEB2 F	CAATACCGTCATCCTCAGCA
H. sapiens ZEB2 F	CCAATCCCAGGAGGAAAAAC
ERV3 F	ATGGGAAGCAAGGGAACTAAT
ERV3 R	CCCAGCGAGCAATACAGAATTT

F, forward primer; R, reverse primer. All sequences listed from 5'-3'.

Immunoblots

Immunoblotting was performed using the NOVEX (Invitrogen) system. Briefly, proteins were separated on 4–12% Bis-Tris polyacrylamide gel electrophoresis (PAGE) gels and transferred onto nitrocellulose membranes. Membranes were blocked for one hour in 3% milk in TBS-T. Antibodies used for immunoblot are E-cadherin (BD Pharmingen 610404), N-cadherin (BD Pharmingen 610920), vimentin (Sigma F1804), α-tubulin (Sigma T6793), GAPDH (GeneTex GTX627408), HMGA2 (Biocheck 59170AP), Twist1 (Cell Signaling 4119), Snail1 (Cell Signaling 4719), Sip1 (SCBT sc-48789), Slug (Abcam ab27568), IκBα (pS32, Cell Signaling 2859), IκBα (SCBT sc-371), RelA (pS536, Cell Signaling 3031), RelA (SCBT sc-372), and M2-Flag (Sigma F1804).

Enzyme-Linked Immunosorbant Assay (ELISA)

Supernatants from 2D and 3D cultures untreated or treated with TNF and TGFβ for 96 hours were harvested and filtered (0.22 μm). ELISA kits (R&D DY338) were used to measure Activin levels in the supernatants (100 μL aliquots), as per manufacturer's protocol.

Transwell Assays

Monolayers and spheroid cultures were disaggregated by incubation with 0.05% trypsin. Spheroid cultures were also subjected to intermittent gentle trituration to facilitate disaggregation. Transwell assays were performed to measure migration and invasion according to the manufacturer's protocol (BD Biosciences). 1×10^5

cells (migration) or 5 x 10^4 cells (invasion) were seeded in plain DMEM in the top well of a transwell control plate (BD 354578) or Matrigel invasion plate (BD 354480). The bottom well was loaded with DMEM containing either 10% FBS or 1% FBS + 1μM S1P as a chemoattractant, and the plates were incubated for eight hours (migration) or twenty-four hours (invasion) at 37°C and 5% CO_2. Afterwards, cells on the upper side of the membrane were removed, and the remaining cells were fixed in 100% methanol and stained with 0.1% crystal violet. The stained cells were imaged and quantified using Adobe® Photoshop.

Tumor Model

Monolayer or spheroid A549 cultures that had been left untreated or treated with TNF and TGFβ were trypsinized and resuspended in DMEM/0.5% FBS. Cells were subcutaneously (SQ) injected into female outbred Crl:NU/NU nude mice (Charles River). Five mice were injected per experimental condition. Mice were sacrificed forty days post-injection. The primary SQ tumors were removed and weighed. Additionally, the lungs were removed, fixed in formalin, and surface lung metastases were counted. To quantify the amount of total tumor burden in the formalin fixed lung tissue, genomic DNA was extracted (Gilbert et al., 2007) and assayed for the presence of human genomic material as described using QRT-PCR primers specific to human endogenous retrovirus-3 (ERV3) (Nitz et al., 2008; Thulke et al., 2003).

This study was carried out in strict accordance with recommendation from the Animal Care and Use Committee (ACUC) of the University of Virginia. The

protocol was approved by ACUC Number 3914. All experiments were terminated after 40 days at which time SQ tumors were less than 1.0 cm^3 in size, restricting tumor burden. All efforts were made to minimize pain and suffering.

Statistics

All data are presented as mean ± SD of three independent biological experiments. When two experimental groups were compared, values were log_2-transformed, and a one-tailed Student's *t* test in Microsoft Excel was performed. Differences were considered statistically significant when indicated by $p \leq 0.05$ (indicated by *), $p \leq 0.01$ (**), or $p \leq 0.005$ (***).

CHAPTER 3: CREATION OF A HUMAN CELL CULTURE MODEL FOR STUDYING EPITHELIAL-TO-MESENCHYMAL TRANSITION IN NON-SMALL CELL LUNG CANCER

INTRODUCTION

Cancer progression from carcinoma *in situ* to advanced metastatic disease is a multistep process mediated by carcinoma cell-activated stroma interactions, angiogenesis, and recruitment of pro-inflammatory cells (Cirri & Chiarugi, 2012; Korkaya, Liu, & Wicha, 2011). An emerging hypothesis proposes that this milieu of intercellular interactions, growth factors, and cytokines known as the tumor microenvironment, stimulates the epithelial-to-mesenchymal transition (EMT) within tumor cells (Fuxe & Karlsson, 2012; Thiery et al., 2009; Yang & Weinberg, 2008). EMT induces intracellular architecture remodeling and decreased cellular adhesion and polarization. Carcinoma cells that have undergone EMT are characteristically motile, invasive and highly metastatic. Over the past several years, EMT has also been recognized as a de-differentiation program attributed to generation of tumor-initiating or cancer-initiating cells (CICs) that possess self-renewing and multipotent characteristics (Floor et al., 2011; Mani et al., 2008; Morel et al., 2008; Scheel & Weinberg, 2012)

Although multiple cytokines and growth factors can induce EMT, one of the most potent and thoroughly studied factors is TGFβ (Fuxe & Karlsson, 2012; Heldin et al., 2012; Wendt et al., 2012; Zu et al., 2012). Stimulation of cells with TGFβ results in expression of the EMT master-switch transcription factors, *TWIST1*/*Twist*, *SNAI1*/*Snail*, *SNAI2*/*Slug*, and *ZEB2*/*SIP1*, that together differentially regulate genes to repress epithelial markers while promoting the mesenchymal phenotype (Heldin et al., 2012; Zu et al., 2012). TNF activates NF-κB to synergize with TGFβ to potentiate the transition (Asiedu et al., 2011;

Bates & Mercurio, 2003). A prevailing hypothesis in the field is that exposure of carcinoma cells to these soluble factors within the tumor microenvironment promotes EMT, de-differentiation, and the formation of CICs (Korkaya et al., 2011; Scheel et al., 2011; Thiery et al., 2009).

Although NF-κB has been associated with EMT (Chua et al., 2007; Huber et al., 2004) and CIC formation (Kendellen et al., 2013; Shostak & Chariot, 2011; Yamamoto et al., 2013) in breast cancer models, the role of this transcription factor in stimulating EMT and developing CICs in NSCLC has not been thoroughly examined. Here, using a three-dimensional (3D) cell culture model, we demonstrate that coordinated activation of TNF and TGFβ signaling cascades effectively induces EMT and the expression of genes related to de-differentiation and self-renewal. Further, we show that mesenchymal NSCLC cells possess constitutively active NF-κB, and that inhibition of NF-κB decreases EMT, CIC formation, and metastatic potential.

RESULTS

A model to study EMT in NSCLC

TNF has been shown to potentiate TGFβ-mediated EMT through the activation of co-stimulatory pathways (Asiedu et al., 2011; Bates & Mercurio, 2003; Câmara & Jarai, 2010; Kawata et al., 2012; Shintani et al., 2013; Takahashi et al., 2007). To confirm this observation in our 3D model, a time course was performed using both cytokines in tandem and alone. Multicellular spheroid cultures were created using a modified hanging droplet method (Kelm

et al., 2003). After two days, spheroids were suspended in polyHEMA-coated plates and treated every two days with the indicated cytokines to induce EMT (Figure 3A). Samples were collected from untreated (0 days) and cytokine-treated cultures (1-8 days). Epithelial (E-cadherin) and mesenchymal (N-cadherin and vimentin) markers were measured by immunoblot. Treatment with TNF resulted in a modest increase in N-cadherin but failed to show differences in other markers (Figure 3B). Consistent with the induction of EMT, TGFβ treatment resulted in a loss of E-cadherin expression and an increase in N-cadherin and vimentin. Moreover, co-stimulation with TNF and TGFβ yielded a more mesenchymal phenotype and persisted throughout the eight day time course (Figure 3B). Importantly, stimulation with TNF and TGFβ effectively induced EMT in multiple NSCLC cell lines within four days of treatment (Figure 3C). Based on results in Figure 3, we used the four day timeframe throughout our remaining experiments.

3D cultures undergo EMT more efficiently than 2D cultures

To determine whether 3D A549 cultures undergo EMT more efficiently than two-dimensional (2D) monolayer cultures, we measured expression of epithelial and mesenchymal markers in response to stimulation with TNF and TGFβ as described in Figure 3. Following cytokine treatment, 3D cultures show significant loss of *CDH1*/E-cadherin expression when compared to 2D cultures (Figure 4A). Moreover, the spheroids also possess increased expression of

A.

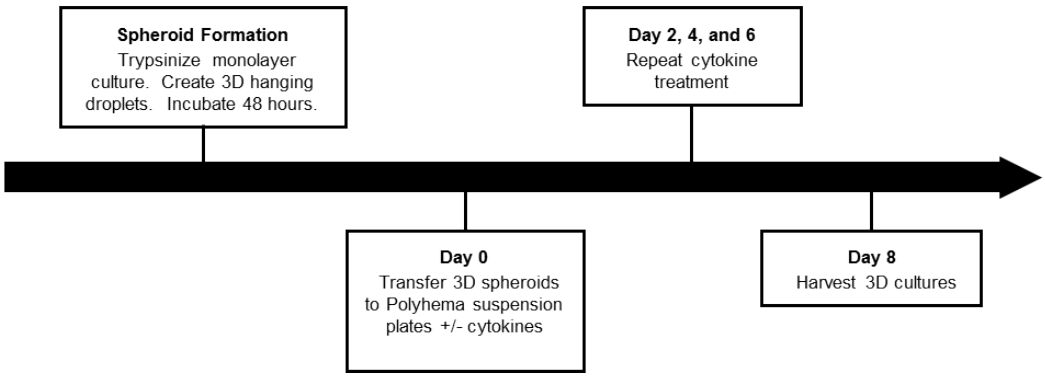
Spheroid Formation
Trypsinize monolayer culture. Create 3D hanging droplets. Incubate 48 hours.
Day 2, 4, and 6
Repeat cytokine treatment
Day 0
Transfer 3D spheroids to Polyhema suspension plates +/- cytokines
Day 8
Harvest 3D cultures

B.

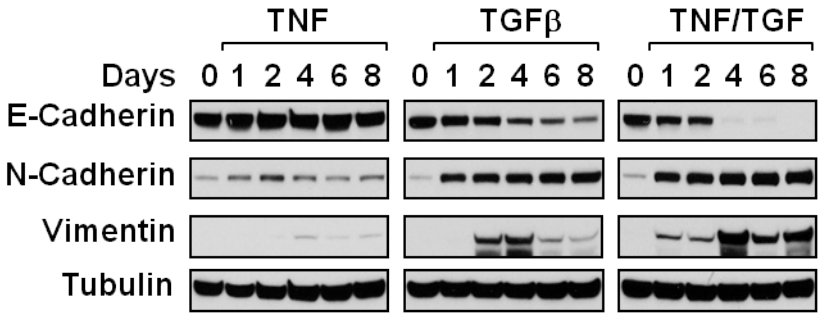
TNF
TGFβ
TNF/TGF
Days 0 1 2 4 6 8 0 1 2 4 6 8 0 1 2 4 6 8
E-Cadherin
N-Cadherin
Vimentin
Tubulin

C.

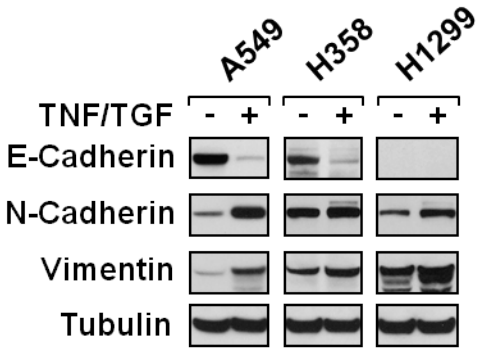
A549
H358
H1299
TNF/TGF - + - + - +
E-Cadherin
N-Cadherin
Vimentin
Tubulin

Figure 3: Establishing a three-dimensional multicellular culture model for EMT studies. (A) Schematic illustrating the protocol used to create a 3D mesenchymal cell population from confluent monolayers. **(B)** Spheroid cultures of A549 cells were treated with TNF, TGFβ, or both TNF and TGFβ every 48 hours for the indicated times. Immunoblot analysis measured changes in epithelial (E-cadherin) and mesenchymal (N-cadherin and vimentin) markers over an eight day time course. **(C)** 3D cultures of multiple NSCLC cell lines (A549, H358, H1299) were incubated for 96 hours in the absence or presence of TNF and TGFβ. Epithelial and mesenchymal markers were subsequently measured by immunoblot. Results from Figures 3B and 3C are representative examples from at least three independent experiments. Tubulin acts as a protein loading control. **Experiments conducted by Drs. Manish Kumar and Natalya Baranova.**

mesenchymal markers *VIM*/vimentin, *HMGA2 (*high-mobility group AT-hook 2), and the EMT master-switch transcription factors, *TWIST1*/*Twist*, *SNAI1/Snail*, *SNAI2/Slug* and *ZEB2/SIP1* (Figures 4A and 4B). Immunoblot analysis of spheroid cultures confirm that the differential mRNA expression resulted in a corresponding change in protein levels (Figure 4C). Results shown in Figures 3 and 4 illustrate significant EMT induction in 3D cultures as measured by changes in mesenchymal markers, EMT master-switch transcription factor expression, and cellular morphology.

Mesenchymal NSCLC cells are invasive and endogenously express genes known to promote self-renewal

Phenotypically, mesenchymal cells have high migration rates and secrete enzymes that degrade extracellular matrix to facilitate cellular invasion. Using *in vitro* transwell assays, we measured the migratory and invasive capabilities of A549 cells grown as either 2D or 3D cultures. Interestingly, untreated 3D spheroid cultures showed higher migration rates than 2D monolayer cultures (Figure 5A, left). However, treatment of 3D cultures with TNF and TGFβ further potentiated migration when compared to untreated 3D cultures. Spheroids treated with cytokines invaded through Matrigel more effectively than any other condition (Figure 5A, right). Additionally, cytokine-treated A549 spheroids displayed upregulated expression of *MMP9*, *LOX*, and *COL22A1* (collagen) (Figure 5B), genes known to potentiate invasion. These results demonstrate that culturing 3D spheroids in the presence of TNF and TGFβ establishes a highly

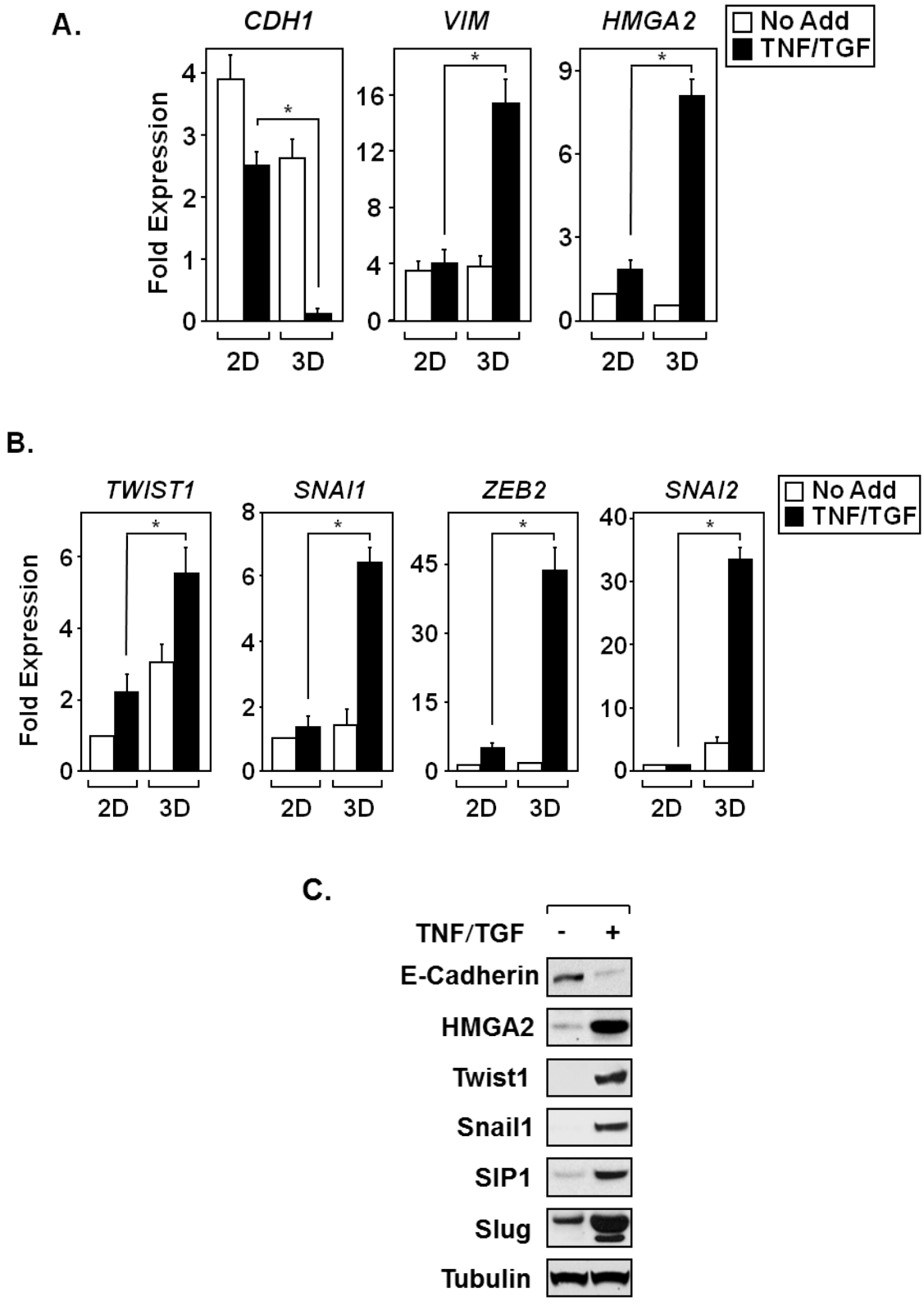
A.
CDH1
VIM
HMGA2
No Add
TNF/TGF
Fold Expression
2D
3D
B.
TWIST1
SNAI1
ZEB2
SNAI2
No Add
TNF/TGF
Fold Expression
2D
3D
C.
TNF/TGF
-
+
E-Cadherin
HMGA2
Twist1
Snail1
SIP1
Slug
Tubulin

Figure 4: Three-dimensional cultures show enhanced sensitivity to cytokine treatment. (A and B) Monolayer (2D) and 3D cultures of A549 cells were left alone (No Add) or treated with TNF and TGFβ (TNF/TGF) for 96 hours. Expression of epithelial markers (*CDH1*), mesenchymal markers (*VIM, HMGA2*), and EMT master-switch transcription factors (*TWIST1, SNAI1, ZEB2, SNAI2*) were measured by QRT-PCR. **(C)** Immunoblot analysis of 3D A549 cultures, left alone (No Add) or treated with TNF and TGFβ (TNF/TGF), was performed on E-cadherin, HMGA2, Twist1, Snail1, Sip1, Slug, and Tubulin. Results in Figure 4A and 4B were normalized to *GAPDH*, and are calculated mean ± SD. A one-tailed Student's *t* test in Microsoft Excel was performed to compare values; * indicates $p < 0.05$. N=3. Immunoblots in Figure 4C are representative examples from at least three independent experiments. **Experiments conducted by Drs. Manish Kumar and Natalya Baranova.**

invasive mesenchymal population. Finally, cytokine-treated spheroids showed endogenous upregulation of markers associated with dedifferentiation and maintenance of CICs (Chen et al., 2008; Leis et al., 2012; Levina et al., 2010; Takahashi et al., 2007), including *KLF4, SOX2, POU5F1/Oct4, MYCN*, and *KIT* (Figure 5C). Data shown in Figure 5 indicate that co-stimulation of spheroids with TNF and TGFβ promotes phenotypic changes in A549 cells that result in increased invasion and expression of gene products associated with stem-like properties.

Mesenchymal cells are highly metastatic and display cancer-initiating phenotypes

To examine whether induction of EMT promotes the development of CICs *in vivo*, we utilized a xenograft tumor model in nude mice. TNF- and TGFβ–treated 2D and 3D cultures were disaggregated, and cell suspensions were SQ injected into the right flank of nude mice. Forty days later, animals were sacrificed and SQ tumors were resected and weighed while the lungs were excised and scored for surface metastases. To our surprise, cells derived from TNF and TGFβ treated spheroids failed to produce SQ tumors (Figure 6A, left). However, examination of the lung surface in these mice revealed extensive metastasis (Figure 6A, right). The only plausible explanation for these results is that mesenchymal cells from 3D cultures invaded and metastasized to the lung without developing SQ tumors. Measuring the extent of metastasis under limiting cell dilution proves a reliable test for the presence of enriched CICs in epithelial-

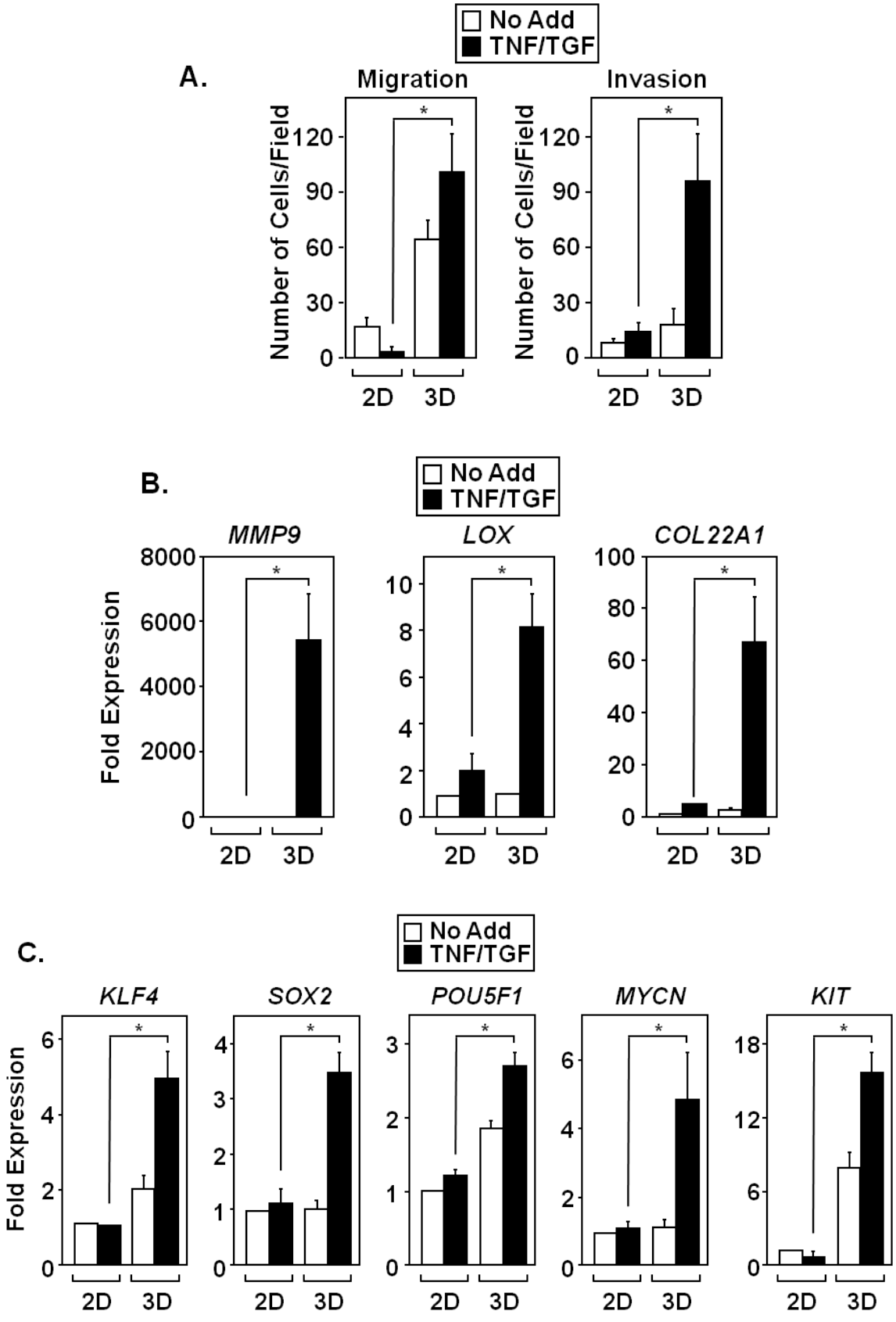
A.
No Add
TNF/TGF
Migration
Invasion
Number of Cells/Field
0
30
60
90
120
2D
3D
*
B.
No Add
TNF/TGF
MMP9
LOX
COL22A1
Fold Expression
0
2000
4000
6000
8000
0
2
4
6
8
10
0
20
40
60
80
100
2D
3D
*
C.
No Add
TNF/TGF
KLF4
SOX2
POU5F1
MYCN
KIT
Fold Expression
0
2
4
6
0
1
2
3
4
0
1
2
3
0
2
4
6
0
6
12
18
2D
3D
*

Figure 5: Efficient induction of EMT promotes invasion and the expression of genes required to maintain CICs. Monolayer and 3D A549 cultures were left alone (No Add) or treated with TNF and TGFβ (TNF/TGF) for 96 hours. **(A)** Cells were disaggregated and subsequently subjected to migration and invasion assays. **(B and C)** Expression of invasion (*MMP9, LOX, COL22A1*) and stem cell markers (*KLF4, SOX2, POU5F1, MYCN, and KIT*) was measured by QRT-PCR. Results in Figures 5 are calculated mean ± SD. A one-tailed Student's *t* test in Microsoft Excel was performed to compare values; * indicates $p < 0.05$. N=3. Results from 5B and 5C were normalized to *GAPDH*. **Experiments conducted by Drs. Manish Kumar and Natalya Baranova.**

derived tumors (Al-Hajj et al., 2003). Therefore, experiments were repeated using one thousand cells per SQ injection. Cell suspensions, derived from TNF and TGFβ treated spheroids, produced more surface lung metastases under limiting cell dilution than cytokine-treated monolayers or untreated 3D cultures (Figure 6B, left). Limiting cell dilution assays indicate that induction of EMT in 3D cultures produces a CIC population that effectively metastasizes to lung. As expected, analysis of DNA isolated from mouse lungs confirmed the presence of metastatic burden and verified that the lesions were of human origin (Figure 6B, right). We conclude from the experiments in Figure 6 that de-differentiation, CIC formation, and metastatic potential are all significantly enhanced in EMT-induced spheroid cultures.

Mesenchymal A549 cells produce soluble factors capable of inducing EMT

Results shown in Figures 3-6 demonstrate that TNF and TGFβ-stimulated NSCLC spheroid (3D) cultures effectively undergo EMT over a four day period. Since the half-life of recombinant cytokines is relatively short in growth media (Facoetti et al., 2010), we postulated that upon stimulation, A549 cells produce autocrine factors that maintain the mesenchymal state. To test the hypothesis that cytokine-treated spheroid cultures produce soluble factors capable of mediating EMT, we harvested conditioned media (CM) from 2D and 3D A549 cells that had been left alone or stimulated with cytokines. Naïve 3D (N3D) cultures were then incubated with CM for 96 hours, and EMT markers were measured by immunoblot. Supernatants obtained from cytokine-treated 3D

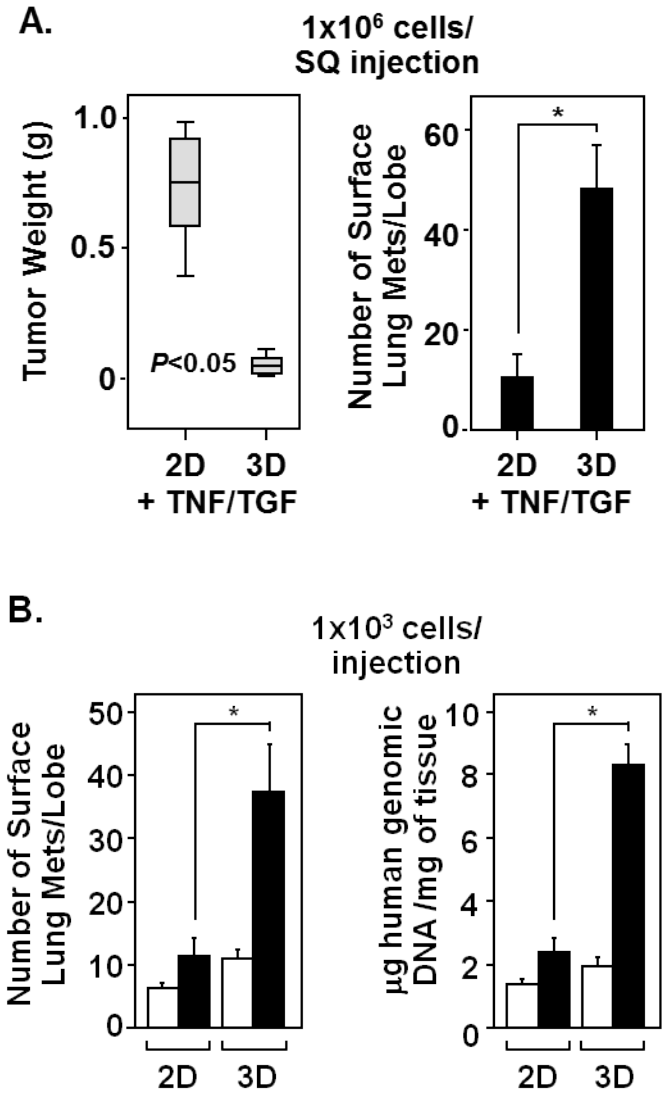
A.
1x10^6 cells/
SQ injection
Tumor Weight (g)
1.0
0.5
0
P<0.05
2D
3D
+ TNF/TGF
Number of Surface
Lung Mets/Lobe
60
40
20
0
*
2D
3D
+ TNF/TGF
B.
1x10^3 cells/
injection
Number of Surface
Lung Mets/Lobe
50
40
30
20
10
0
*
2D
3D
µg human genomic
DNA /mg of tissue
10
8
6
4
2
0
*
2D
3D

Figure 6: Cytokine-treated 3D cultures contain CICs with increased metastatic potential. (A) Monolayer and 3D A549 cultures were treated with TNF and TGFβ for 96 hours. Cells were disaggregated and SQ injected into nude mice (1×10^6 cells/animal). Forty days later, the primary SQ tumors were resected and weighed. Additionally, the lungs were excised and the number of surface metastases was determined. **(B)** Monolayer and 3D A549 cultures were either left untreated or treated with TNF and TGFβ. Limiting cell numbers (1×10^3/animal) were SQ injected into nude mice to evaluate the presence of CICs. Metastasis was evaluated by surface lung tumor count, and lung tumor burden was evaluated using genomic QRT-PCR to detect human DNA in total lung tissue. Weight and lung metastases data from Figure 6 are mean ± SD of five mice per condition. A one-tailed Student's *t* test in Microsoft Excel was performed to compare values; * indicates $p < 0.05$. N=3. Genomic QRT-PCR data from Figure 6B are normalized to total lung tissue (mg). **Experiments conducted by Dr. Manish Kumar.**

cultures effectively down-regulated E-cadherin while up-regulating N-cadherin and vimentin (Figure 7A). This effect was not due to residual TNF or TGFβ remaining in the culture media, as supernatant obtained from cytokine-treated 2D cultures was unable to elicit the same response. Production of autocrine factors required both TNF and TGFβ cytokines, since CM from spheroid cultures treated with TNF or TGFβ alone did not induce EMT in N3D cultures, as assayed by downregulation of E-cadherin and increased expression of N-cadherin and vimentin (Figure 7B). Results shown in Figures 7A and 7B indicate that 3D cultures treated with both TNF and TGFβ produce autocrine factors capable of inducing EMT in a paracrine-dependent manner in naïve 3D cultures.

Gene expression profiling of mesenchymal cultures identifies several NF-κB-governed candidate autocrine factors for potentiating CIC phenotypes

To identify potential autocrine factors responsible for inducing EMT, we performed microarray and bioinformatic analysis using a "top-down" approach. Microarray analysis performed on 2D and 3D A549 cultures either left alone or stimulated with TNF and TGFβ showed massive and reproducible changes in gene expression (Figure 7C). Microarray analysis identified 4064 differentially regulated genes specific to the 3D treated versus untreated cultures. Of these, 1351 genes showed increased expression upon stimulation. This 1351 gene list was then analyzed for overlap with a library of 1636 genes encoding secreted/extracellular proteins (Secreted Protein Database, SPD) (Chen et al., 2005). As illustrated in the Venn diagram in Figure 7D, a 128 gene overlap was

identified between differentially upregulated genes in cytokine-treated 3D cultures and the SPD library. Many of the genes in this overlap encode secreted protein ligands that are highly upregulated following the induction of EMT in 3D cultures (Table 2). Interestingly, a number of these genes are known NF-κB targets, including *GAL* (Toscano et al., 2011), *CSF2* (Li et al., 2013), *CCL5* (Werts et al., 2007), *PDGFB* (Au et al., 2005) *IL-11* (Yde et al., 2011) and *IL-1B* (Yde et al., 2011). Therefore, we hypothesized that NSCLC CICs display constitutive NF-κB activity, in part to sustain expression and secretion of autocrine factors essential for upkeep of their phenotype.

NF-κB is constitutively active in 3D cultures and is required for induction of EMT

TNF, a potent NF-κB activator, enhances induction of EMT in NSCLC cell lines, which corresponds with upregulation of several NF-κB target genes that encode secreted ligands. Therefore, we assessed whether EMT induction results in activation of NF-κB signaling by immunoblot. Interestingly, mesenchymal A549 spheroids displayed constitutive IKK activity as measured by phospho-specific antibodies that detect IκBα (pS32) and RelA (pS536) (Figure 8A). Changes in E-cadherin and vimentin levels confirmed efficient EMT in the cytokine-treated spheroids. Moreover, QRT-PCR experiments demonstrated increased expression of NF-κB-regulated genes *IL8* and *KDM6B/JMJD3* in mesenchymal 3D cultures (Figure 8B). Collectively, these data indicate that

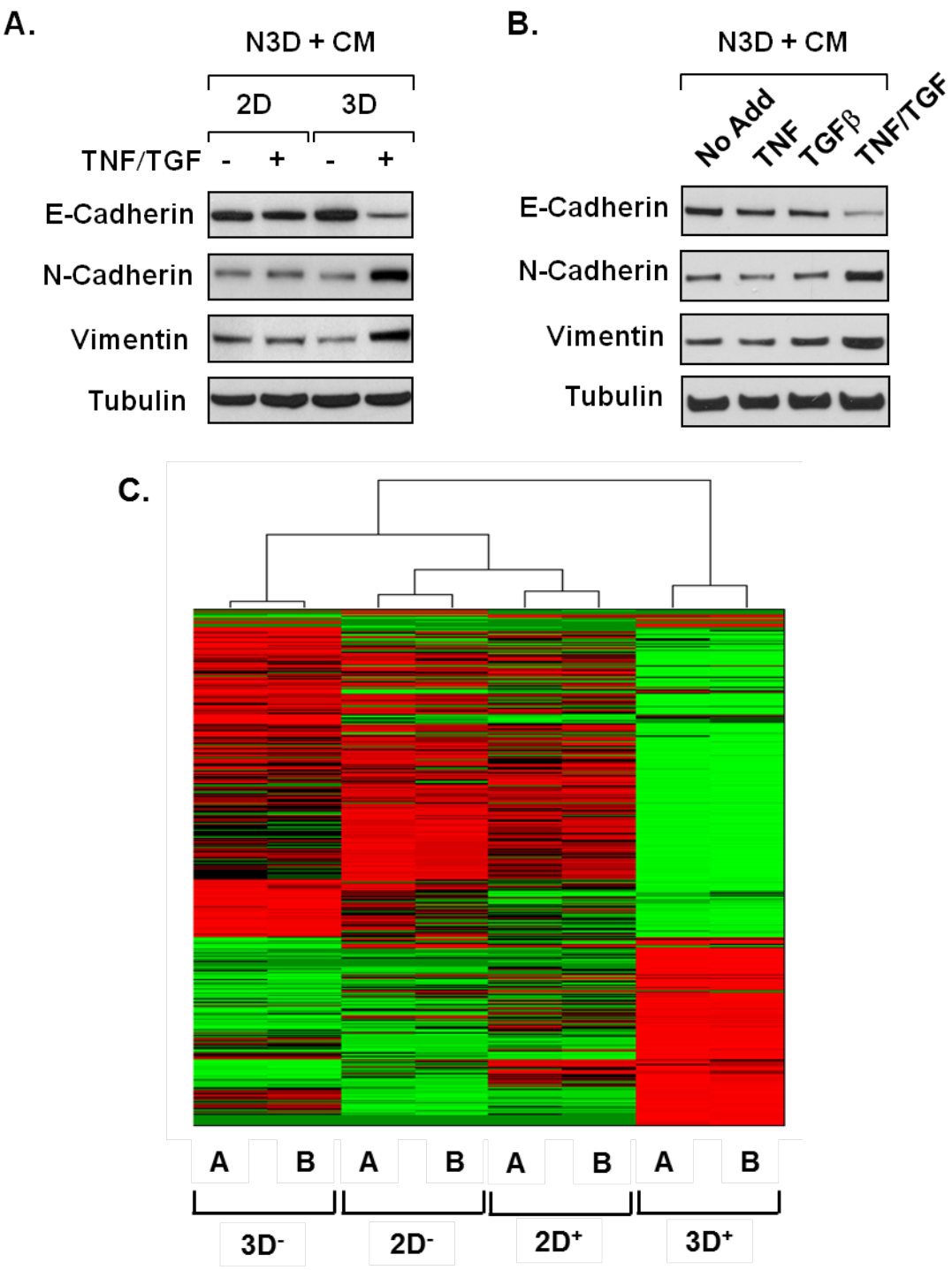
A.
N3D + CM
2D
3D
TNF/TGF - + - +
E-Cadherin
N-Cadherin
Vimentin
Tubulin
B.
N3D + CM
No Add
TNF
TGFβ
TNF/TGF
E-Cadherin
N-Cadherin
Vimentin
Tubulin
C.
A B A B A B A B
3D⁻ 2D⁻ 2D⁺ 3D⁺

D.

Figure 7: Mesenchymal A549 cells produce paracrine factors capable of inducing EMT in naïve 3D cultures. (A) Naïve 3D (N3D) cultures were incubated with conditioned media (CM) harvested from 2D or 3D cultures left untreated (-) or stimulated (+) with TNF and TGFβ. Immunoblot analysis measured changes in epithelial and mesenchymal markers. Tubulin served as a protein loading control. **(B)** Immunoblots confirm that CM harvested from 3D cultures stimulated with both TNF and TGFβ effectively induced changes in mesenchymal markers, compared to CM from 3D cultures left alone (No Add), or those stimulated with TNF or TGFβ alone. Data in Figures 7A and 7B are representative examples from at least three independent experiments. **(C)** All differentially expressed genes (4064) between untreated (-) and TNF and TGFβ stimulated (+) 2D and 3D cultures were organized and visualized by two-way cluster (gene and sample) using MATLAB clustergram. Upregulated and downregulated genes are represented in the heat map in red and green, respectively. Duplicate array results (A and B) for of each condition clustered together and display similar expression profiles, indicating strong reproducibility of the data. Gene expression patterns indicate that arrays from $2D^-$, $2D^+$, and $3D^-$ cluster together, but gene expression profiles in $3D^+$ profile are unique. These results indicate that the changes between $3D^-$ and $3D^+$ and display the greatest change in differential gene expression. **(D)** Venn diagram indicating the 128 gene overlap (orange) between the 1636 genes from the Secreted Protein Database (SPD, red), and the 1351 unique genes that are upregulated in 3D treated cultures (yellow, 5% FDR threshold was applied). **The experiments in**

Figure 7B were conducted by Dr. Manish Kumar. Bioinformatic analysis was conducted by Drs. Xiaoxiang Xiu and Stephen Hoang.

TABLE 2: Most Upregulated Genes Encoding Secreted Ligands Following Cytokine Stimulation in 3D

Rank	Symbol	GenBank	FC ($3D^- \rightarrow 3D^+$)
1	*GAL*	NM_015973.3	220
2	*CSF2*	NM_000758.3	201
3	*INHBA*	NM_002192.2	160
4	*PDGFB*	NM_002608.2	111
5	*CCL5*	NM_002985.2	100
6	*IL11*	NM_000641.3	98
7	*BMP6*	NM_001718.4	58
8	*PTHLH*	NM_002820.2	41
9	*EDIL3*	NM_005711.3	40
10	*CRLF1*	NM_004750.4	15
11	*CYR61*	NM_001554.4	15
12	*CSF3*	NM_000759.3	14
13	*IL8*	NM_000584.3	5
14	*PDGFA*	NM_002607.5	4
15	*CCL2*	NM_002982.3	4

Table 2: Mesenchymal NSCLC significantly upregulate secreted ligands, several of which are transcriptionally governed by NF-κB. Microarray and bioinformatic analysis identified 128 genes that belong to the Secreted Protein Database and that are significantly upregulated in 3D cultures following TNF and TGFβ treatment. Of these, the 15 most upregulated genes that encode secreted ligands are shown. The FDR-adjusted *p*-values for the fold induction were ≤0.05.

cytokine-treatment of 3D A549 cultures results in the increased phosphorylation of IKK-regulated substrates and constitutive NF-κB transcriptional activation.

To determine the importance of NF-κB activity during induction of EMT in NSCLC cell lines, stable clonal pools expressing the super-repressor IκBα (SR-IκBα) were generated. The SR-IκBα is resistant to proteasomal degradation, consequently sequestering NF-κB in the cytosol. Cells expressing the SR-IκBα protein therefore display an inhibition of NF-κB-mediated transcription (Mayo et al., 1997). Figure 8C (top) confirms expression of Flag-tagged SR-IκBα in A549 stable cells (A549.I) compared to empty vector control cells (A549.V). Furthermore, nuclear protein extracts from A549.I spheroid cultures, treated with TNF and TGFβ, lacked NF-κB DNA binding activity as compared to A549.V extracts (Figure 8C, bottom). QRT-PCR assays show repressed cytokine-mediated induction of *IL8* and *BIRC3/cIAP-2* in A549.I cells when compared to control cells A549.V (Figure 8D). These data verify that SR-IκBα expression in the A549.I cell line effectively blocks NF-κB transcriptional activity.

Characterization of NF-κB in potentiating the mesenchymal phenotype

NF-κB has been shown to regulate the expression of EMT master-switch transcription factors in multiple model systems (Allison et al., 2012; Barberà et al., 2004; Chua et al., 2007; Julien et al., 2007), and NF-κB governs several candidate autocrine maintenance factors identified by microarray analysis. Therefore, we hypothesized that inhibition of NF-κB activity in the A549.I cell line would dampen EMT induction. Immunoblot analysis confirmed that A549.I cells

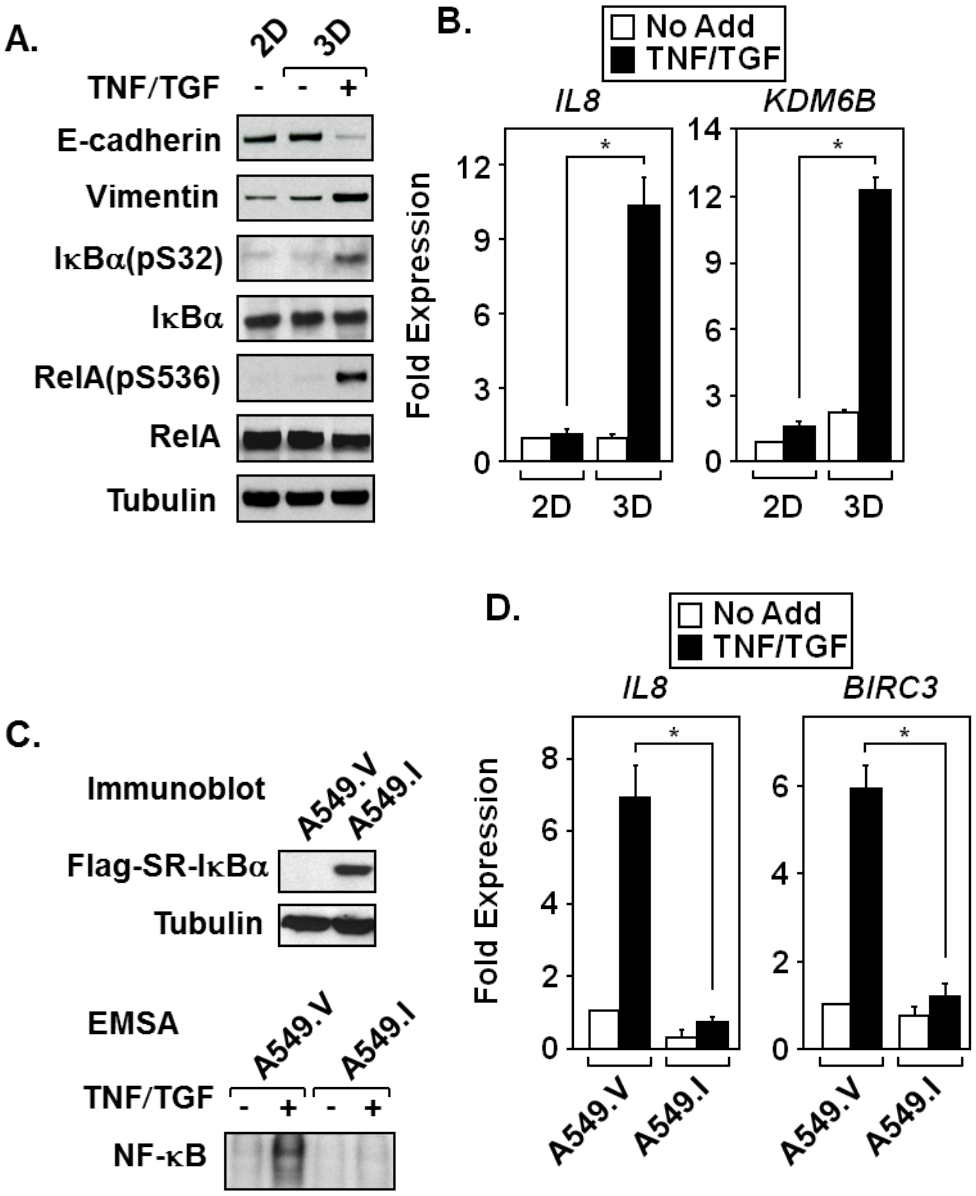
A.
2D
3D
TNF/TGF
- - +
E-cadherin
Vimentin
IκBα(pS32)
IκBα
RelA(pS536)
RelA
Tubulin
B.
No Add
TNF/TGF
IL8
KDM6B
Fold Expression
0
3
6
9
12
14
2D
3D
C.
Immunoblot
A549.V
A549.I
Flag-SR-IκBα
Tubulin
EMSA
TNF/TGF
- + - +
NF-κB
D.
No Add
TNF/TGF
IL8
BIRC3
Fold Expression
0
2
4
6
8
A549.V
A549.I

Figure 8: Mesenchymal cells display constitutive NF-κB activity. Monolayer and 3D cultures of A549 cells were incubated with cytokines for 96 hours. **(A)** Mesenchymal A549 cells display constitutive NF-κB activated pathways, as determined using phospho-specific antibodies to IκBα and RelA. **(B)** Untreated and TNF and TGFβ stimulated 2D and 3D cultures of A549 cells were harvested and analyzed for expression of NF-κB regulated genes by QRT-PCR. **(C and D)** Three-dimensional cultures of A549.V (vector control) and A549.I (SR-IκB) were incubated for 96 hours in the absence or presence of TNF and TGFβ. **(C)** Immunoblots confirm the expression of the Flag-tagged SR-IκB in the A549.I line, which successfully blocked nuclear translocation and DNA binding, as measured by EMSA. **(D)** QRT-PCR confirmed the inability of A549.I cell to upregulate NF-κB-regulated genes following TNF and TGFβ treatment. Immunoblots in Figure 8A are a representative example from three independent experiments. Results in Figure 8B and 8D are calculated mean ± SD. A one-tailed Student's *t* test in Microsoft Excel was performed to compare values; * indicates $p < 0.05$. N=3. Values in Figures 8B and 8D were normalized to *GAPDH*. **Experiments conducted by Dr. Manish Kumar.**

fail to downregulate E-cadherin expression or upregulate mesenchymal markers (vimentin and N-cadherin) compared to control cells (Figure 9A). Moreover, cytokine-treated A549.I cells showed only minimal upregulation of *TWIST1*, *ZEB2,* and *SNAI2* gene expression following TNF and TGFβ treatment (Figure 9B). These results indicate that NF-κB is required to upregulate *TWIST1*, *ZEB2* and *SNAI2,* while expression of *SNAI1* appears independent of NF-κB-dependent transcription in the A549.I cell line. These results suggest that the expression of critical EMT master-switch transcription factors requires NF-κB activity.

Next, we assessed whether NSCLC required NF-κB for invasion using transwell assays. Inhibiting NF-κB activity in A549 (A549.I) cells abolished invasion through Matrigel when compared to the control lines (Figure 9C). Because data shown in Figure 8 indicate that NF-κB is required for NSCLC to undergo EMT, we tested the A549.V and A549.I cell lines for their ability to metastasize to lung using a nude mouse model. As expected, cytokine-treated A549.I cells failed to form lung metastases (Figure 9D, left). The inability of these cells to metastasize to lung was not due to a loss of cell viability or an inability to form primary tumors, since untreated A549.I formed SQ tumors with similar growth rates as A549.V cells (Figure 9D, right). Thus, data shown in Figure 9 indicates that TNF and TGFβ treated 3D NSCLC cultures require NF-κB to upregulate master-switch transcription factors, induce EMT, and promote invasive properties. Moreover, without NF-κB transcriptional activity, A549 cells lose their ability to metastasize to lung without impacting primary tumor growth.

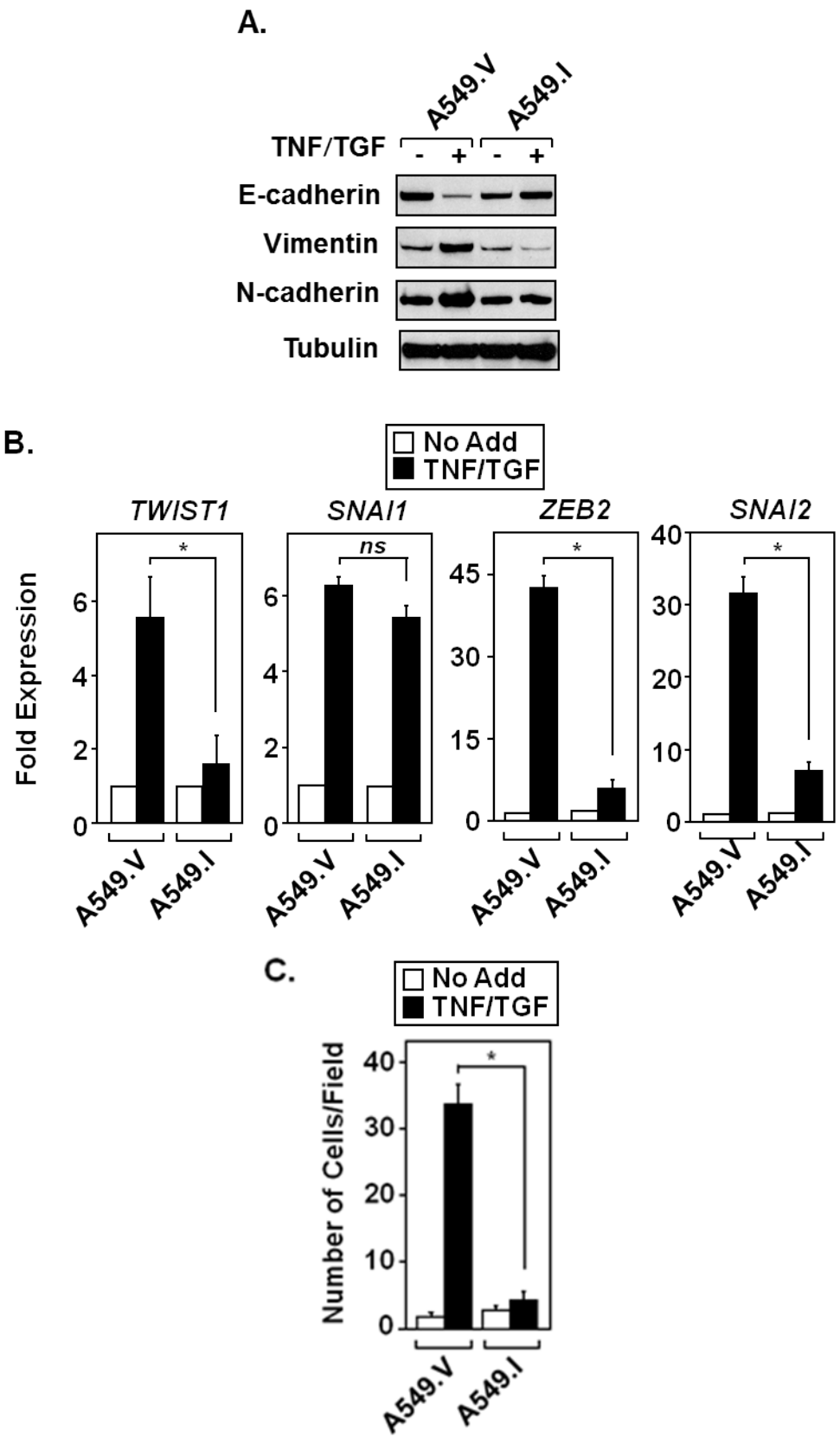
A.
A549.V
A549.I
TNF/TGF
- + - +
E-cadherin
Vimentin
N-cadherin
Tubulin
B.
No Add
TNF/TGF
TWIST1
SNAI1
ZEB2
SNAI2
Fold Expression
*
ns
*
*
0
2
4
6
0
15
30
45
0
10
20
30
40
A549.V
A549.I
C.
No Add
TNF/TGF
Number of Cells/Field
*
0
10
20
30
40
A549.V
A549.I

D.

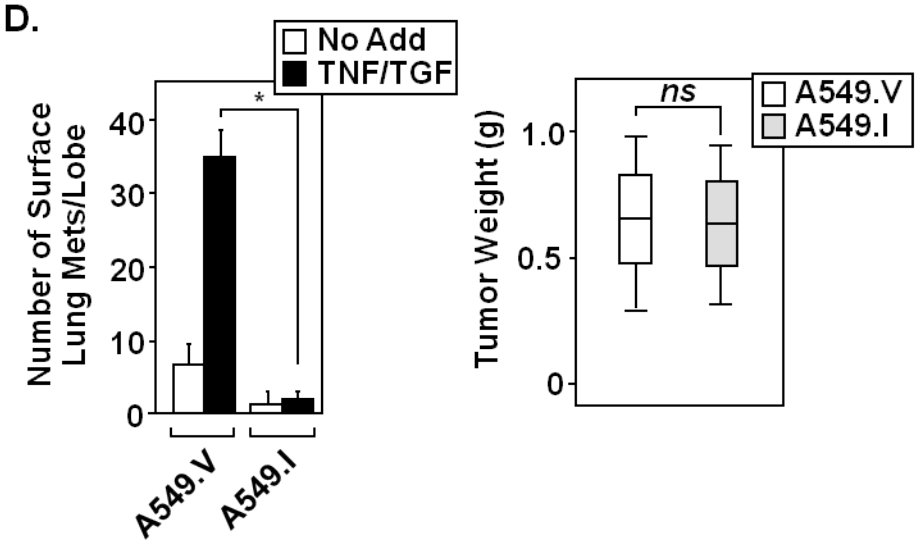
No Add
TNF/TGF
Number of Surface Lung Mets/Lobe
40
30
20
10
0
*
A549.V
A549.I
Tumor Weight (g)
1.0
0.5
0
ns
A549.V
A549.I

Figure 9: NF-κB is required for the maintenance of CICs and lung metastasis. **(A)** A549.I cells fail to show changes in mesenchymal markers, as determined by immunoblot analysis. **(B)** NF-κB is required to upregulate mRNA expression of master-switch transcription factors. **(C)** A549 spheroid cultures, expressing empty vector or the Flag-IκB super-repressor, were left alone (No Add) or treated with TNF and TGFβ (TNF/TGF) for 96 hours. The cells were disaggregated and subjected to invasion assays. **(D)** A549.V and A549.I 3D cultures were left alone (No Add) or treated with TNF and TGFβ (TNF/TGF) for 96 hours. The cells were disaggregated and SQ injected into nude mice (1 x 10^6/animal). Forty days later, animals were sacrificed, and the number of surface lung metastases was determined. In addition, SQ tumors were excised and wet tumor weight was determined. Data presented in Figure 9 are mean ± SD. A one-tailed Student's *t* test in Microsoft Excel was performed to compare values; * indicates $p < 0.05$. Tests indicating $p > 0.05$ were considered not significant (*ns*). Data in Figure 9B were normalized to *GAPDH* expression. **Experiments conducted by Dr. Manish Kumar.**

DISCUSSION

NF-κB regulates EMT to potentiate metastatic progression of NSCLC

We implemented a simple and relatively quick 3D culture system to examine the importance of NF-κB signaling during EMT induction and CIC propagation within NSCLC cell lines. In response to TNF and TGFβ exposure, A549 spheroid cultures displayed a loss of E-cadherin and elevated expression of mesenchymal markers, N-cadherin and vimentin. The increased expression of mesenchymal protein markers likely occurs due to induction of the EMT master-switch transcription factors, *TWIST1*, *SNAI1*, *SNAI2*, and *ZEB2*. Furthermore, spheroid populations of mesenchymal A549 cells show elevated expression of endogenous transcription factors known to potentiate dedifferentiation, including *KLF4*, *SOX2*, *POU5F1*, *MYCN* and *KIT*.

Interestingly, mesenchymal A549 cells from spheroid cultures formed no primary SQ tumors in nude mice, but rather extravasated into the circulatory system to metastasize to the lung. In contrast, cells from untreated A549 spheroid populations formed SQ tumors at the injection site while producing significantly fewer lung metastases. We further demonstrated that EMT-induced A549 3D cultures effectively metastasize to lung under limiting cell dilutions, confirming the presence of an enriched “stem-like” CIC population.

Since IKK and NF-κB pathways have been linked to EMT and development of CICs (Barberà et al., 2004; Chua et al., 2007; Huber et al., 2004; Julien et al., 2007; Pham et al., 2007; Wu et al., 2009), we examined whether mesenchymal A549 cells upregulate NF-κB transcriptional activity. Surprisingly,

EMT-induced spheroid A549 cultures displayed chronic IKK activity as measured by phosphorylation of IκBα (pS32) and RelA (pS536), and by constitutive expression of *IL8* and *KDM6B* transcripts.

Moreover, cytokine-treated spheroid A549 cultures maintained the activation of IKK signaling pathways well beyond the half-life of the TNF and TGFβ cytokines added to the culture media. These results suggest that mesenchymal A549 spheroid cultures must produce autocrine factors capable of maintaining the EMT phenotype. Importantly, constitutive NF-κB activity proves essential for effective EMT partially through its ability to upregulate the master-switch transcription factors *TWIST1*, *ZEB2,* and *SNAI2*. As a result, the loss of NF-κB activity prohibited cytokine-treated spheroid A549 cells from becoming invasive and also abolished lung metastasis in the mouse xenograft model. This work firmly establishes a role for NF-κB in the induction of EMT and for the development of NSCLC CICs that promote metastasis. As a number of secreted ligands that are downstream of NF-κB are upregulated following EMT in our model system (Table 2), it would be particularly interesting to see which, if any, of these soluble factors can act in an autocrine manner to potentiate CIC phenotypes.

Other experiments to support the enrichment of CICs in cytokine-treated spheroid cultures

The gold standard for demonstrating cancer-initiating cell characteristics is the ability for a pool of cells to form tumors in nude mice under limiting dilution.

Our laboratory effectively demonstrated that A549 spheroid cultures treated with cytokines are enriched for CICs, as similar numbers of lung metastases were found in mice injected with either a million or a thousand cells (Figure 6). However, several other experiments could be conducted to further confirm CIC enrichment within cytokine-treated A549 3D cultures. First, we hypothesize that cytokine-treated NSCLC spheroid cultures are inherently more resistant to chemoradiotherapy (CRT). We could test this hypothesis by treating spheroid cultures with cytokines or leaving them untreated, dissociating them, replating the cells as a monolayer, and exposing them to cytotoxic drugs or radiation. Demonstration of reduced levels of apoptosis in TNF/TGFβ-treated cells in response to CRT would support this hypothesis. *ABCG1*, a gene encoding an ABC transporter that functions as a drug pump, is upregulated ~5-fold in spheroid cultures following cytokine treatment. It would be interesting to expose these cells to Hoescht 33342 and see if they extrude this dye at higher rates than cells from untreated spheroid cultures, another hallmark of CICs.

Sorting cytokine-treated spheroid cultures by flow cytometry for cell surface antigens commonly expressed on NSCLC CICs would enable quantification and isolation of the CIC pool within the mixed population. The two most common surface antigens found in NSCLC CICs are CD133 (Eramo et al., 2008) and CD44 (Leung et al., 2010). According to microarray analysis, *CD133* is not upregulated following cytokine treatment of A549 spheroid cultures. However, *CD44* is induced greater than two-fold following stimulation of 3D cultures (data not shown). First, this upregulation would require confirmation by

QRT-PCR and potentially immunoblot. As dissociating the spheroid cultures with trypsin would likely cleave membrane-tethered CD44, an antibody recognizing an epitope found within the intracellular CD44 domain would be required. Following confirmation of *CD44* induction after TNF and TGFβ treatment, we could sort the dissociated spheroid cultures by CD44 expression and perform various assays on the $CD44^+$ and $CD44^-$ pools of cells. We hypothesize that cells expressing CD44 would demonstrate increased resistance to chemoradiotherapy, display elevated levels of genes associated with multipotency, and possess increased capacities for tumorigenicity.

Cytokine-treated NSCLC spheroid cultures as a model for bone metastasis

Tumor-related bone disease, caused by metastasis of solid tumors such as breast, prostate, and lung, or by multiple myeloma, sharply decreases quality of life while increasing morbidity and mortality. NSCLC patients presenting with bone metastases have a median survival of less than six months (Al Husaini, Wheatley-Price, Clemons, & Shepherd, 2009). An estimated 30 to 40% of patients with advanced lung cancer will develop bone metastases throughout the course of their disease. Therefore, efforts have been made to 1) identify key factors governing bone metastasis and 2) model bone metastasis *in vivo*.

Under physiological conditions, bone homeostasis is maintained by two types of cells, osteoblasts and osteoclasts. Osteoblasts (OB) deposit bone by synthesizing very dense collagen as well as other proteins in smaller amounts that are then crosslinked to form the organic component of bone. Osteoclasts

(OC) promote bone resorption, also referred to as osteolysis. These processes are tightly regulated to ensure that the appropriate amount of bone tissue is maintained over the lifespan of an organism. During metastasis of NSCLC cells to bone, deregulation of this balance occurs, resulting in enhanced osteolysis by OCs (bone resorption) and repressed bone deposition. Bone metastasis is mediated by interactions between the NSCLC cells and the bone microenvironment. Soluble factors secreted by the tumor cells are essential for this process (Al Husaini et al., 2009). Several genes encoding known promoters of bone metastasis, *PTHLH, IL-11,* and *IL-8*, were identified as being highly upregulated only in 3D A549 cultures following cytokine treatment (Table 2).

Recently, Kuo et al. showed that miR-33a inhibits metastasis of A549 cells to bone by directly targeting mRNA encoding *PTHLH*, which encodes parathyroid hormone-related protein (PTHrP), a protein known to stimulate OC activity (Kuo et al., 2013). Deng and colleagues examined gene expression changes in cultured human lung squamous carcinoma cells with or without culturing in the presence of neonatal mouse calvaria (skulls). Interestingly, one of the most upregulated genes was *PTHLH*. Silencing of *PTHLH* in the lung squamous carcinoma cells attenuated their ability to invade *in vitro* (Deng et al., 2007). Another group demonstrated the indispensability of PTHrP in forming bone metastases by SCLC cells using a PTHrP neutralizing antibody. Interestingly, the authors showed that this protein's role in promoting metastasis is unique to the bone, as the neutralizing antibody failed to block metastasis to other organs, including lung, liver, kidney, and lymph node (Miki et al., 2004). A similar role

has been demonstrated for PTHrP in breast cancer metastases specifically to bone, not soft tissues (Guise et al., 1996). Of genes specifically upregulated in 3D cultures following cytokine treatment that encode secreted ligands, *PTHLH* is the eighth-most induced gene. This suggests that cells within our cytokine-treated A549 spheroid cultures may have a predilection to metastasize to bone.

A number of studies have shown a role for interleukin-8 (IL-8) in stimulating creation of osteoclasts and subsequent bone resportion (Bendre et al., 2003, 2005). Importantly, this phenomenon has been demonstrated not only in metastatic breast cancer cells but also in A549 cells. Conditioned media from A549 cells stimulated osteoclast formation, but this process was reduced by 60% by pre-incubating the conditioned media with an IL-8 neutralizing antibody (Bendre et al., 2005). A role for IL-8 in promoting bone metastases derived from breast cancer cells has also been established (Singh et al., 2006). *IL8* is the fourteenth-most upregulated gene following cytokine treatment that encodes a secreted ligand (Table 2). Moreover, the product of the fifth-most upregulated gene in Table 2, IL-11, promotes bone metastasis in both breast and prostate cancer (Kingsley et al., 2007).

The strong upregulation of these soluble factors that have been implicated in promoting bone metastasis, selectively in 3D cultures following cytokine treatment, suggest that stimulated A549 spheroid cultures are enriched for CICs that are primed to metastasize to bone. This hypothesis is strengthened by the multitude of data that this chapter presents supporting the migratory, invasive, self-renewing, and metastatic phenotypes of these mesenchymal A549 cells.

Unfortunately, we did not look at bone metastasis in the mice used in these experiments. It would be fascinating to repeat the A549 xenograft experiments outlined in Figure 6 and look for bone metastases in mice injected with treated versus untreated cells. Moreover, these experiments could be repeated with or without injection with neutralizing antibodies for PTHRP, IL-11, and IL-8. If administration of these antibodies were to yield decreases in number and/or size of bone metastases, as well as increases in bone mineral density, these findings would specifically implicate these factors in promoting NSCLC bone metastasis. Confirmation of upregulation of these targets following cytokine treatment in spheroid cultures formed with other NSCLC cell lines, including H460 (squamous cell) and H1299 (large cell), would inspire confidence that EMT is a method by which CICs primed to metastasize to bone can be generated. Xenograft experiments using these other NSCLC cell lines would confirm this hypothesis.

Chapter Acknowledgements

This chapter was adapted from a manuscript entitled “NF-κB regulates mesenchymal transition for the induction of non-small cell lung cancer initiating cells.” The authors of this manuscript include Manish Kumar, David Allison, Stephen Hoang, Natalya Baranova, J. Jacob Wamsley, Adam Katz, Stefan Bekiranov, David Jones, and Marty Mayo.

CHAPTER 4: NF-κB-MEDIATED UPREGULATION OF *INHBA/ACTIVIN A* IS REQUIRED FOR MAINTENANCE OF NON-SMALL CELL LUNG CANCER-INITIATING PHENOTYPES

INTRODUCTION

Activins are pleiotropic growth factors and morphogens in the TGFβ superfamily

The TGFβ superfamily consists of over forty structurally related ligands that regulate diverse cellular processes such as proliferation, differentiation, migration, and invasion. Activins and Inhibins comprise a subset of this superfamily. They are comprised of dimers of Inhibin α or Inhibin β subunits linked by a single disulfide bond. Five β subunits (βA-βE) and one α subunit have been identified. β subunits can homodimerize or heterodimerize to produce Activins. Three different forms of bioactive Activin have been purified and characterized: Activins A and B, homodimers of the βA and βB subunits, and Activin AB, a heterodimer of the βA and βB subunits. The βC, βD, and βE subunits are far less characterized. βD has only been identified in *Xenopus laevis* (Oda et al., 1995), and βC and βE polypeptides appear to be restricted to the liver (Fang et al., 1996; Hotten et al., 1995). Since Activin A is the most abundant and best-studied Activin variant, and little is known about Activins B and AB, we will refer to Activin A as Activin throughout the remainder of the introduction. Inhibin β subunits can also heterodimerize with the α subunit to produce Inhibins, natural antagonists of Activins.

Activin and Inhibin were initially identified in 1978 as reproductive hormones governing the hypothalamic-pituitary-gonadal axis. Activin was shown to promote follicle-stimulating hormone (FSH) release from cultured gonadotropes (Ling et al., 1986; Lorenzen, et al., 1978), whereas Inhibin blocked

FSH secretion. However, these ligands are now known to regulate a plethora of cellular processes, including differentiation, proliferation, pluripotency, and apoptosis. Like other TGFβ superfamily members, Activin exerts its effects through two transmembrane receptors with intracellular serine/threonine kinase activity. Mature ligands initiate signaling by binding one of two type II receptors, ActRIIA or ActRIIB, stimulating its kinase activity. The active type II receptor then binds and phosphorylates the type I receptor, Alk4. Next, Alk4 phosphorylates either SMAD2 or SMAD3, which subsequently binds SMAD4. This competent heterodimeric transcription factor then translocates to the nucleus to govern Activin target gene expression. In addition to this canonical SMAD signaling pathway, Activin can also exert its effects through activating mitogen-activated protein kinase (MAPK) pathways, including extracellular-signal-regulated kinase (ERK), p38 (MAPK14) and c-Jun N-terminal kinases (JNK) (Antsiferova & Werner, 2012).

Both soluble and membrane-bound Activin antagonists exist. Inhibins compete with Activin to bind ActRIIA or ActRIIB. However, no type I receptor has been identified for Inhibin, so it inhibits Activin signaling by sequestering type II receptors following its binding to the membrane protein betaglycan/TGFBR3. Two secreted glycoproteins, follistatin and follistatin-like protein 3, bind Activin dimers and block the domains required for interaction with the type II receptors. Membrane proteins cripto and BAMBI also can interfere with access of Activin to its receptors (Wakefield & Hill, 2013).

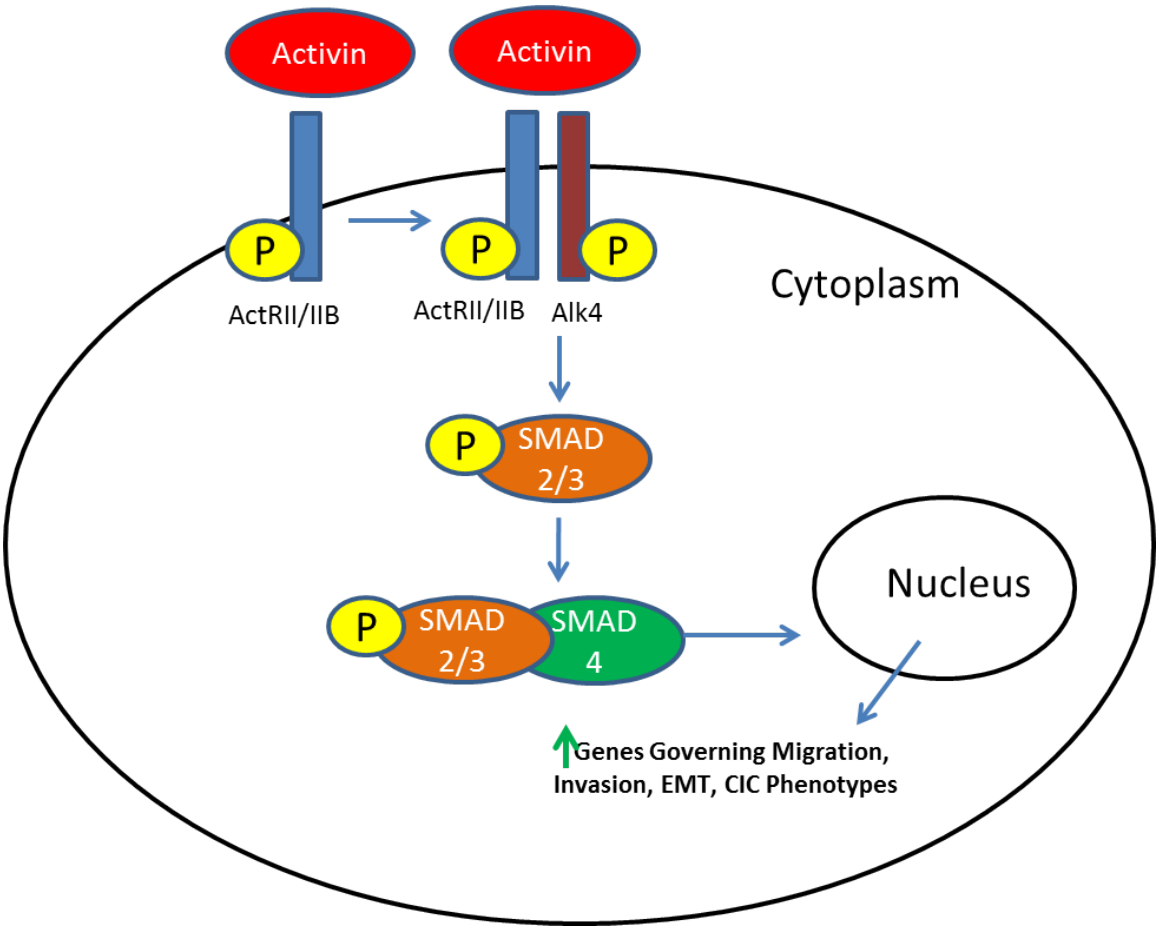
Activin
Activin
P
P
P
ActRII/IIB
ActRII/IIB
Alk4
Cytoplasm
P
SMAD
2/3
Nucleus
P
SMAD
2/3
SMAD
4
Genes Governing Migration,
Invasion, EMT, CIC Phenotypes

Figure 10: Canonical Activin Signaling. Activin (red) initiates the signaling cascade by binding its type II receptor (blue) and activating its kinase activity. Active ActRII or ActRIIB binds and phosphorylates Alk4 (purple), stimulating its kinase activity. Alk4 then phosphorylates one of two regulatory SMADs (R-SMADs), SMAD2 or SMAD3 (orange). Phosphorylated SMAD2/3 then bind the co-SMAD, SMAD4 (green), to form a transcriptionally competent heterodimer that translocates to the nucleus and binds Activin target genes.

Activin governs self-renewal and other stem cell characteristics

Human embryonic stem cells (hESCs) are capable of self-renewal as well as differentiation into a multitude of somatic cell types from each of the three primary germ layers, ectoderm, endoderm, and mesoderm. When cultured *in vitro*, hESCs mimic the differentiation process that occurs *in vivo*. These characteristics make them valuable tools for studying mechanisms controlling differentiation and development. Moreover, hESCs could potentially be used in clinical transplants to promote tissue regeneration (Passier & Mummery, 2003). However, maintenance of their self-renewing and pluripotent statuses *in vitro* requires growth on a mouse embryonic feeder (mEF) layer that secretes soluble factors into the media. A chief concern is that contaminants from mEF feeder layers could render the cells unsuitable for transplant. To solve this problem, researchers have focused efforts to identifying the soluble factors required for maintaining pluripotency (Vazin & Freed, 2010).

A number of studies have demonstrated sufficiency, to a degree, of Activin in maintaining pluripotency of hESCs. In the absence of mEF feeder layers, Activin was sufficient to maintain pluripotency, as assayed by levels of Oct4 and Nanog and the ability to form teratomas in mice. However, the addition of nicotinamide and keratinocyte growth factor (KGF) was required to support continued proliferation and growth in addition to pluripotency. Conversely, culturing hESC with follistatin on a mEF feeder layer precipitated differentiation, indicating that mEF-secreted Activin is necessary for maintaining stem-like properties in hESC (Beattie et al., 2005). A similar study found that Activin can

maintain self-renewal of hESC in a feeder-free culture, as determined by levels of Oct4, Nanog, bFGF, and Nodal, as well as the ability to form teratomas (Xiao, Yuan, & Sharkis, 2006). Interestingly, Activin maintains multipotency of mesenchymal stem cells derived from several different organs by upregulating Sox2, and Activin levels decrease rapidly following differentiation (Djouad et al., 2010).

Controversy regarding the required destruction of live embryos to obtain human embryonic stem cells has generated interest in developing other model systems for pluripotency. Human induced pluripotent stem cells (hiPSC) are generated from adult fibroblasts by "forcing" the expression of four transcription factors essential in governing pluripotency, Oct3/4, Sox2, Klf4, and c-Myc (Takahashi et al., 2007). As with hESC, feeder-free culture of these artificial human stem cells is essential for their clinical applications, including transplantation, to avoid contamination with proteins from other species. Since human iPS cells resemble hESC in cell surface antigens, proliferation rates, morphology, gene expression, and pluripotent phenotype, it follows that human iPS cells also require Activin to maintain pluripotency in the absence of a feeder layer (Tomizawa et al., 2013).

Activin is upregulated in many solid malignancies

In addition to its role in embryonic and gonadal sex development, Activin also regulates homeostasis of muscle, bone, and other tissues. On a cellular level, Activin govern proliferation, apoptosis, and migration (Chen et al., 2006; Phillips et al., 2005). Given this information, a number of studies have examined

a potential role of Activin in cancer progression. Upregulation of Activin, as well as its receptors, has been identified in a number of solid tumors, and it has been shown to drive aberrant proliferation, migration, invasion, and metastasis.

An abundance of evidence exists that implicates Activin in esophageal cancer progression. Within these tumors, *Activin* levels are significantly upregulated when compared to matched normal tissue (Seder et al., 2009a), and Activin levels correlate with lymph node metastasis, advanced stage, and poor prognosis (Yoshinaga et al., 2003), partially by upregulating N-cadherin (Yoshinaga et al., 2004). Stable overexpression of Activin in an esophageal cancer cell lines enhances rates of proliferation, migration, and invasion (Yoshinaga et al., 2008). Moreover, following E-cadherin knockdown in several esophageal cancer cell lines, exogenous Activin A potentiated invasion *in vitro* (Le Bras et al., 2011).

In oral squamous cell carcinoma (OSCC), Activin A overexpression in tissue and in serum is correlated with poor histological differentiation, positive N stage, and perineural invasion. Correspondingly, Activin levels correlate with worse prognoses for both disease-free survival and overall survival. Additionally, *Activin* knockdown reduced rates of OC3 proliferation, migration, and invasion *in vitro* (Chang et al., 2010). These findings suggest that Activin is secreted by OSCC cells to drive tumorigenicity. Additionally, one study found that primary myofibroblasts isolated from OSCC tumors secrete Activin when cultured *in vitro*. SCC9 cells cultured with conditioned media from myofibroblasts secreting Activin displayed increased rates of proliferation, invasion, and MMP activity, and

silencing of Activin in the myofibroblasts reversed these effects. Interestingly, injection of SCC9 cells with myofibroblasts into mice formed significantly larger tumors than SCC9 cells with fibroblasts (Sobral et al., 2011).

In ovarian cancer cell lines, Activin stimulates proliferation and invasion through Matrigel, whereas Inhibin yields opposite phenotypes. Moreover, mice injected with Inhibin-resistant ovarian cancer cell lines resulted in a shorter survival time when compared to those injected with Inhibin-responsive ovarian cancer cells (Steller et al., 2005). Activin levels are elevated in human colorectal tumors, particularly from those in stage IV disease, suggesting that Activin may play a role in advanced colorectal cancer (Wildi et al., 2001). In prostate cancer, Activin is correlated with bone metastasis, Gleason score, and expression of androgen receptor (AR) and prostate-specific antigen (PSA). Activin also promotes the translocation of the AR to the nucleus where it interacts with SMAD3 to promote prostate cancer cell migration to bone matrix *in vitro* (Kang et al., 2009).

The large amount of evidence for Activin as an orchestrator of wound healing suggests that it may play a role in skin tumorigenesis. Using genetically modified mice overexpressing Activin or its receptors, Antsiferova et al. demonstrate that Activin promotes skin tumor formation and progression, partially by blocking proliferation of tumor-suppressive epidermal T cells. Moreover, tissue from human cutaneous basal and squamous cell express significantly higher levels of Activin than matched normal tissue (Antsiferova et al., 2011).

Surprisingly, very little is known about the role of Activin in promoting lung tumorigenesis. Only one study has really examined its role in NSCLC, finding that *Activin* is overexpressed in over 70% of lung adenocarcinomas. Among stage I patients, *Activin* mRNA levels negatively correlate with prognosis. Moreover, the study demonstrates that overexpressing Activin increases lung adenocarcinoma proliferation rates, whereas *Activin* knockdown or treatment with follistatin yields the opposite result (Seder et al., 2009b).

Results shown in Chapter 3 demonstrate that TNF and TGFβ-stimulated NSCLC spheroid cultures effectively undergo EMT over a four day period, and that they secrete autocrine factors to sustain their phenotype (Figure 7). Interestingly, *Activin* is one of the most upregulated genes that encodes a secreted ligand in cytokine-treated NSCLC spheroid cultures (Table 2), suggesting that it may play a role in preserving the cancer-initiating cell (CIC) phenotype. Given this evidence, along with the role of Activin in promoting tumorigenesis within many other organs, its status as a maintenance factor for self-renewal and pluripotency, and the fact that it is a TGFβ superfamily member, we postulated that NSCLC CICs upregulate Activin to maintain their phenotype.

RESULTS

In Chapter 3, we demonstrated that following treatment with TNF and TGFβ, A549 spheroid cultures secrete soluble factors that can induce EMT in naïve 3D cultures (Figure 7A, 7B). Gene expression profiling identified a number of highly upregulated genes that encode secreted ligands, many of these being

NF-κB targets (Table 2). Interestingly, this list included *Inhibin βA* (*INHBA*), which homodimerizes to produce Activin A (Table 2). Importantly, in our microarray data, other members of the TGFβ superfamily, including *NODAL*, the *TGFBs*, and other Inhibin subunits, are not transcriptionally upregulated to the same extent as *INHBA*/Activin A in cytokine-treated cultures (Table 3). These results were confirmed by QRT-PCR (Figure 11). Moreover, *INHA* is not induced following induction of EMT (Figure 11). The unique upregulation of *INHBA* among Inhibin α/β subunits following EMT suggests that these βA subunits predominately homodimerize to produce Activin A, rather than Inhibin or other Activins. Therefore, for the sake of convenience, we refer to Activin A as Activin throughout the remainder of the results. Collectively, our analysis indicates that Activin appears to be an excellent candidate for an autocrine factor capable of inducing EMT in naïve 3D cultures.

Activin is upregulated in established cell lines and in NSCLC cells derived from primary lung tumors

To confirm microarray results shown in Tables 2 and 3, QRT-PCR was performed following exposure to TNF, TGFβ, or both cytokines. Although TGFβ alone modestly increased *Activin* mRNA levels, combined treatment with TNF and TGFβ significantly upregulated *Activin* transcripts (Figure 12A). A549 and H1299 cells increased *Activin* transcript levels in cytokine-treated 3D cultures compared to 2D cultures (Figure 12B). Importantly, the upregulation of Activin

TABLE 3: Differential Expression of TGFβ Superfamily Members Following Cytokine Treatment

Symbol	GenBank	FC ($2D^- \rightarrow 2D^+$)	FC ($3D^- \rightarrow 3D^+$)
INHBA	NM_002192.2	1.0	159.8***
INHBB	NM_002193.2	0.6	0.1**
INHBC	NM_005538.2	1.0	1.0
INHBE	NM_031479.3	5.2	1.6
INHA	NM_002191.3	1.2	0.8
TGFB1	NM_000660.4	1.5	2.9*
TGFB2	NM_001135599.2	1.2	1.0
TGFB3	NM_003239.2	1.0	1.0
NODAL	NM_018055.4	1.0	1.0

Table 3: Cytokine-treated A549 spheroid cultures selectively upregulate *Activin.* The differential expression of select TGFβ superfamily members following cytokine treatment in both 2D and 3D cultures was examined. Values are as indicated: *$p \leq 0.05$, **$p \leq 0.01$, ***$p \leq 0.005$.

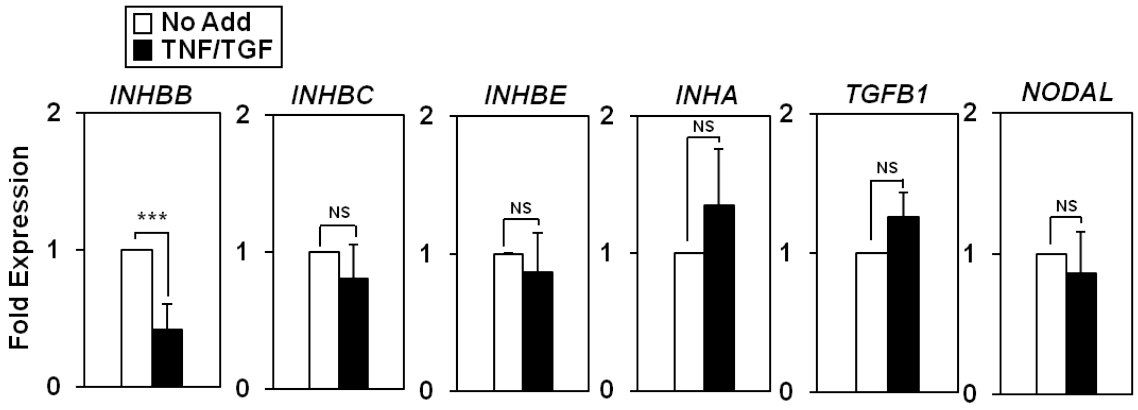
No Add
TNF/TGF
INHBB
INHBC
INHBE
INHA
TGFB1
NODAL
Fold Expression
2
1
0
***
NS

Figure 11: Transcripts encoding members of the TGFβ superfamily are not upregulated in cytokine-treated 3D A549 cultures, as measured by QRT-PCR**.** A one-tailed Student's *t* test in Microsoft Excel was performed to compare values; *** indicates $p < 0.05$. Data were normalized to *GAPDH* expression.

mRNA levels observed in Figure 12A and 12B corresponded with elevated protein levels in the media, as determined by ELISA (Figure 12C).

Next, CM from cytokine-treated 3D A549 cultures were incubated for two hours with either an Activin-specific neutralizing antibody or with rabbit IgG control. CM were then added to N3D cultures for 96 hours, and immunoblot analysis was performed. Similar to results shown in Figure 7A, N3D cultures incubated with supernatants from cytokine-treated spheres effectively downregulated E-cadherin and upregulated N-cadherin, compared to N3D cultures incubated with CM from unstimulated spheroid cultures (Figure 12D). Neutralizing Activin activity attenuated the ability of CM to induce EMT in N3D cultures, indicating that the secretion of Activin into the media is sufficient to induce EMT. Moreover, treatment of N3D cultures with recombinant Activin and TNF was as effective as TGFβ and TNF at inducing N-cadherin and vimentin protein expression (Figure 12E). Experiments in Figure 12D and 12E indicate that Activin is required to induce EMT in N3D A549 cultures.

Since Activin is associated with aggressive cancer phenotypes and with the production of CICs (Lonardo et al., 2011; Topczewska et al., 2006), we examined whether NSCLC cells derived from primary human tumors expressed Activin and whether levels increased following exposure to TNF and TGFβ. Two human NSCLC tumors, an adenocarcinoma (ADC) and a squamous cell carcinoma (SCC), were disaggregated. Spheroid cultures were generated and left untreated or stimulated with TNF and TGFβ. Supernatants were harvested 96 hours later and assayed by ELISA. Supernatants derived from unstimulated

primary human NSCLC spheroid cultures contained high levels of Activin, relative to untreated A549 3D cultures (Figure 12F). Moreover, Activin levels further increased in primary NSCLC cultures following exposure to TNF and TGFβ. These data indicate that spheroid cultures from both established cell lines and primary NSCLC cells express Activin, an event that is potentiated following TNF and TGFβ treatment. Thus, data shown in Figure 12 indicate that TNF and TGFβ-treated spheres produce and secrete Activin, which is capable of inducing EMT in N3D cultures.

NF-κB upregulates **Activin** *to promote expression of EMT markers*

Since we have recently shown that NF-κB is required for EMT and development of CICs in NSCLC (Chapter 3) (Kendellen et al., 2013), and many of the genes encoding potential autocrine factors are NF-κB targets (Table 2), we wanted to determine if *Activin* is transcriptionally regulated by NF-κB. A549 stable cell lines were developed that ectopically express either the vector control (A549.V) or the dominant negative super-repressor IκBα (SR-IκBα, A549.I). A549.I cells fail to induce NF-κB transcription because expression of the SR-IκBα prevents nuclear translocation in response to physiological stimuli.

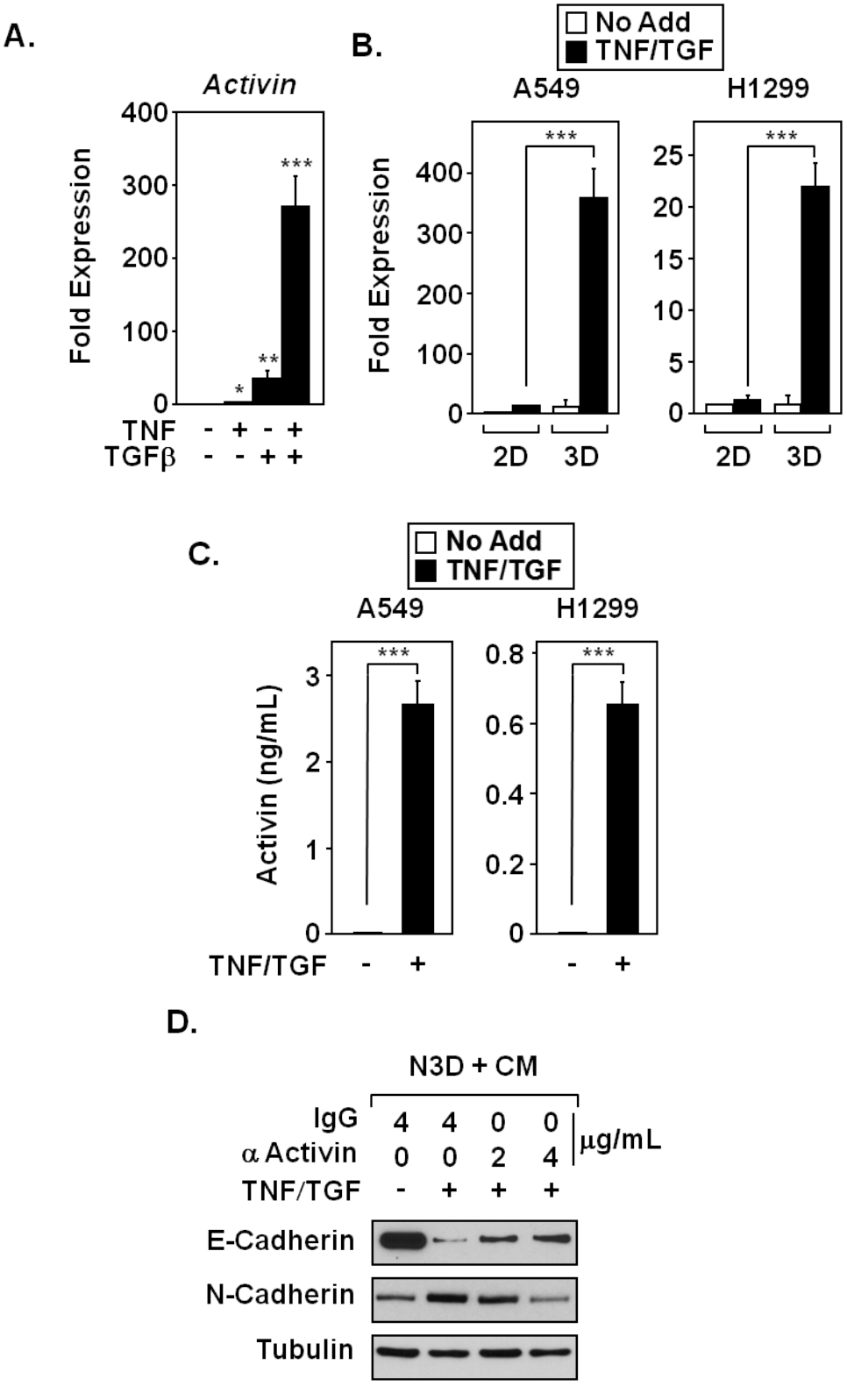
A.
Activin
Fold Expression
400
300
200
100
0
***
**
*
TNF - + - +
TGFβ - - + +
B.
No Add
TNF/TGF
A549
H1299
Fold Expression
400
300
200
100
0
25
20
15
10
5
0
***
***
2D
3D
2D
3D
C.
No Add
TNF/TGF
A549
H1299
Activin (ng/mL)
3
2
1
0
0.8
0.6
0.4
0.2
0
***
***
TNF/TGF - +
- +
D.
N3D + CM
IgG 4 4 0 0
α Activin 0 0 2 4
μg/mL
TNF/TGF - + + +
E-Cadherin
N-Cadherin
Tubulin

E.

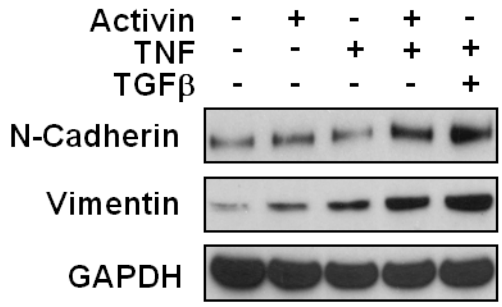
Activin - + - + -
TNF - - + + +
TGFβ - - - - +
N-Cadherin
Vimentin
GAPDH

F.

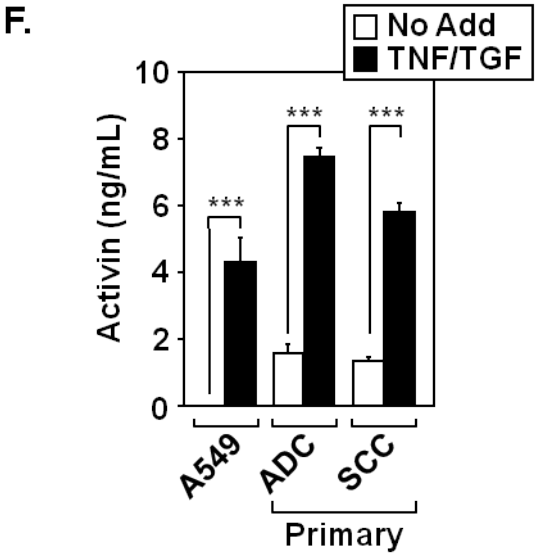
No Add
TNF/TGF
Activin (ng/mL)
10
8
6
4
2
0
***
***
***
A549
ADC
SCC
Primary

Figure 12: Upregulation of Activin in NSCLC lines and primary human lung tumor cells. (A) A549 3D cultures were left untreated (-) or treated (+) with TNF, TGFβ, or both TNF and TGFβ for 96 hours, and *Activin* expression was measured by QRT-PCR. **(B and C)** A549 and H1299 cultures (2D and 3D) were left alone (No Add) or stimulated (TNF/TGF). Activin mRNA and protein levels were measured by QRT-PCR and ELISA, respectively. **(D)** CM from 3D cultures either left untreated (-) or stimulated (+) with TNF and TGFβ were incubated with either IgG control antibody (4 μg/ml) or with Activin neutralizing antibody (2 or 4 μg/ml) for four hours. CM were incubated with N3D cultures for 96 hours, prior to immunoblot analysis. **(E)** Spheroid A549 cultures were either left untreated (-), or stimulated (+) with recombinant Activin (100 ng/mL), TNF, TGFβ, or a combination of cytokines for 96 hours prior to immunoblot analysis. GAPDH served as a protein loading control. **(F)** Spheroid cultures were generated from A549 cells or from primary lung tumor cells isolated from human adenocarcinoma (ADC) or squamous cell carcinoma (SCC) and were left untreated or stimulated with TNF and TGFβ. Activin levels in supernatants were measured by ELISA. QRT-PCR and ELISA results are calculated mean ± SD. A one-tailed Student's *t* test in Microsoft Excel was performed to compare values; *$p \leq 0.05$, **$p \leq 0.01$, ***$p \leq 0.005$, N=3. **Experiments in Figures 12B, 12C and 12F conducted by Dr. Manish Kumar.**

A549.I cells were unable to fully upregulate *Activin* expression following TNF and TGFβ treatment, compared to A549.V control cells (Figure 13A). In contrast, the A549.I line demonstrated full transcriptional induction of bone morphogenic protein 2 (*BMP2)*, another TGFβ superfamily member that is not transcriptionally regulated by NF-κB. As predicted from the QRT-PCR data, A549.I cells secrete less Activin into the media than the A549.V line (Figure 13B). Moreover, when compared to control cells, the A549.I line was unable to produce autocrine factors capable of supporting EMT in naïve 3D cultures (Figure 13C). Although NF-κB has been shown to be required for EMT and for the expansion of CICs (Chapter 3) (Huber et al., 2004; Kendellen et al., 2013; Liu et al., 2010), soluble factors regulated by NF-κB that potentiate EMT and CICs have not been fully elucidated. Data shown in Figures 13A-C indicate that the loss of NF-κB transcriptional activity results in the inability of CM to induce EMT in spheroid cultures, an effect that correlates with a loss of Activin expression and secretion.

Since data shown in Figure 13C could be due to a failure of A549.I cells to undergo EMT in the absence of NF-κB activity, we examined whether CM induced EMT through Activin signaling pathways in A549 cells. To address this question, Activin signaling was blocked using the Alk4/5/7 serine/threonine kinase inhibitor SB431542 (Inman et al., 2002). CM were isolated and incubated with N3D cultures in either the absence or presence of SB431542 (SB). Supernatants from cytokine-treated spheres induced expression of the EMT master-switch transcription factors *SNAI1/Snail*, *SNAI2/Slug*, *TWIST1/Twist* and *ZEB2/Sip1* (Figure 13D). Importantly, treatment of N3D cultures with the

Alk4/5/7 inhibitor blocked the ability of CM to upregulate *SNAI1*, *SNAI2*, and *ZEB2*, but not *TWIST1*. Activin signaling was also required to upregulate *CDH2*/*N-cadherin* and *VIM*/*Vimentin* and to repress *CDH1/E-cadherin* in N3D cultures in response to treatment with CM (Figure 13D). Although SB431542 blocks signaling in response to Activin, Nodal and TGFβ ligands, only Activin is upregulated in A549 3D cultures in response to TNF and TGFβ (Table 3, Figure 11). Thus, the ability of SB431542 to block expression of EMT markers supports the hypothesis that Activin functions as a maintenance factor for the mesenchymal phenotype in NSCLC CIC.

Activin expression is required to maintain EMT in NSCLC

To further examine the contribution of Activin to EMT in NSCLC, we created stable A549 cell lines expressing either non-targeting shRNA control (A549.C) or shRNA to Activin (A549.A). Spheroid cultures with these two cell lines were created and left untreated or stimulated with cytokines. Knockdown of approximately 70% at both the mRNA (Figure 14A) and protein (Figure 14B) levels was achieved.

Next, supernatants isolated from A549.C and A549.A cells were harvested and used to treat N3D cultures. As expected, CM from A549.C cells downregulated E-cadherin and upregulated vimentin protein expression, while supernatants from A549.A were less efficient at modulating these EMT markers (Figure 14C). Since TNF and TGFβ-stimulated NSCLC spheroid cultures

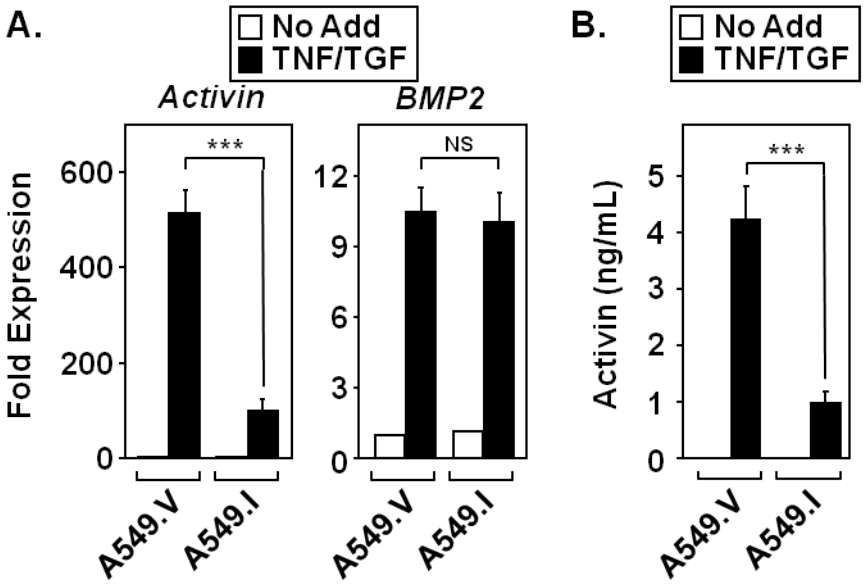
A.
No Add
TNF/TGF
Activin
BMP2
Fold Expression
***
NS
600
400
200
0
12
9
6
3
0
A549.V
A549.I
A549.V
A549.I
B.
No Add
TNF/TGF
Activin (ng/mL)
***
5
4
3
2
1
0
A549.V
A549.I

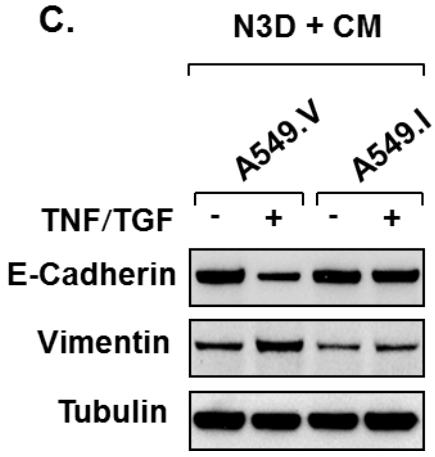
C.
N3D + CM
A549.V
A549.I
TNF/TGF
- + - +
E-Cadherin
Vimentin
Tubulin

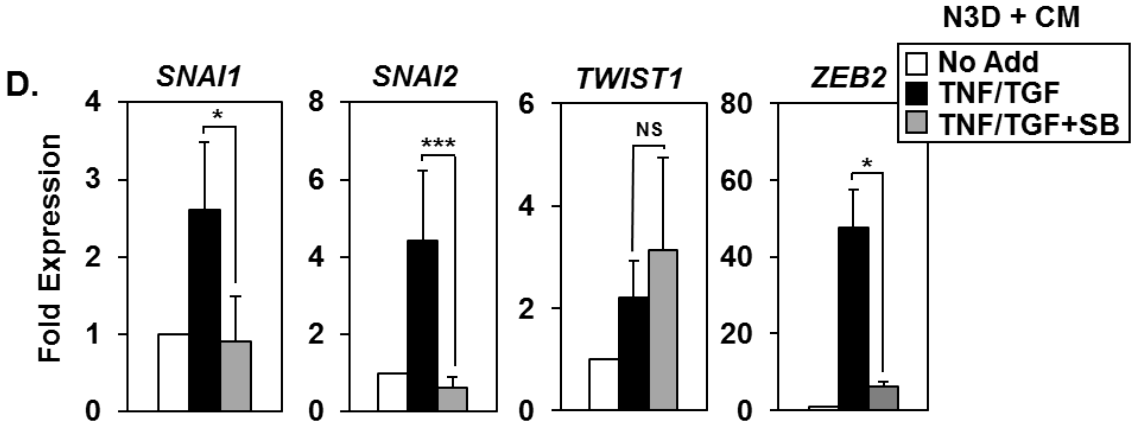
D.
N3D + CM
No Add
TNF/TGF
TNF/TGF+SB
SNAI1
SNAI2
TWIST1
ZEB2
Fold Expression
*
***
NS
*
4
3
2
1
0
8
6
4
2
0
6
4
2
0
80
60
40
20
0

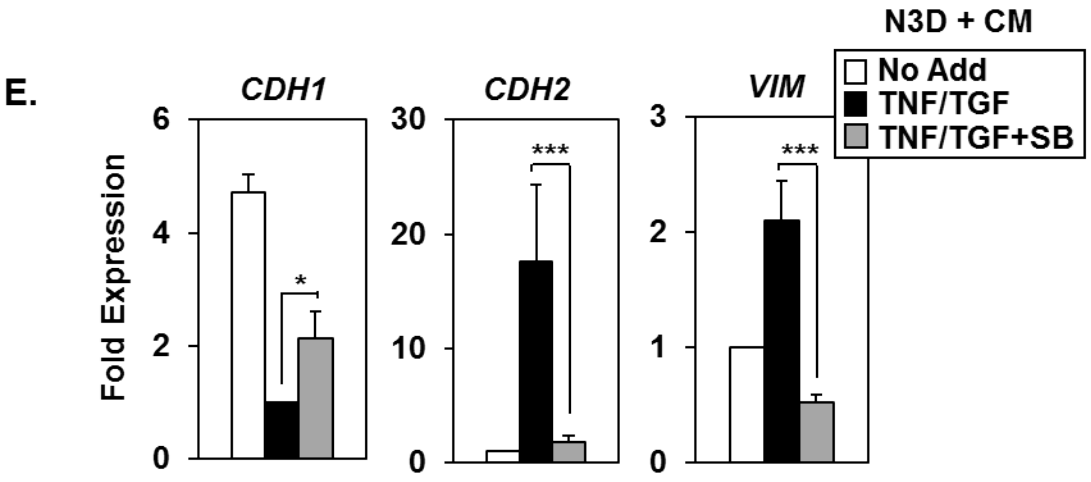
E.
N3D + CM
No Add
TNF/TGF
TNF/TGF+SB
CDH1
CDH2
VIM
Fold Expression
6
4
2
0
30
20
10
0
3
2
1
0
*
***
***

Figure 13: NF-κB upregulates *Activin* to promote EMT. (A and B) Spheroid A549 cultures expressing the non-degradable mutant IκBα (A549.I) or vector control (A549.V) were left alone or stimulated with TNF and TGFβ. *Activin* and *BMP* levels were measured by QRT-PCR, and secreted Activin was assayed by ELISA. **(C)** N3D cultures were incubated with CM from either cytokine-treated 3D A549.V or A549.I cultures. CM from A549.I cells failed to induce changes in mesenchymal markers, compared to CM from A549.V cells, as determined by immunoblot analysis. **(D and E)** N3D cultures were pre-treated for two hours with DMSO or SB431542 (5 μM) prior to incubation with CM from control (No Add) or cytokine-treated (TNF/TGF) 3D cultures. Gene expression was determined by QRT-PCR. QRT-PCR and ELISA results are calculated mean ± SD. A one-tailed Student's *t* test in Microsoft Excel was performed to compare values; *$p \leq 0.05$, **$p \leq 0.01$, ***$p \leq 0.005$, N=3. **Experiments in Figures 13A-C conducted by Dr. Manish Kumar.**

effectively undergo EMT over a four-day period, we hypothesized that A549 cells produce Activin to maintain the mesenchymal state. A549.A cells exhibit statistically significantly lower levels of EMT master-switch transcription factors *SNAI1*, *SNAI2*, and *ZEB2*, compared to control cells (Figure 14D). Interestingly, the knockdown of Activin had no effect on *TWIST1* expression, consistent with our results from Figure 9D. Since mesenchymal cells reprogram to express genes known to promote stem-like properties (Chapter 3) (Mani et al., 2008; Morel et al., 2008; Scheel et al., 2011), we examined endogenous expression of genes involved in self-renewal. Activin was required to sustain expression of *MYCN, SOX2, KLF4*, and *HMGA2* (Figure 14E), supporting the role of Activin as a maintenance factor required for the expression of genes known to induce self-renewal in CICs.

Given that mesenchymal cells are characteristically motile and invasive, we examined whether Activin was also required to sustain expression of gene products that promote cell migration and invasion. The knockdown of Activin resulted in the loss of induction of collagen, type XXII (*COL22A1)*, matrix metalloproteases *MMP2* and *MMP9*, and lysyl oxidase (*LOX)* (Figure 15A). Moreover, Activin expression was required for cell migration and invasion of cytokine-treated spheroid A549 cultures, as assayed in transwell assays (Figure 15B).

Results shown in Chapter 3 indicate that induction of EMT in A549 cells promotes the development of CICs. Interestingly, unlike other models where assays rely on the development of SQ tumors under limiting cell dilution,

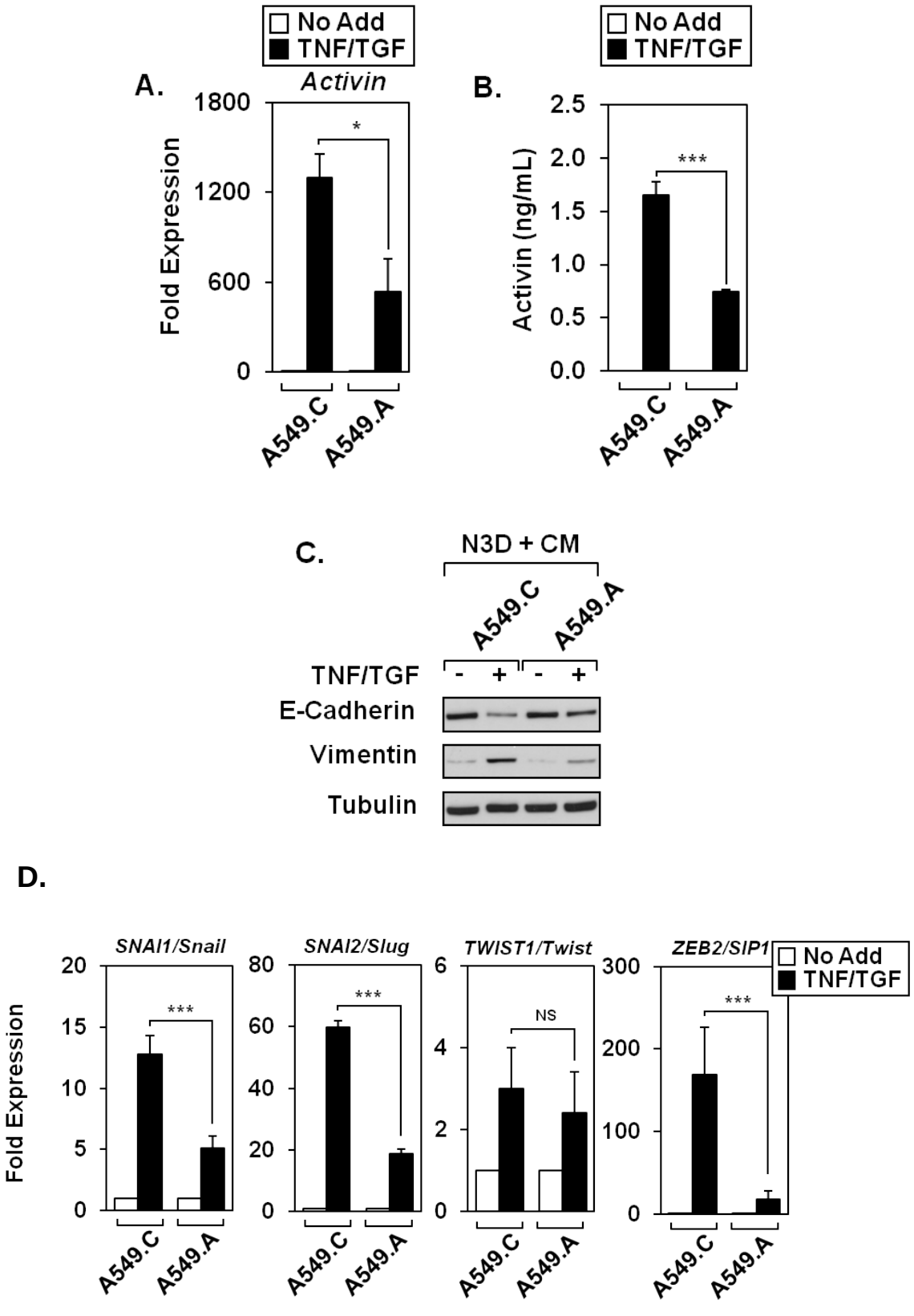
A.
Activin
No Add
TNF/TGF
Fold Expression
1800
1200
600
0
*
A549.C
A549.A
B.
No Add
TNF/TGF
Activin (ng/mL)
2.5
2.0
1.5
1.0
0.5
0.0
***
A549.C
A549.A
C.
N3D + CM
A549.C
A549.A
TNF/TGF
- + - +
E-Cadherin
Vimentin
Tubulin
D.
SNAI1/Snail
SNAI2/Slug
TWIST1/Twist
ZEB2/SIP1
No Add
TNF/TGF
Fold Expression
20
15
10
5
0
80
60
40
20
0
6
4
2
0
300
200
100
0
***
NS
A549.C
A549.A

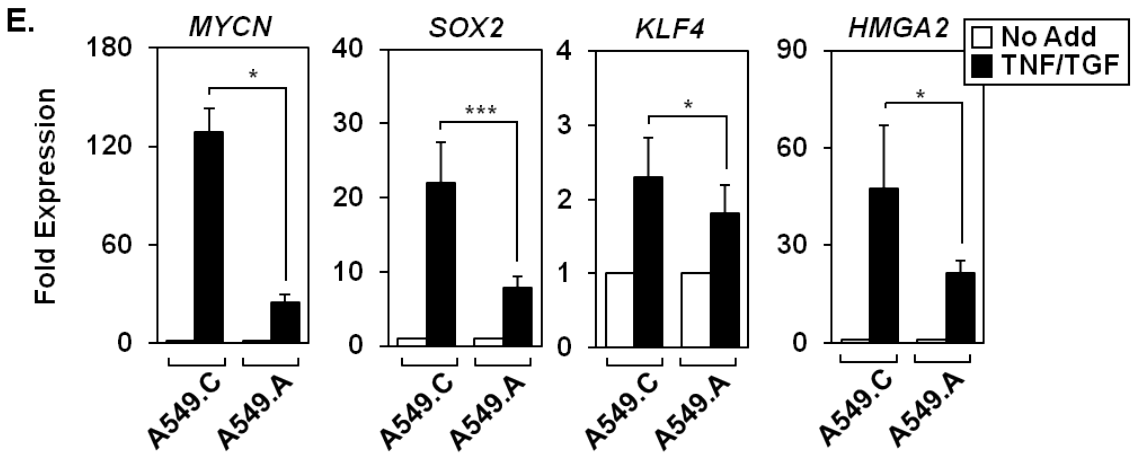
E.
MYCN
SOX2
KLF4
HMGA2
No Add
TNF/TGF
Fold Expression
180
120
60
0
40
30
20
10
0
4
3
2
1
0
90
60
30
0
*
***
*
*
A549.C
A549.A
A549.C
A549.A
A549.C
A549.A
A549.C
A549.A

Figure 14: Activin expression is required to maintain EMT in NSCLC. (A and B) Knockdown of Activin in A549 (A549.A) cells was sustained in cytokine-treated 3D cultures, compared to control cells (A549.C), as determined by QRT-PCR and ELISA. **(C)** N3D cultures were incubated with CM harvested from untreated and cytokine-stimulated 3D A549.C and A549.A cells. Whole cell lysates were assayed by immunoblot analysis. **(D and E)** Knockdown of *Activin* in the A549.A line results in suppressed expression of EMT-master switch transcription factors and genes associated with self-renewal, as determined by QRT-PCR. A one-tailed Student's *t* test in Microsoft Excel was performed to compare values; *$p \leq 0.05$, **$p \leq 0.01$, ***$p \leq 0.005$, N=3. Data shown in Figures 14A, 14D, and 14E were normalized to *GAPDH*.

(Cai et al., 2008; Meuwissen & Berns, 2005), mesenchymal A549 cells do not form SQ tumors. Thus, cytokine-treated spheroid cultures are capable of generating CIC that are highly metastatic under limiting cell dilution without the need for SQ tumor growth. To determine the importance of Activin for metastatic potential of CICs, A549.C and A549.A spheroid cultures were treated with cytokines, disaggregated, and injected SQ into nude mice. Lung surface metastases were numerated after forty days. The knockdown of Activin significantly impaired the ability of A549 cells to metastasize to the lung of nude mice when compared to control cells (Figure 15C). Collectively, our results indicate that TNF and TGFβ-induced expression of Activin is a critical step required to sustain mesenchymal properties and promote CIC metastasis.

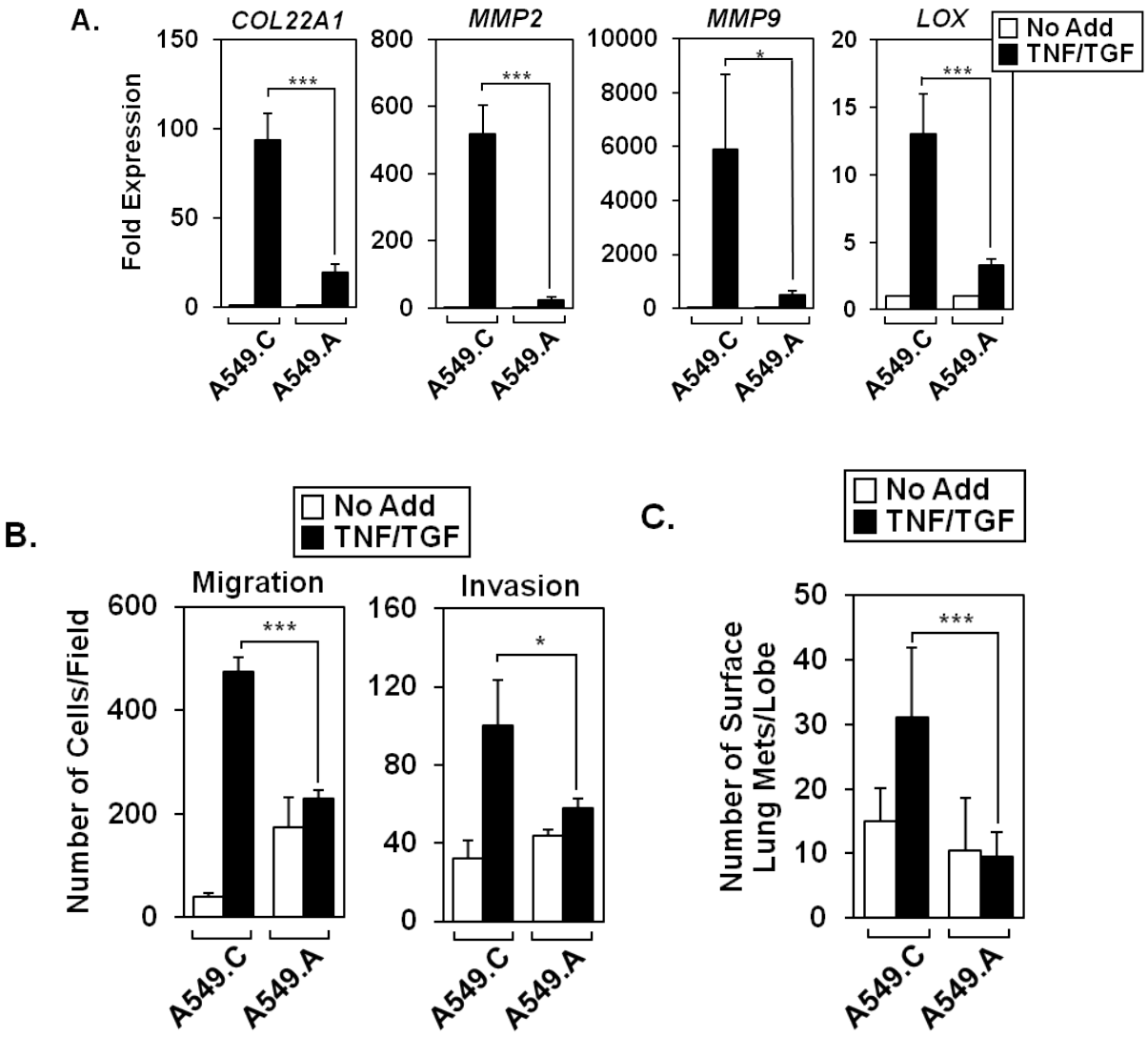
A.
COL22A1
MMP2
MMP9
LOX
No Add
TNF/TGF
Fold Expression
150
100
50
0
800
600
400
200
0
10000
8000
6000
4000
2000
0
20
15
10
5
0
***
***
*
***
A549.C
A549.A
B.
No Add
TNF/TGF
Migration
Invasion
Number of Cells/Field
600
400
200
0
160
120
80
40
0
***
*
A549.C
A549.A
C.
No Add
TNF/TGF
Number of Surface Lung Mets/Lobe
50
40
30
20
10
0
***
A549.C
A549.A

Figure 15: Invasive and metastatic potential of A549 cells is dependent on Activin expression. (A) Loss of Activin activity significantly dampens the expression of genes known to promote NSCLC invasion, as measured by QRT-PCR. **(B)** Unstimulated or cytokine-treated A549.C and A549.A 3D cultures were dissociated and subjected to migration and invasion assays as previously described (Kumar et al., 2013). **(C)** Three-dimensional A549.C and A549.A cultures, either left alone or treated with cytokines were disaggregated and injected subcutaneously (SC) into nude mice (1×10^6 cells/animal). Forty days later, the lungs were removed, and the number of surface metastases was enumerated. Lung metastases data are mean ± SD of five mice per condition, N=2. A one-tailed Student's *t* test in Microsoft Excel was performed to compare values; *$p \leq 0.05$, **$p \leq 0.01$, ***$p \leq 0.005$, N=3. Data shown in Figure 15A were normalized to *GAPDH*. **Experiments in Figure 15B were conducted along with Dr. David Allison.**

DISCUSSION

Work presented in Chapter 3 demonstrates that upon treatment with TNF and TGFβ, spheroid cultures undergo EMT and are enriched for CICs. However, the half-life of cytokines in growth media is short, so we postulated that NSCLC CICs secrete autocrine factors to maintain the mesenchymal phenotype. In parallel, within the cancer patient, disseminating cells abandon the primary tumor microenvironment containing the cytokines responsible for induction of the mesenchymal phenotype. Mechanisms by which NSCLC CICs preserve this phenotype have remained elusive.

Here, we illustrate that only spheroid cultures stimulated with TNF and TGFβ produce soluble factors that can mediate the mesenchymal phenotype in N3D cultures, and the secretion of these factors requires both cytokines. Whole-genome microarray analysis identified *Activin* as a TGFβ superfamily member highly upregulated exclusively in 3D cultures. Signaling through SMADs 2 and 3 has been shown to be essential in EMT. Importantly, the only TGFβ superfamily members that can activate these SMADs are TGFβ, Activin, and Nodal. Microarray data, as well as QRT-PCR, show that of these three ligands, only *Activin* is upregulated in NSCLC spheroid cultures derived from both established cell lines and primary tumor cells. Therefore, we postulated that upon exhaustion of the inducing TGFβ stimulus, cytokine-treated spheroid cultures upregulate *Activin* to sustain SMAD signaling. We demonstrate that neutralizing Activin bioactivity in conditioned media is sufficient to abrogate induction of EMT. Moreover, co-stimulation of N3D cultures with Activin and TNF induced EMT as

efficiently as TNF and TGFβ, supporting the role for Activin as a TGFβ superfamily maintenance factor.

Data in Chapter 3 demonstrate a clear requirement for NF-κB in the induction of EMT in NSCLC. Interestingly, findings presented in this chapter suggest that NF-κB is also required for maintenance of this phenotype. Inhibition of the canonical NF-κB signaling pathway blocks the secretion of autocrine factors that can induce EMT in N3D cultures in a paracrine manner, namely *Activin*. Importantly, we demonstrate a clear requirement for *Activin* in maintaining the CIC phenotype over a four-day period, as measured by transcript levels of master-switch transcription factors, extracellular matrix remodelers, and factors known to mediate self-renewal. These changes in gene expression correlate with decreased capacities for migration, invasion, and metastasis, establishing a clear role for Activin in preserving the NSCLC CIC phenotype (Figure 16).

Activin: More evidence for our system as a model for bone metastasis

In addition to its roles as a cytokine, morphogen, and reproductive hormone, Activin also plays critical roles in bone remodeling. Activin A is one of the most highly expressed TGFβ superfamily members in bone, whereas neither Activins B or AB can be detected (Ogawa et al., 1992). Activin is expressed in both osteoblasts and osteoclasts (Leto, 2010). In tumor-naïve bone marrow stromal cells, Activin stimulates OC differentiation while inhibiting OB differentiation *in vitro* (Vallet et al., 2010). Its critical role in governing bone

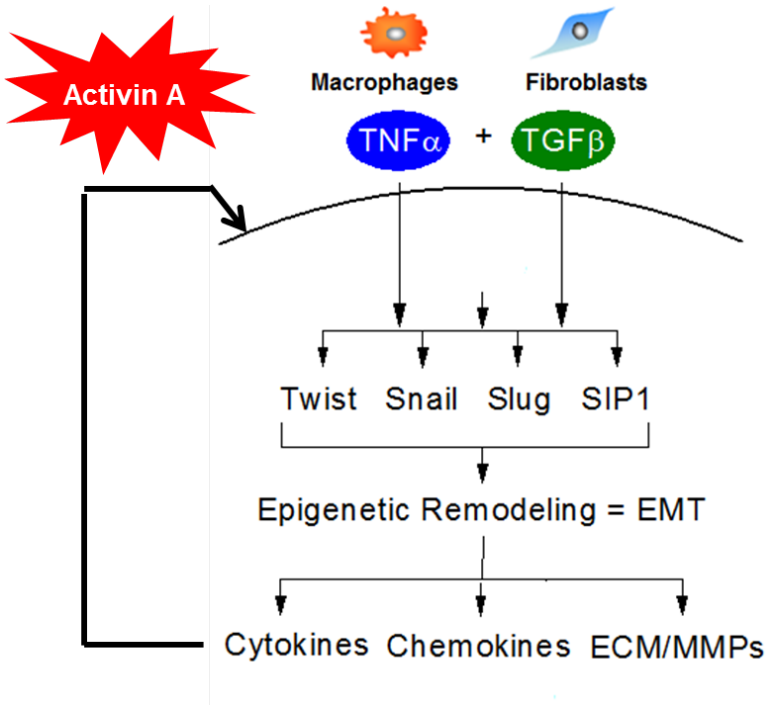

INITIATION

INDUCTION

MAINTENANCE

Figure 16: Activin as a mesenychmal and CIC maintenance factor. TNF and TGFβ initiate the epithelial-to-mesenchymal transition by upregulating the EMT master switch transcription factors, Twist, Snail, SIP1, and Slug. These transcription factors repress epithelial markers while inducing expression of genes encoding mesenchymal proteins, including extracellular matrix proteins, matrix metalloproteases, and chemokines. Also upregulated by these four transcription factors are cytokines, particularly Activin, that act in an autocrine manner to preserve the mesenchymal and cancer-initiating cell phenotypes.

homeostasis under physiological conditions supports Activin as a prime candidate for promoting bone metastasis.

Several studies have demonstrated a role for Activin in promoting bone disease associated with both metastasis and multiple myeloma (MM). One interesting study found that in mice injected with MM cells, administration of a soluble Activin receptor type IIA fusion protein (RAP-011) promoted bone formation, prevented bone destruction, and stimulated osteoblastogenesis, yielding increased bone mass and survival. Similarly, treatment with this fusion protein in mice with metastatic breast cancer blocked bone destruction and the formation of bone metastases (Chantry et al., 2010). Work done by Vallet and colleagues supported these findings. These researchers showed that administration of RAP-011 reversed inhibition of OB differentiation *in vitro*. Moreover, they showed that in an MM mouse model, this decoy receptor decreased OC count within bone, resulting in attenuation of osteolysis (Vallet et al., 2010).

To ensure that these laboratory findings are clinically relevant, a few studies have examined the role of Activin as a biomarker for bone disease and prognosis in humans. In breast cancer patients, Activin serum levels correlate significantly with the presence and number of bone metastases (Incorvaia et al., 2007). Among prostate cancer patients, a significant association between circulating Activin levels and Gleason score, PSA levels, tumor grade, and number of bone metastases has been established (Incorvaia et al., 2007; Leto et al., 2006). Interestingly, in patients with multiple myeloma, Activin is correlated

with the presence and number of osteolytic lesions but not tumor burden, suggesting that Activin specifically promotes bone disease (Vallet et al., 2010).

Data collected from mouse models, as well as evidence that Activin is a biomarker for bone metastasis in breast and prostate cancer patients, have generated interest in testing Activin inhibitors in human clinical trials. The human analogue of RAP-011, termed ACE-011 or Sotatercept, has demonstrated low toxicity in both healthy patients and patients with multiple myeloma (Raje & Vallet, 2010). Importantly, Sotatercept improved bone lesions associated with MM (Vallet et al., 2010), suggesting that it may also be useful in treating bone metastasis. Interestingly, the Activin ligand trap also increased levels of hemoglobin and hematocrit, suggesting that it may also be able to reverse anemia that cancer patients frequently encounter.

Activin: A target for restoring erythropoiesis following bone metastasis and chemotherapy

Anemia, defined as a paucity of healthy red blood cells, is frequently encountered among NSCLC patients. It can be caused by chemotherapy or bone metastasis, resulting in both bone marrow damage and insufficient production of erythropoietin. NSCLC patients are frequently treated with cisplatin-based chemotherapy, and their primary tumors often metastasize to bone, yielding anemia that can be more severe than that encountered in other malignancies. Treatment with recombinant erythropoietin reverses in anemia in

only about half of NSCLC patients, making the identification of other targets a key area of focus (Del Mastro et al., 1999).

The role of Activin in inhibiting bone growth during pathological processes places it at the forefront of molecular targets whose inhibition could reverse anemia. Studies using conditioned media from bone marrow stromal cells on CD34+ human blood cells show that depleting Activin levels in conditioned media using ACE-011 restores erythropoiesis (Iancu-Rubin et al., 2013). Importantly, RAP-011 administration in mice attenuated chemotherapy-induced anemia (Chantry et al., 2010), generating interest in clinical trials for Sotatercept in patients with anemia. Since anemia occurs so frequently in NSCLC patients, a clinical trial was initiated to determine effective doses of Sotatercept to inhibit chemotherapy-induced anemia in NSCLC patients. Unfortunately, the trial was terminated due to persistent low enrollment.

Our results have identified Activin as a novel target for NSCLC patients. Its upregulation in NSCLC CICs is essential for maintaining the cancer-initiating cell characteristics that are essential for metastasis, including invasion and self-renewal. Treatment of NSCLC patients with Sotatercept could shrink the pool of CICs in the primary tumor as well as eradicate circulating CICs, preventing metastasis to distal sites. However, if metastasis to bone has already occurred, then Sotatercept could still be useful for NSCLC patients by slowing osteolysis and reversing anemia associated with chemotherapy and bone metastasis.

Chapter Acknowledgements

This chapter was adapted from a manuscript currently under review with *Cancer Research* entitled “NF-κB-Mediated Upregulation of *INHBA/Activin* Maintains Cancer-Initiating Cell Phenotypes. The authors of this manuscript include J. Jacob Wamsley, Manish Kumar, David Allison, Sheena Clift, Szymon Szymura, Stephen Hoang, Xiaoxiang Xu, David Jones, Stefan Bekiranov, and Marty Mayo.

CHAPTER 5: SPHINGOSINE 1-PHOSPHATE PROMOTES THE CANCER-INITIATING CELL PHENOTYPE IN NON-SMALL CELL LUNG CANCER

INTRODUCTION

Sphingosine-1-Phosphate Signaling

Although sphingolipids are critical constituents of cell membranes, far more interesting functions involve their roles as signaling molecules controlling cell fate. Ceramide and sphingosine both promote apoptosis and senescence. However, sphingosine-1-phosphate (S1P) confers a proliferative signal upon cells. S1P is a bioactive signaling lipid formed by the ATP-dependent phosphorylation of sphingosine by sphingosine kinase (SK). Two isoforms of SK exist, SK1 and SK2. The phosphorylation mark is removed by S1P phosphatase. S1P can be irreversibly hydrolyzed by S1P lyase to produce hexadecenal and ethanolamine phosphate, marking the only point of exit from the sphingolipid metabolic pathway (Pyne et al., 2012). S1P predominately mediates its effects through five differentially expressed G-protein-coupled receptors (GPCR) (S1PR1-5). These transmembrane receptors activate downstream signaling pathways such as PI3K/Akt, Rac/Rho, and MAPK to promote oncogenesis (Heffernan-Stroud & Obeid, 2013).

SK1 and SK2 have minor differences in structure and cellular localization. SK1 is thought to be more inducible, particularly by external agonists. It localizes predominately to the cytoplasm, and following phosphorylation at serine 225 and subsequent activation, translocates to the plasma membrane, where it governs extracellular S1P levels. SK2 appears to have more of a housekeeping role that may be restricted to the nucleus. Interestingly, overexpression of SK1 generally promotes growth, whereas SK2 overexpression induces apoptosis (Spiegel &

Milstien, 2003). However, studies performed in knockout mice indicate that they may have overlapping functions. Single SK1 and SK2 knockout mice exhibit a normal phenotype without compensation for the other isoform. However, double KO mice are embryonic lethal, due to neuronal apoptosis and insufficient angiogenesis and neurogenesis (Mizugishi et al., 2005).

SK1 as an oncogene

The importance of the S1P:sphingosine "rheostat" in controlling cell fate, as well as the documented roles of SK1 in driving proliferation and migration, implicate SK1 as a prime candidate for an oncogene. Several cancer cell lines exhibit increased SK1 expression, and they are frequently reliant on SK1 activity for survival and proliferation. Elevated SK1 levels are found in malignancies of the stomach, lung, brain, kidney, breast, and colon, as well as non-Hodgkin's lymphoma (Heffernan-Stroud & Obeid, 2013; Pyne & Pyne, 2013). Production of S1P by SK1 has been implicated in cancer development by promoting survival, drug resistance, and abnormal proliferation through cross-talk with receptor tyrosine kinases (Heffernan-Stroud & Obeid, 2013).

Evidence also implicates S1P in promoting migratory and invasive phenotypes, hallmarks of CICs. In esophageal cancer cells, TGFβ induces SK1 and SK2, resulting in elevated intracellular S1P levels. Inhibition of either kinase attenuates TGFβ-induced activation of ERK1/2 and promotion of esophageal cancer cell migration and invasion (Miller et al., 2008). Data in breast cancer

cells links S1P to the upregulation of MMP9 and subsequent migratory and invasive phenotypes (Kim et al., 2011).

In addition to driving proliferation, migration, and invasion of carcinoma cells, S1P has also been shown to play an indispensable role in regulating angiogenesis, a rate-limiting step for tumor growth. This was first demonstrated by the fact that S1PR1 knockout mice die *in utero* due to vascular abnormalities (Liu et al., 2000). Moreover, S1P has been shown to bind S1PR1 and S1PR3 on vascular endothelial cells to promote their migration and capillary-like tube formation *in vitro* (Kimura et al., 2000; Lee et al., 1999) and *in vivo* (Oyama et al., 2008). These findings provide further support for S1P as a critical mediator of cancer progression.

In addition to migratory and invasive capacities, CICs are also self-renewing and multipotent. These attributes are conferred by the same factors that govern pluripotency of human embryonic stem cells, such as Oct4, Sox2, c-Kit, N-myc, and Activin, as shown in chapters 3 and 4. Interestingly, a role for S1P in governing proliferation, survival, and pluripotency of hESCs has been established (Avery et al., 2008). These findings led us to examine whether S1P could mediate the CIC phenotypes observed in cytokine-treated 3D cultures.

CICs also exhibit resistance to chemotherapy and other drugs, conferred by upregulation of pathways involved in evasion of apoptosis and the overexpression of cell surface ABC transporters that can efflux drugs. Interestingly, S1P export from breast cancer cells often occurs through ABCC1 and ABCG2, which are frequently upregulated in CICs (Takabe et al., 2010).

PC3 cells are resistant to camptothecin, whereas LNCaP cells are sensitive. Importantly, PC3 exhibit significantly higher levels of *SK1*, *S1PR1*, and *S1PR3* when compared to LNCaP cells, and treatment with camptothecin further potentiated expression of these genes even further (Akao et al., 2006).

Importantly, evidence for the SK1:S1P signaling axis in NSCLC progression has also been established. SK1 levels are upregulated in NSCLC tissue when compared to normal lung tissue, as assayed by both IHC and QRT-PCR (Johnson et al., 2005; Song et al., 2011). Furthermore, a role for S1P in resistance to chemotherapy in NSCLC cells was demonstrated by Schnitzer et al. The authors first showed that hypoxic conditioned medium from A549 cells protected naïve cells from etoposide-induced apoptosis. Interestingly, this effect was not mediated by SK1, as knockdown of only SK2 prior to harvesting the conditioned medium reversed these effects. Incubating the conditioned medium with an S1PR1/S1PR3 antagonist also blocked its ability to protect cells from apoptosis (Schnitzer, Weigert, Zhou, & Brüne, 2009). Based on the evidence implicating SK1 as an oncogene capable of inducing migratory and invasive phenotypes, as well as the ability of S1P to drive self-renewal and drug resistance in multiple malignancies, we hypothesize that deregulation of the S1P signaling pathway contributes to CIC phenotypes observed in NSCLC.

RESULTS

Mesenchymal NSCLC cells upregulate S1P, a powerful chemoattractant

Microarray analysis was performed to identify differentially expressed genes following TNF and TGFβ treatment in A549 spheroid cultures. These results indicate that components of the S1P signaling pathway are upregulated in NSCLC CIC, namely *SK1* (18-fold) and *S1PR3* (3-fold) (data not shown). These findings are supported by studies indicating that SK1 can be induced by either TNF (Xia et al., 2002) or TGFβ (Kono et al., 2007). Interestingly, neither *SK2* nor *S1PR1*, another well-studied S1P receptor, are induced. QRT-PCR confirmed this selective upregulation (Figures 16A and 16B). Consistent with elevated *SK1* levels, A549 cells display increased intracellular S1P levels following TNF/TGF stimulation (Figure 16C). Although the increase in S1P levels observed following EMT is not statistically significant, S1P levels are basally high in A549 cells. Moreover, since we propose that S1P acts as a soluble factor to preserve the mesenchymal phenotype, it is possible that the majority of S1P is rapidly exported from the cell following synthesis, where it acts in an autocrine or paracrine manner. Additional work is required to test this hypothesis.

S1P has been shown to be a powerful chemoattractant for a number of types of non-transformed cells, particularly various types of immune cells. This phenomenon has been explained by the fact that plasma contains 10-fold higher levels of S1P compared to tissue (Liu et al., 2011). Therefore, we hypothesized that this S1P gradient may also provide a mechanism by which NSCLC CICs migrate to the bloodstream following invasion through the basement membrane.

To test this hypothesis, we generated A549 spheroid cultures, treated them with TNF and TGFβ, disaggregated the cultures, and assayed their ability to migrate to DMEM with 1 μM S1P. Data shown in Figure 16D indicate that NSCLC CIC migrate effectively to S1P following invasion through Matrigel, indicating that the S1P gradient may mediate the egress of CICs from lung tissue to the bloodstream, facilitating metastasis.

S1P promotes EMT in NSCLC

Evidence implicating SK1 in promoting migratory and invasive phenotypes in multiple solid cancers led us to speculate that S1P functions as a critical mediator of EMT. Furthermore, S1P has been shown to activate SMAD signaling, presumably by cross-activating the TGFβ type I receptor (Xin et al., 2004). Therefore, we examined the ability of S1P to induce EMT in naïve 3D (N3D) cultures, as assayed by immunoblot for N-cadherin and vimentin. Interestingly, S1P alone failed to induce EMT at a wide variety of concentrations, in stark contrast to previously published results (Milara et al., 2012) (data not shown). However, co-stimulation of N3D cultures with S1P and TNF induced expression of both N-cadherin and vimentin (Figure 13A). These results are similar to those achieved with Activin, presented in Chapter 4 and illustrated in lane 4 of Figure 13A. Just as Activin required TNF treatment to induce EMT, S1P-mediated induction of EMT also requires stimulation of the NF-κB signaling pathway. Together, our findings suggest that Activin and S1P do not induce

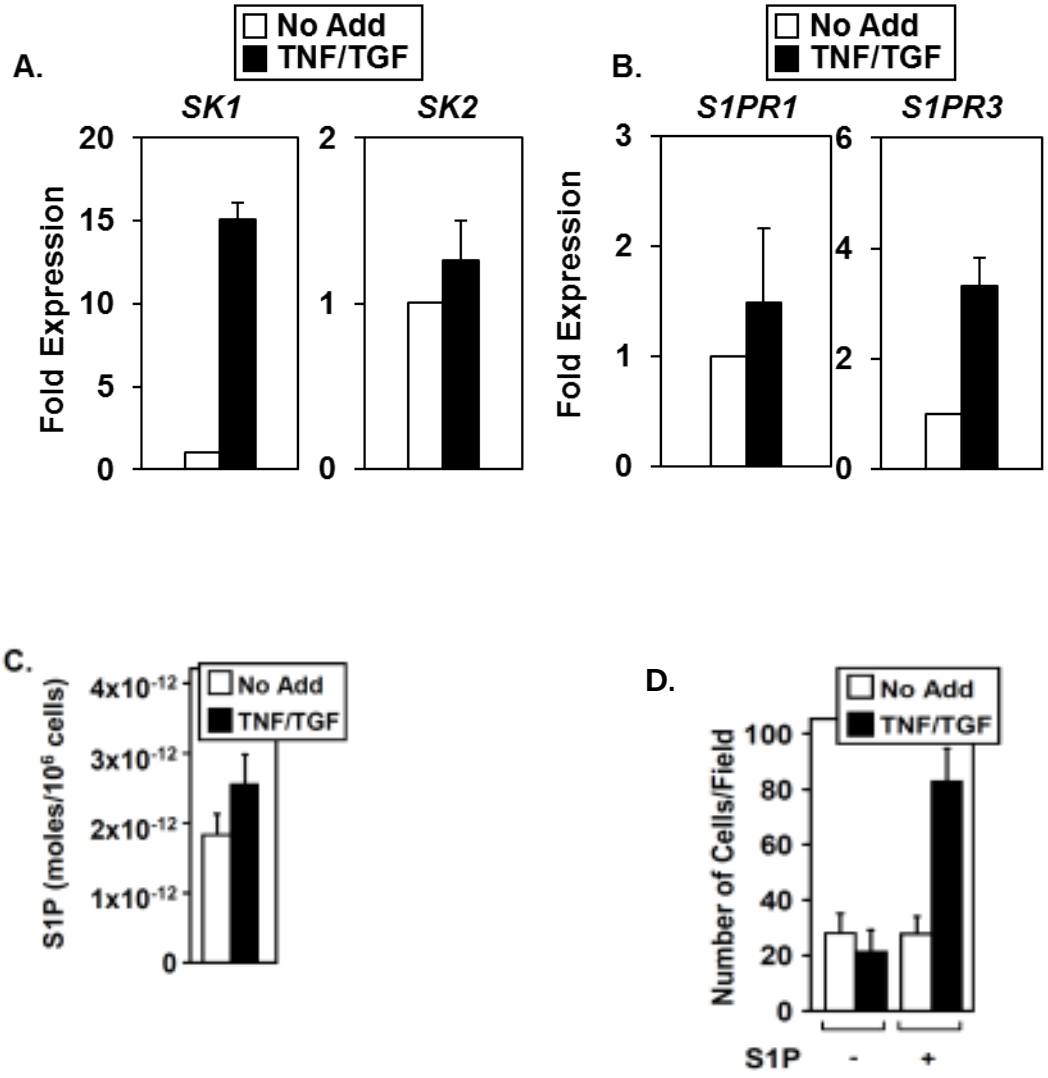
A.
No Add
TNF/TGF
SK1
SK2
Fold Expression
20
15
10
5
0
2
1
0
B.
No Add
TNF/TGF
S1PR1
S1PR3
Fold Expression
3
2
1
0
6
4
2
0
C.
No Add
TNF/TGF
S1P (moles/10^6 cells)
4x10^-12
3x10^-12
2x10^-12
1x10^-12
0
D.
No Add
TNF/TGF
Number of Cells/Field
100
80
60
40
20
0
S1P
-
+

Figure 17: NSCLC 3D cultures upregulate S1P, a powerful chemoattractant for CICs. A and B) QRT-PCR analysis demonstrates that *SK1* and *S1PR3* are upregulated in NSCLC CIC, whereas *SK2* and *SIPR1* are not. **C)** Liquid chromatography-mass spectrometry (LC-MS) was performed to detect the levels of S1P in A549 cells following treatment of 3D cultures with TNF/TGF for a four day period. **D)** Invasion through Matrigel to 1 µM S1P in DMEM was assayed with A549 spheroid cultures left unstimulated or treated with TNF/TGF. For all panels, N=3. Data shown in Figures 17A and 17B were normalized to *GAPDH*.

EMT as efficiently as TGFβ, but their activation of SMADs is sufficient to mediate EMT when the canonical NF-κB pathway is also activated. However, this hypothesis must be confirmed by showing that in our model system, S1P can activate SMAD signaling.

Microarray results and QRT-PCR data demonstrate selective upregulation of *SK1* in NSCLC CIC. Therefore, to continue our studies of this pathway in CIC formation, we utilized a specific pharmacological inhibitor of SK1, SKX96091, created and graciously provided by Sphynx Therapeutics Inc. (Kharel et al., 2011; Zhu et al., 2007). This compound binds SK1 with nanomolar affinity, competing with ATP to inhibit kinase activity. The ability of SK1 inhibition to attenuate TNF and TGFβ-mediated induction of EMT was then measured through a number of assays.

First, we measured mRNA levels of master-switch transcription factors *SNAI1/SNAIL, ZEB2/SIP1, SNAI2/SLUG,* and *TWIST/TWIST1*, as well as the critical maintenance factor *Activin* (Chapter 4), in 3D cultures that were left untreated or treated with TNF and TGFβ, with or without SKX96091. Data shown in Figure 17B illustrate that SK1 activity is necessary for full induction of both *SNAI1/SNAIL* and *TWIST1/TWIST*, as well as *Activin,* when compared to cultures treated with TNF and TGFβ but without the SK1 inhibitor (Figure 17B). Inhibition of SK1 did not attenuate induction of ZEB2/*SIP1* or *SNAI2*/*SLUG* (data not shown). Moreover, blocking SK1 kinase activity abrogated cytokine-mediated induction of the matrix metalloproteases *MMP2* and

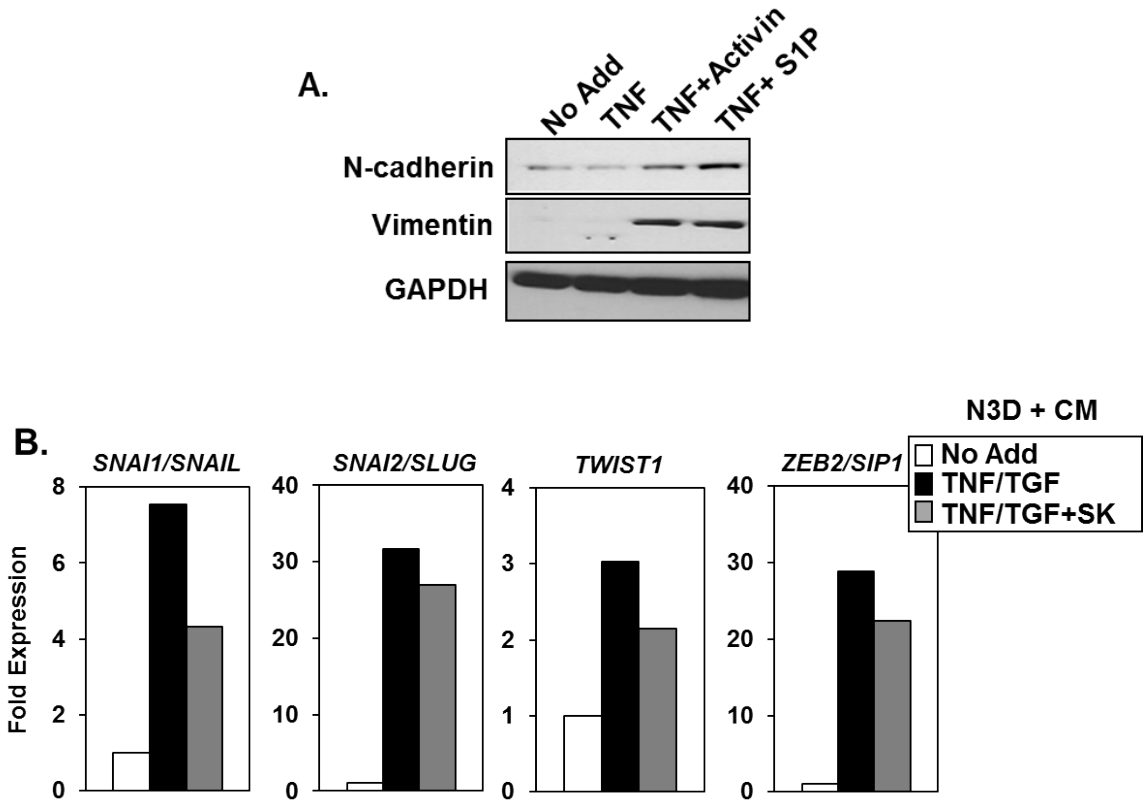
A.
No Add
TNF
TNF+Activin
TNF+ S1P
N-cadherin
Vimentin
GAPDH
B.
N3D + CM
No Add
TNF/TGF
TNF/TGF+SK
SNAI1/SNAIL
SNAI2/SLUG
TWIST1
ZEB2/SIP1
Fold Expression
0
2
4
6
8
10
20
30
40
1
3

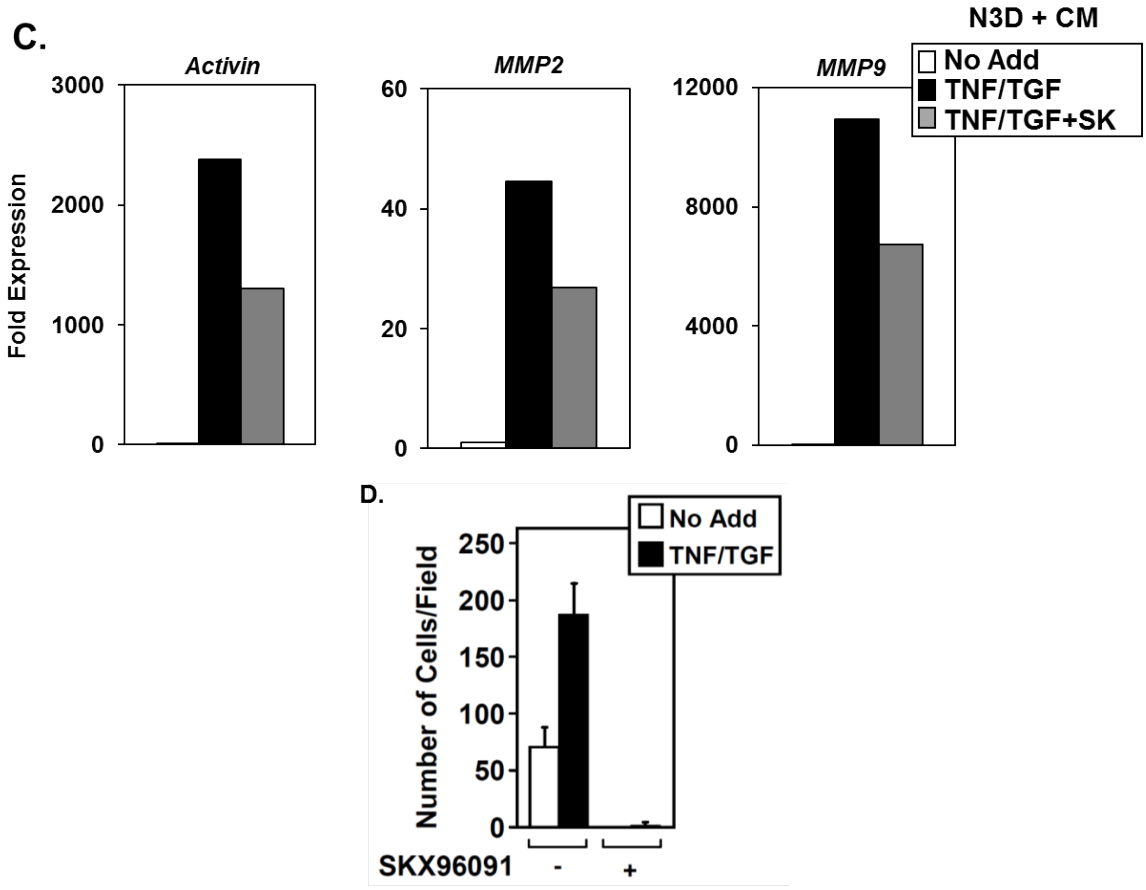
C.
Activin
MMP2
MMP9
N3D + CM
No Add
TNF/TGF
TNF/TGF+SK
Fold Expression
3000
2000
1000
0
60
40
20
0
12000
8000
4000
0
D.
No Add
TNF/TGF
Number of Cells/Field
250
200
150
100
50
0
SKX96091
-
+

Figure 18: SK1-mediated phosphorylation of sphingosine mediates EMT in NSCLC. A) Immunoblot analysis of 3D A549 cultures stimulated with Activin, S1P, TNF, or combinations of the three. Induction of EMT is measured by protein levels of N-cadherin and vimentin. GAPDH serves as a protein loading control. N=2. **B and C)** QRT-PCR analysis of A549 spheroid cultures left untreated, treated with TNF/TGF, or co-stimulated with TNF/TGF and SKX96091 (SK). Induction of EMT was measured by mRNA levels of *INHBA/Activin, SNAI1/SNAIL*, *TWIST1/TWIST*, *MMP2, and MMP9.* N=1. **D)** The ability of A549 3D cultures left untreated, treated with TNF/TGF, or treated with TNF/TGF and SKX96091 to invade through Matrigel to 1 μM S1P was measured via transwell assays. N=3.

MMP9 (Figure 17C). These changes in MMP expression following SK1 inhibition correlate with ablated levels of invasion through Matrigel, using S1P as a chemoattractant (Figure 17D). Taken together, these results indicate that S1P may promote multiple aspects of the epithelial-to-mesenchymal transition by governing expression of two of the key master-switch transcription factors, matrix metalloproteases, and the essential CIC maintenance factor, Activin.

DISCUSSION AND FUTURE DIRECTIONS

Components of the S1P signaling pathway are deregulated in many solid malignancies. SK1 is overexpressed in a number of tumors, and its expression often correlates with poor prognosis in patients. Given the upregulation of *SK1* and *S1PR3* in NSCLC CICs, as assayed by microarray analysis and QRT-PCR (Figure 16A), increased levels of S1P in NSCLC CIC (Figure 16C), and the well-established status of *SK1* as an oncogene, we hypothesized that S1P promotes mesenchymal and CIC phenotypes in NSCLC.

We demonstrated that S1P, in concert with TNF, can induce EMT in N3D cultures (Figure 17A). This finding was consistent with evidence in the literature that S1P can activate SMAD signaling. Moreover, pharmacological inhibition of SK1 inhibited EMT as assayed by attenuated induction of *Activin*, *MMP2, MMP9*, *SNAIL,* and *TWIST*, as well as diminished levels of invasion (Figures 17B-D). Additionally, we demonstrated that S1P is as a potent chemoattractant for NSCLC CICs (Figure 16D). Taken together, these results suggest that S1P drives both invasion through the basement membrane (Figures 17C, 17D) and intravasation into the bloodstream (Figure 16D), initiating the metastatic cascade (Figure 18).

Although preliminary, these findings implicate S1P as a critical mediator of EMT in NSCLC. Further experiments are needed to confirm, and expound upon, these findings. First, pharmacological inhibition experiments must be repeated using the control enantiomer, SKX96115. Second, RNA interference studies should be conducted. Stable knockdown of *SK1* in A549 cells should result in

similar phenotypes as those obtained following its pharmacological inhibition. Additionally, extracellular levels of S1P must be measured following cytokine treatment of A549 spheroid cultures. If S1P functions as a maintenance factor for NSCLC CICs, then one would expect its extracellular levels to be significantly elevated in conditioned media of cytokine-treated spheroid cultures when compared to untreated cultures. Finally, mouse experiments should be conducted to confirm that *in vitro* evidence implicating S1P as a promoter of CIC phenotypes is physiologically relevant. The ability of mesenchymal A549 cells to seed lung metastases should be challenged with the SK1 inhibitor, SKX96091. The ability of RNAi-mediated knockdown of *SK1* to inhibit lung metastasis in A549 cells should also be examined.

Another exciting avenue to pursue would be to attempt to establish a direct link between NF-κB and S1P in our system. The literature suggests that TNF stimulation is sufficient for induction of SK1. It would be interesting to assay *SK1* levels directly in A549.I cells (Figure , lacking functional NF-κB signaling) to see if NF-κB governs the sphingosine-1-phosphate pathway in NSCLC CIC. This would implicate NF-κB in the induction of both autocrine factors examined in this dissertation, Activin and S1P.

A particularly interesting finding was the stark inhibition of invasion upon administration of the SK1 inhibitor to both treated and treated A549 spheroid cultures (Figure 18D). At this time, it is not known whether this is unique to S1P as a chemoattractant, or whether inhibiting SK1 blocks induction of pathways required for migration and invasion to any chemoattractant. SK1 is upregulated

in A549 cultures following TNF and TGFβ treatment, but it is also expressed prior to treatment, albeit at lower levels. Interestingly, untreated spheroid cultures also can migrate and invade *in vitro* (Figure 5A) as well as metastasize *in vivo* (Figure 6B). Therefore, it is possible that even in untreated cultures, SK1 activity is required for the basal levels of migration and invasion observed, by activating pathways required for these actions. On the other hand, this phenomenon may only be observed using S1P as a chemoattractant. This could be explained by the expression of S1P receptors being downstream of SK1 signaling in A549 cells. Cell surface expression of these receptors may be required to "sense" the S1P as a chemoattractant, so their downregulation may block migration to S1P.

Teasing apart the mechanism behind this could be done by repeating these experiments with a different chemoattractant (e.g. 10% FBS). Obtaining inhibition similar to that observed in Figure 18D would suggest that SK1 activity is essential for EMT in NSCLC and the acquired migratory and invasive phenotypes. However, if SK1 inhibition does not block invasion and migration to 10% FBS, then it would appear that the results in Figure 18D can be explained by downregulation of S1P receptors following SK1 inhibition, which could be required for migration to S1P. RNA-mediated interference targeting genes encoding the S1P receptors could then be used to identify which S1P receptors function as sensors for A549 cells.

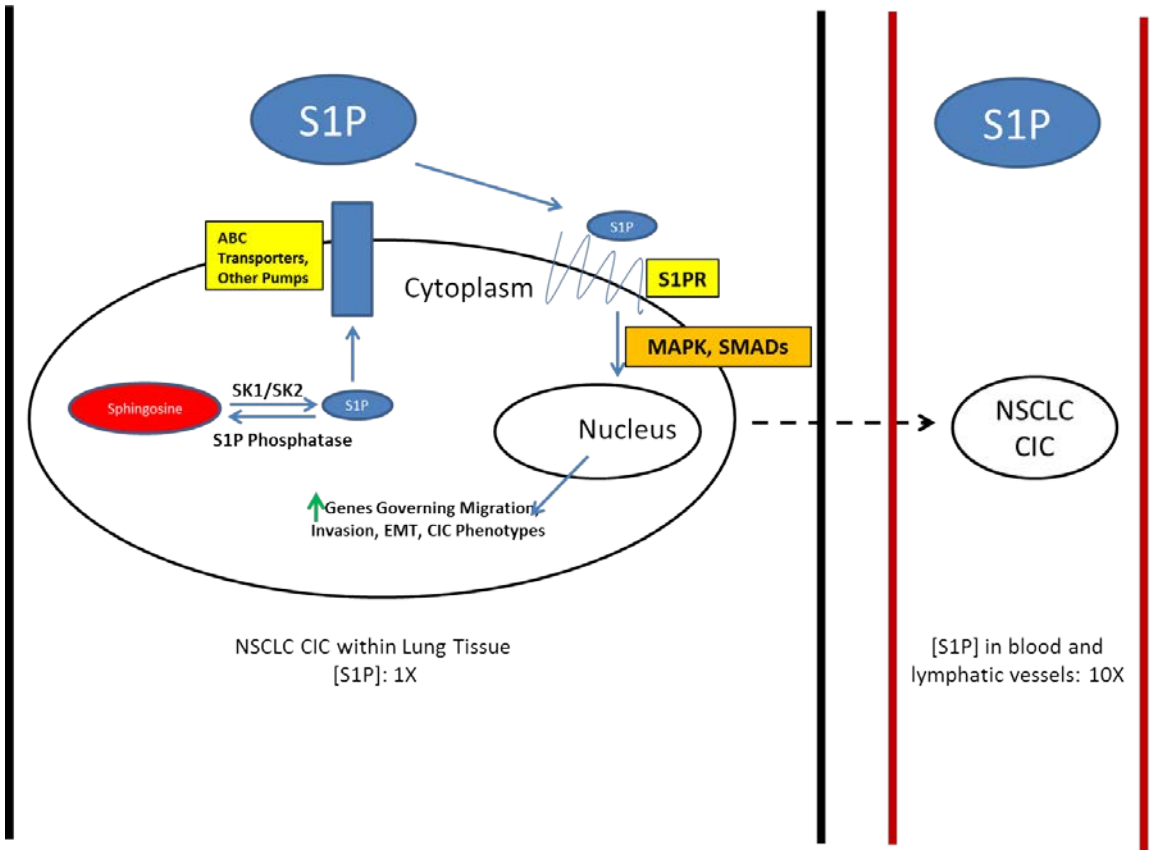
S1P
S1P
ABC
Transporters,
Other Pumps
S1P
Cytoplasm
S1PR
MAPK, SMADs
Sphingosine
SK1/SK2
S1P
S1P Phosphatase
Nucleus
NSCLC
CIC
Genes Governing Migration,
Invasion, EMT, CIC Phenotypes
NSCLC CIC within Lung Tissue
[S1P]: 1X
[S1P] in blood and
lymphatic vessels: 10X

Figure 19: S1P as an NSCLC CIC maintenance factor and chemoattractant. Within the NSCLC CIC, S1P (blue) is reversibly synthesized by either SK1 or SK2 from sphingosine (red). S1P is then exported from the cell by one of several membrane-embedded transport proteins, where it then acts in an autocrine fashion through one of its five G-protein coupled receptors (blue squiggle, yellow label). This receptor then promotes EMT and CIC phenotypes by activating SMADs. SMADs then translocate to the nucleus to regulate gene expression, as delineated in Figures 1 and 10. Intriguingly, S1P may also promote the egress of NSCLC CICs into the body's highway systems, due to the difference in concentrations between lung tissue (within black lines) and blood and lymphatic vessels (within red lines), driving dissemination of cancer-initiating and potentially metastatic cells.

CHAPTER 6: GENERAL DISCUSSION AND FUTURE DIRECTIONS

Despite recent advances made in targeted therapies, non-small cell lung cancer (NSCLC) remains the leading cause of cancer-related death among both men and women in the Western world. Innate and acquired resistance to both traditional and targeted therapies, and the frequency of metastasis, explain these dismal statistics. The epithelial-to-mesenchymal transition (EMT), an evolutionarily conserved de-differentiation program, is believed to promote drug resistance and metastasis by enriching for a pool of cancer-initiating cells (CICs) within the primary tumor. CICs are characteristically migratory, invasive, and self-renewing, enabling them to contribute to multiple steps of the metastatic cascade. Their ability to remodel the underlying extracellular matrix facilitates intravasation, and their self-renewal status promotes colonization of distal sites following dissemination. Furthermore, overexpression of drug efflux pumps, upregulation of anti-apoptotic pathways, and slow rates of proliferation render CICs insensitive to both chemoradiotherapy and targeted tyrosine kinase inhibitors. This drug-resistant, self-renewing pool of cells can regenerate bulk tumor cells successfully eradicated by treatment, contributing to relapse that occurs in patients who initially respond favorably to treatment. Hence, in order to effectively treat NSCLC, the CIC pool must be eradicated. Development of successful stemline treatment requires elucidating the mechanisms that underlie the formation and preservation of CICs.

A spheroid model for EMT and the propagation of CICs

The majority of data generated using cancer cell lines has been collected under the assumption that cells cultured as a monolayer behave as they do under physiological conditions. However, the surface to which cells attach when cultured as a monolayer, polystyrene, is highly artificial and fails to recapitulate cell-ECM interactions. Tissues are three-dimensional (3D) structures, as are the tumors that develop within them. Hence, there has been a recent push toward 3D models that more accurately mimic various aspects of tumor biology (Kunz-Schughart et al., 1998; Li et al., 2011; Pampaloni et al., 2007). Cells grown in spheroid cultures secrete more extracellular matrix (ECM) proteins, the surface to which cells attach *in vivo*, reflecting realistic tumor-stromal interactions. Moreover, gap junctions and intercellular interactions between cell surface adhesion and cell surface receptor proteins are much more prevalent in 3D and *in vivo* than in 2D. These cell-cell and cell-ECM interactions, many of which appear unique to 3D and physiological conditions, activate intracellular and intercellular signaling pathways that drive tumor growth and disease progression.

Rather than using co-culture systems, which introduce contaminating cell types other than NSCLC cells, we treated A549 spheroids with EMT-inducing cytokines prevalent in the tumor microenvironment. TNF is produced predominantly by tumor-associated M2 macrophages, while TGFβ is secreted by fibroblast and endothelial cells. We demonstrate that synergy between these two cytokines effectively and reproducibly induces EMT in spheroid cultures generated by a hanging droplet technique (Figure 3B, 3C, 4, 5). Surprisingly, A549 spheroids show increased migration without requiring exposure to TNF and

TGFβ and despite expressing epithelial markers (Figure 3B, 4A, and 5A). These findings indicate that phenotypic changes occur in 3D cultures prior to cytokine exposure. However, increased invasion is restricted to cytokine-induced A549 spheroid cultures and corresponds with the upregulation of matrix and extracellular remodeling enzymes known to induce invasive properties (Kirschmann et al., 2002; Yu & Stamenkovic, 2000). Together, this suggests that spheroid cultures are more sensitive to EMT-inducing cytokines when compared to NSCLC monolayers. Moreover, spheroid cultures are able to sustain the mesenchymal phenotype over a four-day time course.

Further support for using 3D cell culture models when modeling tumor biology is provided in Chapter 4, where we show that Activin is a critical maintenance factor of the mesenchymal phenotype. The ability to produce autocrine factors that mediate EMT in naïve 3D (N3D) cultures is restricted to spheroid cultures (Figure 7A), suggesting that NSCLC cells cultured as a monolayer lack the ability to preserve the mesenchymal markers that are induced, albeit modestly, following cytokine treatment. Importantly, cytokine-treated 2D cultures do not upregulate *Activin* mRNA levels at all (Figure 8B), nor is Activin even detectable in supernatants of monolayer cultures following stimulation (data not shown). Hence, had we limited our studies of EMT in NSCLC to 2D culture, this critical preservation factor would have never been identified.

Mesenchymal A549 cells possess constitutively active NF-κB signaling that is likely maintained by pro-inflammatory feedback loops

Constitutive NF-κB activation occurs in many different types of hematopoietic malignancies and carcinomas. However, mutations inducing chronic activation of NF-κB signaling are quite rare in epithelial cancers (Ben-Neriah & Karin, 2011). Thus, activation and maintenance of NF-κB signaling likely results from autocrine and paracrine signaling within the tumor microenvironment rather than genetic alterations (Ben-Neriah & Karin, 2011; Korkaya et al., 2011). Our data support this hypothesis, showing that TNF and TGFβ synergize to induce EMT by activating NF-κB (Figures 5A and 5B). However, the half-life of these cytokines in growth media is relatively short, suggesting that maintenance of NF-κB signaling requires autocrine signaling pathways mediated by pro-inflammatory cytokines.

Recent evidence has emerged suggesting that breast CICs activate an epigenetic switch to induce inflammatory circuits involving IL-6, IL-8, and IL-1β that mediate self-renewal of CICs by preserving NF-κB signaling (Ginestier et al., 2010; Iliopoulos et al., 2009; Kendellen et al., 2013; Xie et al., 2012). Ginestier and colleagues showed that breast CICs upregulate the IL-8 receptor CXCR1 to potentiate self-renewal, tumorigenicity and metastasis (Ginestier et al., 2010). Furthermore, Iliopoulos et al. demonstrated that upon transformation with Src, immortalized breast cells induce chronic activation of NF-κB that downregulates Let-7a, a negative microRNA regulator of IL-6. As a result, IL-6 drives an inflammatory feedback loop that sustains canonical NF-κB signaling (Iliopoulos et

al., 2009). IL-6 signaling pathways also downregulate miR200c, an miRNA family involved in suppressing EMT, in a chemically-induced transformed breast cancer cell line. Loss of miR200c subsequently results in constitutive activation of NF-κB through an inflammatory feed-forward signaling circuit (Rokavec et al., 2012). Most recently, both the canonical and non-canonical NF-κB signaling pathways were shown to be essential in maintenance of breast CICs by upregulating IL-6 and IL-1β (Kendellen et al., 2013). Taken together, these results indicate that following EMT, CICs secrete pro-inflammatory cytokines that act in an autocrine manner to preserve NF-κB signaling that underlies the invasive, stem cell-like phenotypes.

NF-κB expression is required for production of autocrine factors (Figure 9C), namely Activin (Figures 9A and 9B), that preserve the mesenchymal phenotype following induction. Hence, it seems intuitive that Activin, a pro-inflammatory cytokine, would be a candidate factor for sustaining canonical NF-κB signaling in NSCLC CICs. However, our data suggest otherwise. A key mechanism by which NF-κB drives EMT is the induction of *Twist* (Li et al., 2012; Pham et al., 2007). Indeed, in our model system, inhibition of the canonical NF-κB signaling pathway blocks expression of *Twist* (Figure 6D). However, pharmacological inhibition of Activin signaling (Figure 9D), as well as *Activin* knockdown (Figure 10D), have no effect on *Twist* expression, suggesting that constitutive NF-κB signaling is preserved by other autocrine factors.

The importance of a feed-forward inflammatory loop to preserve NF-κB signaling is illustrated in Figure 8E. Treatment with just the critical SMAD

maintenance factor, Activin, is insufficient to induce EMT in N3D cultures. However, co-stimulation with TNF to activate NF-κB induces EMT as efficiently as TNF and TGFβ (Figure 8E). These results suggest that Activin works in concert with currently unidentified pro-inflammatory cytokines to sustain CIC phenotypes. Interestingly, the initial NF-κB inducing signal utilized in our model system, TNF, is not upregulated in NSCLC CIC (data not shown), suggesting that other inflammatory cytokines are responsible for upkeep of constitutive NF-κB signaling following induction of EMT.

Additional work is needed to determine the potential involvement of IL-1β, IL-6 and IL-8 as feed-forward mediators of NF-κB activation in mesenchymal NSCLC cell lines. *IL8* (Figure 5B and Table 2) and *IL1B* (Table 2) are both highly upregulated and maintained in mesenchymal A549 cultures. However, *IL6* transcripts do not significantly change in 3D cultures following cytokine treatment (data not shown). Thus, in agreement with IIiopoulos and colleagues (Iliopoulos et al., 2009), IL-6 may not be a common requirement for CICs in lung cancer. An interesting extension of this work would be to repeat the experiment in Figure 8E, replacing TNF with IL-8 or IL-1β. Synergy with Activin in inducing EMT would strongly implicate one of these cytokines as a maintenance factor for NF-κB signaling.

NF-κB specifically upregulates* Activin *to maintain the phenotype of NSCLC CICs

Targeting CICs has been proposed as a promising approach to effectively treat epithelial malignancies (Nurwidya et al., 2012; Yi et al., 2013). However, therapies for their eradication have been limited due to our poor understanding of how this population of cells maintains its mesenchymal phenotype throughout the metastatic process. Treating A549 spheroid cultures with TNF and TGFβ leads to the upregulation and secretion of Activin (Figures 8A-C). This induction was observed in both established cell lines (Figures 8A-C) as well as tumor-derived primary NSCLC cells (Figure 8F). Inhibition of Activin signaling using shRNA silencing or pharmacological inhibition of the Alk4/5/7 receptor indicates that Activin is necessary to induce the expression of EMT master-switch regulators and self-renewing factors required for CIC phenotypes (Figures 9D and 9E). Finally, as an extension to what is understood about Nodal/Activin signaling as a self-renewing factor required for CICs (Lonardo et al., 2011), our studies indicate that Activin expression is required for NSCLC metastasis (Figure 11C). Thus, inhibition of Nodal/Activin signaling is a potentially important molecular target for eradicating circulating CICs responsible for NSCLC metastasis.

In an elegant study by Lonardo and colleagues, Nodal/Activin signaling was reported to be required for tumorigenicity of pancreatic carcinoma by supporting the self-renewal capacity of CICs (Lonardo et al., 2011). Interestingly, primary pancreatic spheroid cultures cultured in basic fibroblast growth factor (bFGF) and epithelial growth factor (EGF) express transcripts encoding Nodal and Activin. Although both recombinant Nodal and Activin support self-renewal activities, the knockdown of Nodal is sufficient to suppress self-renewal

properties of CICs. Thus, in pancreatic CICs, Nodal, not Activin, is the predominant TGFβ family member driving self-renewal phenotypes (Lonardo et al., 2011). This is in contrast to our findings that indicate Activin, not Nodal, drives EMT, expression of pluripotent factors, and metastatic potential of NSCLC CICs.

At the present time, it is not clear why different epithelial CICs demonstrate a distinct requirement for autocrine production of either Nodal or Activin. Although the difference could be due to tissue specificity, this explanation is unlikely since the endoderm is responsible for the development of both the lungs and the pancreas. A more plausible explanation is that exposure of carcinoma spheroid cultures to either growth factors (bFGF and EGF) or cytokines (TNF and TGFβ) dictates whether the CICs upregulate either Nodal or Activin in an autocrine manner. The ability of TNF and TGFβ to upregulate Activin is supported by our observation that cytokine treatment results in constitutive NF-κB activity (Figure 5), which is required to upregulate Activin mRNA expression and secretion (Figures 9A and 9B). Activin is upregulated in NSCLC and correlates with poor clinical outcomes (Seder et al., 2009b). In esophageal carcinoma, Activin, not Nodal, contributes to invasive, aggressive phenotypes (Yoshinaga et al., 2008, 2004). Additional work is needed to determine whether differences in either inflammatory (TNF and TGFβ) or proliferative (bFGF and EGF) cues govern whether the CICs upregulate and respond to either Activin or Nodal in NSCLC.

Inhibiting Nodal/Activin signaling offers a potentially important therapeutic strategy to target carcinoma CICs when used in combination with chemotherapy. Although the use of the Alk4/5/7 inhibitor SB431542 as a single therapy does not block tumor development *in vivo*, combined treatment with both SB431542 and gemcitibine was successful (Lonardo et al., 2011). Interestingly, the chemosensitizing effect was presumably due to the ability of the SB431542 treatment to block self-renewal and promote differentiation. However, targeting the CIC population alone may not be an effective strategy. Lonardo and colleagues found that tumor-associated stroma not only produce Nodal/Activin that can act in an paracrine-dependent manner to support CICs, but that the chemosensitizing effect of the Alk4/5/7 inhibitor SB431542 was lost in pancreatic xenografts. Although the reason for this effect is currently unknown, the authors speculated that it may have to do with the angiogenic nature of the tumor microenvironment and with ineffective drug delivery. Thus, successful chemotherapeutic targeting of CICs will most likely involve the use of multiple agents that abolish Nodal/Activin signaling within the tumor microenvironment.

Another possibility that could explain the inability of Alk4/5/7 inhibitor SB431542 to chemosensitize may have to do with the built-in redundancy of growth factors and inflammatory mediators that support CIC propagation. Although Activin and Nodal maintaining hESC pluripotency and CIC self-renewal, these factors do not act alone. For example, Activin and Nodal have been shown to maintain hESC pluripotency when cultured in the presence of bFGF (Vallier, Alexander, & Pedersen, 2005). In a similar manner, our work supports the role of

TNF as a costimulatory signal required to potentiate EMT in response to recombinant Activin (Figure 8E). In light of the recent work by Kendellen and colleagues (Kendellen et al., 2013), it will be important to determine if inflammatory cytokines, such as IL-1β and IL-8, work in concert with Activin to preserve the CIC phenotype.

Targeting both CICs and bulk carcinoma cells to eradicate NSCLC

It has become increasingly clear that in order to effectively treat non-small cell lung cancer, the population of CICs must be eliminated. Existing therapies that target the bulk carcinoma cells may initially yield promising results in some patients, as measured by shrinkage of the primary tumor. However, failure to destroy the robust, hardy CIC pool will inevitably lead to relapse. Work presented in this dissertation identifies two novel autocrine factors that potentiate the invasive and self-renewing capacities of CICs. Targeting these soluble factors may prove more effective in eradicating the CIC pool than attempting to disrupt the activity of the EMT master-switch and the self-renewal/"stem-like" transcription factors that drive CIC phenotypes. These transcription factors do not have catalytic clefts that enable binding of drug molecules, and neutralizing antibodies targeting them do not exist. Soluble decoy receptors, such as Sotatercept, have demonstrated specificity and efficacy, providing optimism that they may be effective in destroying CICs.

However, our findings also suggest that exclusively targeting CICs may be insufficient. Like many other laboratories, we demonstrate that cytokines present

within the tumor microenvironment induce EMT within a subset of the bulk carcinoma cells, causing them to become cancer-initiating cells with stem-like properties. Hence, even eradicating the standing population of CICs will not ensure that other CICs will not be generated from the bulk tumor cells via EMT. Therefore, further advances made in targeting the more differentiated cells still need to be made. These may include more optimization of chemotherapy regimen and identifying more molecular targets that drive non-CIC proliferation, in addition to EGFR and ALK. New driving mutations particularly need to be identified in squamous cell and large cell carcinomas, as all targetable mutations in NSCLC have been almost exclusively found in adenocarcinoma. Therefore, one could envision a scenario in which a patient with an activating EGFR mutation suffering from chemotherapy-induced anemia would be treated with both an EGFR TKI, to slow proliferation of the bulk tumor cells, as well as Sotatercept, to target CICs within the body. With all of the new evidence implicating CICs in disease relapse, as well as findings that CICs can be created via EMT in differentiated carcinoma cells, it will be interesting to see if there is an increase in clinical trials that utilize therapies that concomitantly target both pools of cells.

REFERENCES

Aberle DR, Adams, AM, Berg, CD, Black WC, Clapp JD, Fagerstrom RM, et al. Reduced lung-cancer mortality with low-dose computed tomographic screening. The New England Journal of Medicine 2011;365: 395–409.

Aisner, DL and Marshall CB. Molecular pathology of non-small cell lung cancer: a practical guide. American Journal of Clinical Pathology 2012;138:332–46.

Akao Y, Banno Y, Nakagawa Y, Hasegawa N, Kim T-J, Murate T, et al. High expression of sphingosine kinase 1 and S1P receptors in chemotherapy-resistant prostate cancer PC3 cells and their camptothecin-induced up-regulation. Biochemical and Biophysical Research Communications 2006;342:1284–90.

Al-Hajj M, Wicha MS, Benito-Hernandez A, Morrison SJ, and Clarke MF. Prospective identification of tumorigenic breast cancer cells. Proceedings of the National Academy of Sciences of the United States of America 2003;100:3983–8.

Al Husaini H, Wheatley-Price P, Clemons M, and Shepherd FA. Prevention and management of bone metastases in lung cancer: a review. Journal of Thoracic Oncology 2009;4:251–9.

Alison MR, Lim SML, and Nicholson LJ. Cancer stem cells: problems for therapy? The Journal of Pathology 2011;223:147–61.

Allison DF, Wamsley JJ, Kumar M, Li D, Gray LG, Hart GW, et al. Modification of RelA by O-linked N-acetylglucosamine links glucose metabolism to NF-κB acetylation and transcription. Proceedings of the National Academy of Sciences of the United States of America 2012;109:16888–93.

Al-Saad S, Al-Shibli K, Donnem T, Persson M, Bremnes RM, and Busund L-T. The prognostic impact of NF-kappaB p105, vimentin, E-cadherin and Par6 expression in epithelial and stromal compartment in non-small-cell lung cancer. British Journal of Cancer 2008;99:1476–83.

Antsiferova M, Huber M, Meyer M, Piwko-Czuchra A, Ramadan T, MacLeod AS, et al (2011). Activin enhances skin tumourigenesis and malignant progression by inducing a pro-tumourigenic immune cell response. Nature Communications;2:576.

Antsiferova M and Werner S. The bright and the dark sides of activin in wound healing and cancer. Journal of Cell Science 2012;125:3929–37.

Asiedu MK, Ingle JN, Behrens MD, Radisky DC, and Knutson KL. TGFβ/TNFα-mediated epithelial-mesenchymal transition generates breast cancer stem cells with a claudin-low phenotype. Cancer Research 2011;71:4707–19.

Au PYB, Martin N, Chau H, Moemeni B, Chia M, Liu F-F, et al. The oncogene PDGF-B provides a key switch from cell death to survival induced by TNF. Oncogene 2005; 24:3196–205.

Avery K, Avery S, Shepherd J, Heath PR, and Moore H. Sphingosine-1-phosphate mediates transcriptional regulation of key targets associated with survival, proliferation, and pluripotency in human embryonic stem cells. Stem Cells and Development 2008;17:1195–205.

Bach PB, Mirkin JN, Oliver TK, Azzoli CG, Berry DA, Brawley OW, et al. Benefits and harms of CT screening for lung cancer: a systematic review. JAMA : The Journal of the American Medical Association 2012;307:2418–29.

Barberà MJ, Puig I, Domínguez D, Julien-Grille S, Guaita-Esteruelas S, Peiró S, et al. Regulation of Snail transcription during epithelial to mesenchymal transition of tumor cells. Oncogene 2004;23:7345–54.

Bassères DS and Baldwin AS. Nuclear factor-kappaB and inhibitor of kappaB kinase pathways in oncogenic initiation and progression. Oncogene 2006;25:6817–30.

Bates RC and Mercurio AM. Tumor Necrosis Factor Stimulates the Epithelial-to-Mesenchymal Transition of Human Colonic Organoids. Molecular Biology of the Cell 2003;14:1790–1800.

Beattie GM, Lopez AD, Bucay N, Hinton A, Firpo MT, King CC, et al. Activin A maintains pluripotency of human embryonic stem cells in the absence of feeder layers. Stem Cells 2005;23:489–95.

Ben-Neriah Y and Karin M. Inflammation meets cancer, with NF-κB as the matchmaker. Nature Immunology 2011;12:715–23.

Bendre MS, Margulies AG, Walser B, Akel NS, Bhattacharrya S, Skinner RA, et al. Tumor-derived interleukin-8 stimulates osteolysis independent of the receptor activator of nuclear factor-κB ligand pathway. Cancer Research 2005;65:11001–9.

Bendre MS, Montague DC, Peery T, Akel NS, Gaddy D, and Suva LJ. Interleukin-8 stimulation of osteoclastogenesis and bone resorption is a mechanism for the increased osteolysis of metastatic bone disease. Bone 2003;33:28–37.

Bolós V, Peinado H, Pérez-Moreno MA, Fraga MFF, Esteller M, and Cano A. The transcription factor Slug represses E-cadherin expression and induces epithelial to mesenchymal transitions: a comparison with Snail and E47 repressors. Journal of Cell Science 2002;116:499–511.

Cai KX, Tse LY, Leung C, Tam PKH, Xu R, and Sham MH. Suppression of lung tumor growth and metastasis in mice by adeno-associated virus-mediated expression of vasostatin. Clinical Cancer Research 2008;14:939–49.

Câmara J and Jarai G. Epithelial-mesenchymal transition in primary human bronchial epithelial cells is Smad-dependent and enhanced by fibronectin and TNF-alpha. Fibrogenesis & Tissue Repair 2010;3:2.

Chang K-P, Kao H-K, Liang Y, Cheng M-H, Chang Y-L, Liu S-C, et al. Overexpression of activin A in oral squamous cell carcinoma: association with poor prognosis and tumor progression. Annals of Surgical Oncology 2010;17:1945–56.

Chantry AD, Heath D, Mulivor AW, Pearsall S, Baud'huin M, Coulton L, et al. Inhibiting activin-A signaling stimulates bone formation and prevents cancer-induced bone destruction in vivo. Journal of Bone and Mineral Research 2010;25:2633–46.

Chen W, Li Z, Bai L, and Lin Y. NF-kappaB in lung cancer, a carcinogenesis mediator and a prevention and therapy target. Frontiers in Bioscience 2011;16:1172–85.

Chen Y, Zhang Y, Yin Y, Gao G, Li S, Jiang Y, et al. SPD--a web-based secreted protein database. Nucleic Acids Research 2005;33:D169–73.

Chen Y-C, Hsu H-S, Chen Y-W, Tsai T-H, How C-K, Wang C-Y, et al. Oct-4 expression maintained cancer stem-like properties in lung cancer-derived CD133-positive cells. PLoS ONE 2008;3.

Chen Y-G, Wang Q, Lin S-L, Chang CD, Chuang J, Chung J, et al. Activin signaling and its role in regulation of cell proliferation, apoptosis, and carcinogenesis. Experimental Biology and Medicine 2006;231:534–44.

Cheng Z-X, Sun B, Wang S-J, Gao Y, Zhang Y-M, Zhou H-X, et al. Nuclear factor-κB-dependent epithelial to mesenchymal transition induced by HIF-1α activation in pancreatic cancer cells under hypoxic conditions. PLoS ONE 2011;6:e23752.

Chiou S-H, Wang M-L, Chou Y-T, Chen C-J, Hong C-F, Hsieh W-J, et al. Coexpression of Oct4 and Nanog enhances malignancy in lung

adenocarcinoma by inducing cancer stem cell-like properties and epithelial-mesenchymal transdifferentiation. Cancer Research 2010;70:10433–44.

Chua HL, Bhat-Nakshatri P, Clare SE, Morimiya A, Badve S, and Nakshatri H. NF-kappaB represses E-cadherin expression and enhances epithelial to mesenchymal transition of mammary epithelial cells: potential involvement of ZEB-1 and ZEB-2. Oncogene 2007;26:711–24.

Cirri P and Chiarugi P. Cancer-associated-fibroblasts and tumour cells: a diabolic liaison driving cancer progression. Cancer Metastasis Reviews 2012;31:195–208.

Cowden Dahl KD, Symowicz J, Ning Y, Gutierrez E, Fishman DA, Adley BP, et al. Matrix metalloproteinase 9 is a mediator of epidermal growth factor-dependent e-cadherin loss in ovarian carcinoma cells. Cancer Research 2008;68:4606–13.

Cufer T, Ovcaricek T, and O'Brien MER. Systemic therapy of advanced non-small cell lung cancer: major-developments of the last 5-years. European Journal of Cancer 2013;49:1216–25.

Camidge DR, Bang Y, Kwak EL, Shaw AT, Iafrate AJ, Maki RG, et al. Progression-free survival (PFS) from a phase I study of crizotinib (PF-02341066) in patients with ALK-positive non-small cell lung cancer (NSCLC). ASCO Annual Meeting Abstracts 2011.

D'Addario G, Früh M, Reck M, Baumann P, Klepetko W, and Felip E. Metastatic non-small-cell lung cancer: ESMO Clinical Practice Guidelines for diagnosis, treatment and follow-up. Annals of Oncology: Official Journal of the European Society for Medical Oncology 2010;21:v116–9.

Del Mastro L, Gennari A, and Donati S. Chemotherapy of non-small-cell lung cancer: role of erythropoietin in the management of anemia. Annals of Oncology 1999;10(S5):S91–4.

Deng X, Tannehill-Gregg SH, Nadella MVP, He G, Levine A, Cao Y, and Rosol TJ. Parathyroid hormone-related protein and ezrin are up-regulated in human lung cancer bone metastases. Clinical and Experimental Metastasis 2007;24:107–19.

Djouad F, Jackson WM, Bobick BE, Janjanin S, Song Y, Huang GTJ, et al. Activin A expression regulates multipotency of mesenchymal progenitor cells. Stem Cell Research and Therapy 2010:1,11.

Eramo A, Lotti F, Sette G, Pilozzi E, Biffoni M, Di Virgilio A, et al. Identification and expansion of the tumorigenic lung cancer stem cell population. Cell Death and Differentiation 2008;15:504–14.

Facoetti A, Pasi F, and Nano R. Some Considerations for the Study of TGFβ in Medium of Irradiated T98G Cells: Activation, Release and Consumption. Anticancer Research 2010;30:3341–3344.

Fang J, Yin W, Smiley E, Wang SQ, and Bonadio J. Molecular cloning of the mouse activin beta E subunit gene. Biochemical and Biophysical Research Communications 1996;228:669–74.

Floor S, van Staveren WCG, Larsimont D, Dumont JE, and Maenhaut C. Cancer cells in epithelial-to-mesenchymal transition and tumor-propagating-cancer stem cells: distinct, overlapping or same populations. Oncogene 2011;30:4609–21.

Fuxe J, and Karlsson MCI. TGF-β-induced epithelial-mesenchymal transition: a link between cancer and inflammation. Seminars in Cancer Biology 2012;22:455–61.

Gaikwad A, Gupta A, Hare S, Gomes M, Sekhon H, Souza C, et al. Primary adenocarcinoma of lung: a pictorial review of recent updates. European Journal of Radiology 2012;81:4146–55.

Gao D, Vahdat LT, Wong S, Chang JC, and Mittal V. Microenvironmental regulation of epithelial-mesenchymal transitions in cancer. Cancer Research 2012;72:4883–9.

Gatzemeier U, Pluzanska A, Szczesna A, Kaukel E, Roubec J, De Rosa F, et al. Phase III study of erlotinib in combination with cisplatin and gemcitabine in advanced non-small-cell lung cancer: the Tarceva Lung Cancer Investigation Trial. Journal of Clinical Oncology: Official Journal of the American Society of Clinical Oncology 2007;25:1545–52.

Giaccone G, Herbst RS, Manegold C, Scagliotti G, Rosell R, Miller V, et al. Gefitinib in combination with gemcitabine and cisplatin in advanced non-small-cell lung cancer: a phase III trial--INTACT 1. Journal of Clinical Oncology: Official Journal of the American Society of Clinical Oncology 2004;22:777–84.

Gilbert MTP, Haselkorn T, Bunce M, Sanchez JJ, Lucas SB, Jewell LD, et al. The isolation of nucleic acids from fixed, paraffin-embedded tissues-which methods are useful when? PLoS ONE 2007;2:e537.

Ginestier C, Liu S, Diebel ME, Korkaya H, Luo M, Brown M, et al. CXCR1 blockade selectively targets human breast cancer stem cells in vitro and in xenografts. The Journal of Clinical Investigation 2010;120:485–97.

Gottschling S, Schnabel PA, Herth FJF, and Herpel E. Are we missing the target? Cancer stem cells and drug resistance in non-small cell lung cancer. Cancer Genomics and Proteomics 2012;9:275–86.

Group NMAC. Chemotherapy in addition to supportive care improves survival in advanced non-small-cell lung cancer: a systematic review and meta-analysis of individual patient data from 16 randomized controlled trials. Journal of Clinical Oncology: Official Journal of the American Society of Clinical Oncology 2008;26:4617–25.

Guise TA, Yin JJ, Taylor SD, Kumagai Y, Dallas M, Boyce BF, et al. Evidence for a causal role of parathyroid hormone-related protein in the pathogenesis of human breast cancer-mediated osteolysis. The Journal of Clinical Investigation 1996; 98:1544–9.

Hasegawa Y, Takanashi S, Kanehira Y, Tsushima T, Imai T, and Okumura K. Transforming growth factor-β1 level correlates with angiogenesis, tumor progression, and prognosis in patients with non-small cell lung carcinoma. Cancer 2001;91:964–71.

Hayden MS and Ghosh S. Shared principles in NF-κB signaling. Cell 2008;132:344–62.

Heffernan-Stroud LA and Obeid LM. Sphingosine kinase 1 in cancer. Advances in Cancer Research 2013;117:201–35.

Heldin C-H, Vanlandewijck M, and Moustakas A. Regulation of EMT by TGFβ in cancer. FEBS Letters 2012;586:1959–70.

Herbst RS, Giaccone G, Schiller JH, Natale RB, Miller V, Manegold C, et al. Gefitinib in combination with paclitaxel and carboplatin in advanced non-small-cell lung cancer: a phase III trial--INTACT 2. Journal of Clinical Oncology: Official Journal of the American Society of Clinical Oncology 2004;22:785–94.

Herbst RS, Prager D, Hermann R, Fehrenbacher L, Johnson BE, Sandler A, et al. TRIBUTE: a phase III trial of erlotinib hydrochloride (OSI-774) combined with carboplatin and paclitaxel chemotherapy in advanced non-small-cell lung cancer. Journal of Clinical Oncology: Official Journal of the American Society of Clinical Oncology 2005;23:5892–9.

Hermann PC, Huber SL, Herrler T, Aicher A, Ellwart JW, Guba M, et al. Distinct populations of cancer stem cells determine tumor growth and metastatic activity in human pancreatic cancer. Cell Stem Cell 2007;1:313–23.

Ho MM, Ng AV, Lam S, and Hung JY. Side population in human lung cancer cell lines and tumors is enriched with stem-like cancer cells. Cancer Research 2007;67:4827–33.

Hoberg JE, Popko AE, Ramsey CS, and Mayo MW. IκB kinase alpha-mediated derepression of SMRT potentiates acetylation of RelA/p65 by p300. Molecular and Cellular Biology 2006;26:457–71.

Hoberg JE, Yeung F, and Mayo MW. SMRT derepression by the IκB kinase α: a prerequisite to NF-κB transcription and survival. Molecular Cell 2004;16:245–55.

Horbelt D, Denkis A, and Knaus P. A portrait of Transforming Growth Factor β superfamily signalling: Background matters. The International Journal of Biochemistry & Cell Biology 2012;44:469–74.

Hotten G, Neidhardt H, Schneider C, and Pohl J. Cloning of a New Member of the TGF-β Family: A Putative New Activin βC Chain. Biochemical and Biophysical Research Communications 1995;206:608–613.

Huber MA, Azoitei N, Baumann B, Grünert S, Sommer A, Pehamberger H, et al. NF-κB is essential for epithelial- mesenchymal transition and metastasis in a model of breast cancer progression. The Journal of Clinical Investigation 2004;114:569–581.

Hung J-J, Yang M-H, Hsu H-S, Hsu W-H, Liu J-S, and Wu K-J. Prognostic significance of hypoxia-inducible factor-1alpha, TWIST1 and Snail expression in resectable non-small cell lung cancer. Thorax 2009;64:1082–9.

Iancu-Rubin C, Mosoyan G, Wang J, Kraus T, Sung V, and Hoffman R. Stromal cell-mediated inhibition of erythropoiesis can be attenuated by Sotatercept (ACE-011), an activin receptor type II ligand trap. Experimental Hematology 2013;41:155–166.

Iliopoulos D, Hirsch HA, and Struhl K. An epigenetic switch involving NF-kappaB, Lin28, Let-7 MicroRNA, and IL6 links inflammation to cell transformation. Cell 2009;139: 693–706.

Incorvaia L, Badalamenti G, Rini G, Arcara C, Fricano S, Sferrazza C, et al. MMP-2, MMP-9 and activin A blood levels in patients with breast cancer or

prostate cancer metastatic to the bone. Anticancer Research 2007;27:1519–25.

Inman GJ, Nicolás FJ, Callahan JF, Harling JD, Gaster LM, Reith AD, et al. SB-431542 is a potent and specific inhibitor of transforming growth factor-beta superfamily type I activin receptor-like kinase (ALK) receptors ALK4, ALK5, and ALK7. Molecular Pharmacology 2002;62:65–74.

Ito H, Matsuo K, Tanaka H, Koestler DC, Ombao H, Fulton J, et al. Nonfilter and filter cigarette consumption and the incidence of lung cancer by histological type in Japan and the United States: analysis of 30-year data from population-based cancer registries. International Journal of Cancer 2011;128:1918–28.

Johnson KR, Johnson KY, Crellin HG, Ogretmen B, Boylan AM, Harley RA, et al. Immunohistochemical distribution of sphingosine kinase 1 in normal and tumor lung tissue. The Journal of Histochemistry and Cytochemistry: Official Journal of the Histochemistry Society 2005;53:1159–66.

Julien S, Puig I, Caretti E, Bonaventure J, Nelles L, van Roy F, et al. Activation of NF-kappaB by Akt upregulates Snail expression and induces epithelium mesenchyme transition. Oncogene 2007;26:7445–56.

Kang H, Huang H, Hsieh C, Li C, Shyr C, Tsai M, et al. Activin A Enhances Prostate Cancer Cell Migration Through Activation of Androgen Receptor and Is Overexpressed in Metastatic Prostate Cancer. Journal of Bone and Mineral Research 2009;24:1180–1193.

Kasai K, Sato Y, Kameya T, Inoue H, Yoshimura H, Kon S, et al. Incidence of latent infection of Epstein-Barr virus in lung cancers--an analysis of EBER1 expression in lung cancers by in situ hybridization. The Journal of Pathology 1994;174:257–65.

Kase S, Sugio K, Yamazaki K, Okamoto T, Yano T, and Sugimachi K. Expression of E-cadherin and β-Catenin in Human Non-Small Cell Lung Cancer and the Clinical Significance. Clinical Cancer Research 2000;6:4789–4796.

Katsenos S, Karachaliou I, and Archondakis S. Mixed squamous and large-cell carcinoma of the lung: a case study and literature review. Journal of Cancer Research and Therapeutics 2012;8:445–7.

Kawata M, Koinuma D, Ogami T, Umezawa K, Iwata C, Watabe T, et al. TGF-β-induced epithelial-mesenchymal transition of A549 lung adenocarcinoma cells is enhanced by pro-inflammatory cytokines derived from RAW 264.7 macrophage cells. Journal of Biochemistry 2012;151:205–16.

Kelm JM, Timmins NE, Brown CJ, Fussenegger M, and Nielsen LK. Method for generation of homogeneous multicellular tumor spheroids applicable to a wide variety of cell types. Biotechnology and Bioengineering 2003;83:173–80.

Kendellen MF, Bradford JW, Lawrence CL, Clark KS, and Baldwin AS. Canonical and non-canonical NF-κB signaling promotes breast cancer tumor-initiating cells. Oncogene 2013.

Kharel Y, Mathews TP, Gellett AM, Tomsig JL, Kennedy PC, Moyer ML, et al. Sphingosine kinase type 1 inhibition reveals rapid turnover of circulating sphingosine 1-phosphate. The Biochemical Journal 2011;440:345–53.

Kim DY, Ahn M-J, Shi Y, De Pas TM, Yang P-C, Riely GJ, et al. Results of a global phase II study with crizotinib in advanced ALK-positive non-small cell lung cancer (NSCLC). ASCO Annual Meeting Abstracts 2012.

Kim E-S, Kim J-S, Kim SG, Hwang S, Lee CH, and Moon A. Sphingosine 1-phosphate regulates matrix metalloproteinase-9 expression and breast cell invasion through S1P3-Gαq coupling. Journal of Cell Science 2011;124:2220–30.

Kim S-H, Choe C, Shin Y-S, Jeon M-J, Choi S-J, Lee J, et al. Human lung cancer-associated fibroblasts enhance motility of non-small cell lung cancer cells in co-culture. Anticancer Research 2013;33:2001–9.

Kimura T, Watanabe T, Sato K, Kon J, Tomura H, Tamama K, et al. Sphingosine 1-phosphate stimulates proliferation and migration of human endothelial cells possibly through the lipid receptors, Edg-1 and Edg-3. The Biochemical Journal 2000;348:71–6.

Kingsley LA, Fournier PGJ, Chirgwin JM, and Guise TA. Molecular biology of bone metastasis. Molecular Cancer Therapeutics 2007;6:2609–17.

Kirschmann DA, Seftor EA, Fong SFT, Nieva DRC, Sullivan CM, Edwards EM, et al. A molecular role for lysyl oxidase in breast cancer invasion. Cancer Research 2002;62:4478–83.

Klein F, Amin Kotb WFM, and Petersen I. Incidence of human papilloma virus in lung cancer. Lung Cancer 2009;65:13–8.

Kono Y, Nishiuma T, Nishimura Y, Kotani Y, Okada T, Nakamura S-I, et al. Sphingosine kinase 1 regulates differentiation of human and mouse lung fibroblasts mediated by TGF-β1. American Journal of Respiratory Cell and Molecular Biology 2007;37: 395–404.

Korkaya H, Liu S, and Wicha MS. Breast cancer stem cells, cytokine networks, and the tumor microenvironment. The Journal of Clinical Investigation 2011;121:3804–9.

Kumar M, Allison DF, Baranova NN, Wamsley JJ, Katz AJ, Bekiranov S, et al. NF-κB Regulates Mesenchymal Transition for the Induction of Non-Small Cell Lung Cancer Initiating Cells. PLoS ONE 2013;8:e68597.

Kunz-Schughart LA, Kreutz M, and Knuechel R. Multicellular spheroids: a three-dimensional in vitro culture system to study tumour biology. International Journal of Experimental Pathology 1998;79:1–23.

Kuo P-L, Liao S-H, Hung J-Y, Huang M-S, and Hsu Y-L. MicroRNA-33a functions as a bone metastasis suppressor in lung cancer by targeting parathyroid hormone related protein. Biochimica et Biophysica Acta 2013;1830:3756–66.

Lapidot T, Sirard C, Vormoor J, Murdoch B, Hoang T, Caceres-Cortes J, et al. A cell initiating human acute myeloid leukaemia after transplantation into SCID mice. Nature 1994;367:645–8.

Le Bras GF, Allison GL, Richards NF, Ansari SS, Washington MK, and Andl CD. CD44 upregulation in E-cadherin-negative esophageal cancers results in cell invasion. PLoS ONE 2011;6:e27063.

Lee MJ, Thangada S, Claffey KP, Ancellin N, Liu CH, Kluk M, et al. Vascular endothelial cell adherens junction assembly and morphogenesis induced by sphingosine-1-phosphate. Cell 1999;99:301–12.

Leis O, Eguiara A, Lopez-Arribillaga E, Alberdi MJ, Hernandez-Garcia S, Elorriaga K, et al. Sox2 expression in breast tumours and activation in breast cancer stem cells. Oncogene 2012;31:1354–65.

Leto G. Activin A and bone metastasis. Journal of Cellular Physiology 2010;225:302–9.

Leto G, Incorvaia L, Badalamenti G, Tumminello FM, Gebbia N, Flandina C, et al. Activin A circulating levels in patients with bone metastasis from breast or prostate cancer. Clinical and Experimental Metastasis 2006;23:117–22.

Leung EL-H, Fiscus RR, Tung JW, Tin VP-C, Cheng LC, Sihoe AD-L, et al. Non-small cell lung cancer cells expressing CD44 are enriched for stem cell-like properties. PLoS ONE 2010;5:e14062.

Levina V, Marrangoni A, Wang T, Parikh S, Su Y, Herberman R, et al. Elimination of human lung cancer stem cells through targeting of the stem cell factor-c-kit autocrine signaling loop. Cancer Research 2010;70:338–46.

Li C-W, Xia W, Huo L, Lim S-O, Wu Y, Hsu JL, et al. Epithelial-mesenchymal transition induced by TNF-α requires NF-κB-mediated transcriptional upregulation of Twist1. Cancer Research 2012;72:1290–300.

Li F, Zeng H, and Ying K. The combination of stem cell markers CD133 and ABCG2 predicts relapse in stage I non-small cell lung carcinomas. Medical Oncology 2011; 28:1458–62.

Li Q, Chen C, Kapadia A, Zhou Q, Harper MK, Schaack J, et al. 3D models of epithelial-mesenchymal transition in breast cancer metastasis: high-throughput screening assay development, validation, and pilot screen. Journal of Biomolecular Screening 2011;16:141–54.

Li Y, Ohms SJ, Sun C, and Fan J. NF-κB controls Il2 and Csf2 expression during T cell development and activation process. Molecular Biology Reports 2013;40:1685–92.

Ling N, Ying SY, Ueno N, Shimasaki S, Esch F, Hotta M, et al. Pituitary FSH is released by a heterodimer of the beta-subunits from the two forms of inhibin. Nature 1986;321:779–82.

Liu J, Hsu A, Lee K-F, Cramer DE, and Lee M-J. To stay or to leave: Stem cells and progenitor cells navigating the S1P gradient. *World journal of biological chemistry 2011*, *2*(1), 1–13. doi:10.4331/wjbc.v2.i1.1

Liu M, Sakamaki T, Casimiro MC, Willmarth NE, Quong AA, Ju X, et al. The canonical NF-kappaB pathway governs mammary tumorigenesis in transgenic mice and tumor stem cell expansion. Cancer Research 2010;70:10464–73.

Liu Y, Wada R, Yamashita T, Mi Y, Deng CX, Hobson JP, et al. Edg-1, the G protein-coupled receptor for sphingosine-1-phosphate, is essential for vascular maturation. The Journal of Clinical Investigation 2000;106:951–61.

Lonardo E, Hermann PC, Mueller M-T, Huber S, Balic A, Miranda-Lorenzo I, et al. Nodal/Activin signaling drives self-renewal and tumorigenicity of pancreatic cancer stem cells and provides a target for combined drug therapy. Cell Stem Cell 2011;9: 433–46.

Lorenzen JR, Channing CP, and Schwartz NB. Partial characterization of FSH suppressing activity (folliculostatin) in porcine follicular fluid using the metestrous rat as an in vivo bioassay model. Biology of Reproduction 1978;19:635–40.

Maemondo M, Inoue A, Kobayashi K, Sugawara S, Oizumi S, Isobe H, et al. Gefitinib or Chemotherapy for Non–Small-Cell Lung Cancer with Mutated EGFR. The NEw England Journal of Medicine 2010;362:2380-8.

Mani SA, Guo W, Liao MJ, Eaton EN, Ayyanan A, Zhou AY, et al. The epithelial-mesenchymal transition generates cells with properties of stem cells. Cell 2008; 133:704–715.

Mayo MW, Wang CY, Cogswell PC, Rogers-Graham KS, Lowe SW, Der CJ, et al. Requirement of NF-kappaB activation to suppress p53-independent apoptosis induced by oncogenic Ras. Science 1997;278:1812–5.

Meuwissen R and Berns A. Mouse models for human lung cancer. Genes & Development 2005;19:643–64.

Meyer MJ, Fleming JM, Ali MA, Pesesky MW, Ginsburg E, and Vonderhaar BK. Dynamic regulation of CD24 and the invasive, CD44posCD24neg phenotype in breast cancer cell lines. Breast Cancer Research 2009;11:R82.

Miki T, Yano S, Hanibuchi M, Kanematsu T, Muguruma H, and Sone S. Parathyroid hormone-related protein (PTHrP) is responsible for production of bone metastasis, but not visceral metastasis, by human small cell lung cancer SBC-5 cells in natural killer cell-depleted SCID mice. International Journal of Cancer;108:511–5.

Milara J, Navarro R, Juan G, Peiró T, Serrano A, Ramón M, et al. Sphingosine-1-phosphate is increased in patients with idiopathic pulmonary fibrosis and mediates epithelial to mesenchymal transition. Thorax 2012;67:147–56.

Miller AV, Alvarez SE, Spiegel S, and Lebman DA. Sphingosine kinases and sphingosine-1-phosphate are critical for transforming growth factor beta-induced extracellular signal-regulated kinase 1 and 2 activation and promotion of migration and invasion of esophageal cancer cells. Molecular and Cellular Biology 2008; 28:4142–51.

Min C, Eddy SF, Sherr DH, and Sonenshein GE. NF-κB and epithelial to mesenchymal transition of cancer. Journal of Cellular Biochemistry 2008;104:733–44.

Mitsudomi T, Morita S, Yatabe Y, Negoro S, Okamoto I, Tsurutani J, et al. Gefitinib versus cisplatin plus docetaxel in patients with non-small-cell lung cancer harbouring mutations of the epidermal growth factor receptor (WJTOG3405): an open label, randomised phase 3 trial. The Lancet Oncology 2010;11:121–8.

Mizugishi K, Yamashita T, Olivera A, Miller GF, Spiegel S, and Proia RL. Essential role for sphingosine kinases in neural and vascular development. Molecular and Cellular Biology 2005;25:11113–21.

Morel A-P, Lièvre M, Thomas C, Hinkal G, Ansieau S, and Puisieux A. Generation of breast cancer stem cells through epithelial-mesenchymal transition. PLoS ONE 2008;3:e2888.

Nitz MD, Harding MA, and Theodorescu D. Invasion and metastasis models for studying RhoGDI2 in bladder cancer. Methods in Enzymology 2008;439:219–33.

Noë V, Fingleton B, Jacobs K, Crawford HC, Vermeulen S, Steelant W, et al. Release of an invasion promoter E-cadherin fragment by matrilysin and stromelysin-1. Journal of Cell Science 2001;114:111–118.

Nurwidya F, Murakami A, Takahashi F, and Takahashi K. Lung cancer stem cells: tumor biology and clinical implications. Asia-Pacific Journal of Clinical Oncology 2012;8: 217–22.

O'Brien CA, Pollett A, Gallinger S, and Dick JE. A human colon cancer cell capable of initiating tumour growth in immunodeficient mice. Nature 2007;445:106–10.

Oda S, Nishimatsu S, Murakami K, and Ueno N. Molecular cloning and functional analysis of a new activin beta subunit: a dorsal mesoderm-inducing activity in Xenopus. Biochemical and Biophysical Research Communications 1995;210:581–8.

Ogawa Y, Schmidt DK, Nathan RM, Armstrong RM, Miller KL, Sawamura SJ, et al. Bovine bone activin enhances bone morphogenetic protein-induced ectopic bone formation. The Journal of Biological Chemistry 1992;267:14233–7.

Oshimori N, and Fuchs E. The harmonies played by TGF-β in stem cell biology. Cell Stem Cell 2012;11:751–64.

Oyama O, Sugimoto N, Qi X, Takuwa N, Mizugishi K, Koizumi J, et al. The lysophospholipid mediator sphingosine-1-phosphate promotes angiogenesis in vivo in ischaemic hindlimbs of mice. Cardiovascular Research 2008;78:301–7.

Pampaloni F, Reynaud EG, and Stelzer EHK. The third dimension bridges the gap between cell culture and live tissue. Nature Reviews: Molecular Cell Biology 2007; 8:839–45.

Passier R, and Mummery C. Origin and use of embryonic and adult stem cells in differentiation and tissue repair. Cardiovascular Research 2003;58:324–335.

Petersen I. The morphological and molecular diagnosis of lung cancer. Deutsches Ärzteblatt International 2011;108:525–31.

Pham CG, Bubici C, Zazzeroni F, Knabb JR, Papa S, Kuntzen C, et al. Upregulation of Twist-1 by NF-kappaB blocks cytotoxicity induced by chemotherapeutic drugs. Molecular and Cellular Biology 2007;27:3920–35.

Phillips DJ, Jones KL, Clarke IJ, Scheerlinck J-PY, and de Kretser DM. Activin A: from sometime reproductive factor to genuine cytokine. Veterinary Immunology and Immunopathology 2005;108:23–7.

Pyne NJ, Tonelli F, Lim KG, Long JS, Edwards J, and Pyne S. Sphingosine 1-phosphate signalling in cancer. Biochemical Society Transactions 2012;40:94–100.

Pyne S and Pyne NJ. New perspectives on the role of sphingosine 1-phosphate in cancer. Handbook of Experimental Pharmacology 2013;216:55–71.

Raparia K, Villa C, DeCamp MM, Patel JD, and Mehta MP. Molecular profiling in non-small cell lung cancer: a step toward personalized medicine. Archives of Pathology & Laboratory Medicine 2013;137:481–91.

Raje N and Vallet S. Sotatercept, a soluble activin receptor type 2A IgG-Fc fusion protein for the treatment of anemia and bone loss. Current Opinion in Molecular Therapeutics 2010;12:586–97.

Rokavec M, Wu W, and Luo J-L. IL6-mediated suppression of miR-200c directs constitutive activation of inflammatory signaling circuit driving transformation and tumorigenesis. Molecular Cell 2012;45:777–89.

Scheel C, Eaton EN, Li SH-J, Chaffer CL, Reinhardt F, Kah K-J, et al. Paracrine and autocrine signals induce and maintain mesenchymal and stem cell states in the breast. Cell 2011;145:926–40.

Scheel C and Weinberg RA. Phenotypic plasticity and epithelial-mesenchymal transitions in cancer and normal stem cells? International Journal of Cancer 2011; 129:2310–4.

Scheel C and Weinberg RA. Cancer stem cells and epithelial-mesenchymal transition: concepts and molecular links. Seminars in Cancer Biology 2012;22:396–403.

Schnitzer SE, Weigert A, Zhou J, and Brüne B. Hypoxia enhances sphingosine kinase 2 activity and provokes sphingosine-1-phosphate-mediated chemoresistance in A549 lung cancer cells. Molecular Cancer Research 2009:7;393–401.

Seder CW, Hartojo W, Lin L, Silvers AL, Wang Z, Thomas DG, et al. INHBA overexpression promotes cell proliferation and may be epigenetically regulated in esophageal adenocarcinoma. Journal of Thoracic Oncology 2009a;4:455–62.

Seder CW, Hartojo W, Lin L, Silvers AL, Wang Z, Thomas DG, et al. Upregulated INHBA Expression May Promote Cell Proliferation and Is Associated with Poor Survival in Lung Adenocarcinoma. Neoplasia 2009b;11:388–396.

Sequist LV, Waltman, BA, Dias-Santagata D, Digumarthy S, Turke AB, Fidias P. Genotypic and histological evolution of lung cancers acquiring resistance to EGFR inhibitors. Science Translational Medicine 2011;3:75ra26.

Shih J-Y, Tsai M-F, Chang T-H, Chang Y-L, Yuan A, Yu C-J, et al. Transcription repressor slug promotes carcinoma invasion and predicts outcome of patients with lung adenocarcinoma. Clinical Cancer Research 2005;11:8070–8.

Shintani Y, Abulaiti A, Kimura T, Funaki S, Nakagiri T, Inoue M, et al. Pulmonary Fibroblasts Induce Epithelial Mesenchymal Transition and Some Characteristics of Stem Cells in Non-Small Cell Lung Cancer. The Annals of Thoracic Surgery 2013;96:425-33.

Shintani Y, Okimura A, Sato K, Nakagiri T, Kadota Y, Inoue M, et al. Epithelial to mesenchymal transition is a determinant of sensitivity to chemoradiotherapy in non-small cell lung cancer. The Annals of Thoracic Surgery 2011;92:1794–804.

Shostak K and Chariot A. NF-κB, stem cells and breast cancer: the links get stronger. Breast Cancer Research 2011;13:214.

Siegel R, Naishadham D, and Jemal A. Cancer statistics, 2013. CA: A Cancer Journal for Clinicians 2013;63:11–30.

Singh SK, Hawkins C, Clarke ID, Squire JA, Bayani J, Hide T, et al. Identification of human brain tumour initiating cells. Nature 2004;432:396–401.

Smyth GK. Linear Models and Empirical Bayes Methods for Assessing Differential Expression in Microarray Experiments. Statistical Applications in Genetics and Molecular Biology 2004;3.

Sobral LM, Bufalino A, Lopes MA, Graner E, Salo T, and Coletta RD. Myofibroblasts in the stroma of oral cancer promote tumorigenesis via secretion of activin A. Oral Oncology 2011;47: 840–6.

Song L, Xiong H, Li J, Liao W, Wang L, Wu J, et al. Sphingosine kinase-1 enhances resistance to apoptosis through activation of PI3K/Akt/NF-κB pathway in human non-small cell lung cancer. Clinical Cancer Research 2011;17:1839–49.

Spiegel S and Milstien S. Sphingosine-1-phosphate: an enigmatic signalling lipid. Nature Reviews: Molecular Cell Biology 2003;4:397–407.

Steller MD, Shaw TJ, and Vanderhyden BC. Inhibin Resistance Is Associated with Aggressive Tumorigenicity of Ovarian Cancer Cells. Molecular Cancer Research 2005;50-61.

Sung J-M, Cho H-J, Yi H, Lee C-H, Kim H-S, Kim D-K, et al. Characterization of a stem cell population in lung cancer A549 cells. Biochemical and Biophysical Research Communications 2008;371:163–7.

Takabe K, Kim RH, Allegood JC, Mitra P, Ramachandran S, Nagahashi M, et al. Estradiol induces export of sphingosine 1-phosphate from breast cancer cells via ABCC1 and ABCG2. The Journal of Biological Chemistry 2010;285:10477–86.

Takahashi E, Nagano O, Ishimoto T, Yae T, Suzuki Y, Shinoda T, et al. Tumor necrosis factor-α regulates transforming growth factor-β-dependent epithelial-mesenchymal transition by promoting hyaluronan-CD44-moesin interaction. The Journal of Biological Chemistry 2010;285:4060–73.

Takahashi K, Tanabe K, Ohnuki M, Narita M, Ichisaka T, Tomoda K, et al. Induction of pluripotent stem cells from adult human fibroblasts by defined factors. Cell 2007;131:861–72.

Takase O, Yoshikawa M, Idei M, Hirahashi J, Fujita T, Takato T, et al. The role of NF-κB signaling in the maintenance of pluripotency of human induced pluripotent stem cells. PLoS ONE 2013;8:e56399.

Thiery JP, Acloque H, Huang RYJ, and Nieto MA. Epithelial-mesenchymal transitions in development and disease. Cell 2009;139:871–90.

Thulke S, Radonic A, Siegert W, and Nitsche A. Highly sensitive quantification of human cells in chimeric NOD/SCID mice by real-time PCR. Haematologica 2003;88:e84-85.

Tirino V, Camerlingo R, Bifulco K, Irollo E, Montella R, Paino F, et al. TGF-β1 exposure induces epithelial to mesenchymal transition both in CSCs and non-CSCs of the A549 cell line, leading to an increase of migration ability in the CD133+ A549 cell fraction. Cell Death & Disease 2013;4:e620.

Tomizawa M, Shinozaki F, Sugiyama T, Yamamoto S, Sueishi M, and Yoshida . Activin A is essential for Feeder-free culture of human induced pluripotent stem cells. Journal of Cellular Biochemistry 2013;114:584–8.

Topczewska JM, Postovit L-M, Margaryan NV, Sam A, Hess AR, Wheaton WW, et al. Embryonic and tumorigenic pathways converge via Nodal signaling: role in melanoma aggressiveness. Nature Medicine 2006;12:925–32.

Toscano MA, Campagna L, Molinero LL, Cerliani JP, Croci DO, Ilarregui JM, et al. Nuclear factor (NF)-κB controls expression of the immunoregulatory glycan-binding protein galectin-1. Molecular Immunology 2011;48:1940–9.

Valastyan S and Weinberg RA. Tumor metastasis: molecular insights and evolving paradigms. Cell 2011;147:275–92.

Vallet S, Mukherjee S, Vaghela N, Hideshima T, Fulciniti M, Pozzi S, et al. Activin A promotes multiple myeloma-induced osteolysis and is a promising target for myeloma bone disease. Proceedings of the National Academy of Sciences 2010; 107:5124–9.

Vallier L, Alexander M, and Pedersen RA. Activin/Nodal and FGF pathways cooperate to maintain pluripotency of human embryonic stem cells. Journal of Cell Science 2005;118:4495–509.

Vazin T and Freed WJ. Human embryonic stem cells: derivation, culture, and differentiation: a review. Restorative Neurology and Neuroscience 2010;28:589–603.

Wakefield LM and Hill CS. Beyond TGFβ: roles of other TGFβ superfamily members in cancer. Nature Reviews Cancer 2013;13:328–41.

Weinstein, I. B. (2002). Cancer. Addiction to oncogenes--the Achilles heal of cancer. *Science (New York, N.Y.)*, *297*(5578), 63–4. doi:10.1126/science.1073096

Wendt MK, Tian M, and Schiemann WP. Deconstructing the mechanisms and consequences of TGF-β-induced EMT during cancer progression. Cell and Tissue Research 2012;347:85–101.

Werts C, le Bourhis L, Liu J, Magalhaes JG, Carneiro LA, Fritz JH, et al. Nod1 and Nod2 induce CCL5/RANTES through the NF-κB pathway. European Journal of Immunology 2007;37:2499–508.

Wildi S, Kleeff J, Maruyama H, Maurer CA, Büchler MW, and Korc M. Overexpression of activin A in stage IV colorectal cancer. Gut 2001;49:409–17.

Witta SE, Gemmill RM, Hirsch FR, Coldren CD, Hedman K, Ravdel L, et al. Restoring E-cadherin expression increases sensitivity to epidermal growth factor receptor inhibitors in lung cancer cell lines. Cancer Research 2006;66:944–950.

Wu C-Y, Tsai Y-P, Wu M-Z, Teng S-C, and Wu K-J. Epigenetic reprogramming and post-transcriptional regulation during the epithelial-mesenchymal transition. Trends in Genetics 2012;28:454–63.

Wu Y and Zhou BP. TNFα/NF-κB/Snail pathway in cancer cell migration and invasion. British Journal of Cancer 2010;102:639–44.

Wu Y, Deng J, Rychahou PG, Qiu S, Evers BM, and Zhou BP. Stabilization of snail by NF-kappaB is required for inflammation-induced cell migration and invasion. Cancer Cell 2009;15:416–28.

Wu Z, Irizarry RA, Gentleman R, Martinez-Murillo F, and Spencer F. A Model-Based Background Adjustment for Oligonucleotide Expression Arrays. Journal of the American Statistical Association 2004;99:909–917.

Xia P, Wang L, Moretti PAB, Albanese N, Chai F, Pitson SM, et al. Sphingosine kinase interacts with TRAF2 and dissects tumor necrosis factor-alpha signaling. The Journal of Biological Chemistry 2002;277:7996–8003.

Xiao L, Yuan X, and Sharkis SJ. Activin A maintains self-renewal and regulates fibroblast growth factor, Wnt, and bone morphogenic protein pathways in human embryonic stem cells. Stem Cells 2006;24:1476–86.

Xie G, Yao Q, Liu Y, Du S, Liu A, Guo Z, et al. IL-6-induced epithelial-mesenchymal transition promotes the generation of breast cancer stem-like cells analogous to mammosphere cultures. International Journal of Oncology 2012;40:1171–9.

Xin C, Ren S, Kleuser B, Shabahang S, Eberhardt W, Radeke H, et al. Sphingosine 1-phosphate cross-activates the Smad signaling cascade and mimics transforming growth factor-beta-induced cell responses. The Journal of Biological Chemistry 2004;279:35255–62.

Xu J, Lamouille S, and Derynck R. TGF-beta-induced epithelial to mesenchymal transition. Cell Research 2009;19:156–72.

Yamamoto M, Taguchi Y, Ito-Kureha T, Semba K, Yamaguchi N, and Inoue J-I. NF-κB non-cell-autonomously regulates cancer stem cell populations in the basal-like breast cancer subtype. Nature Communications 2013;4:2299.

Yanagawa J, Walser TC, Zhu LX, Hong L, Fishbein MC, Mah V, et al. Snail promotes CXCR2 ligand-dependent tumor progression in non-small cell lung carcinoma. Clinical Cancer Research 2009;15:6820–9.

Yang J and Weinberg RA. Epithelial-mesenchymal transition: at the crossroads of development and tumor metastasis. Developmental Cell 2008;14:818–29.

Yauch RL, Januario T, Eberhard DA, Cavet G, Zhu W, Fu L, et al. Epithelial versus mesenchymal phenotype determines in vitro sensitivity and predicts clinical activity of erlotinib in lung cancer patients. Clinical Cancer Research 2005;1:8686–98.

Yde P, Mengel B, Jensen MH, Krishna S, and Trusina A. Modeling the NF-κB mediated inflammatory response predicts cytokine waves in tissue. BMC Systems Biology 2011;5:115.

Yeung F, Hoberg JE, Ramsey CS, Keller MD, Jones DR, Frye RA, and Mayo MW. Modulation of NF-κB-dependent transcription and cell survival by the SIRT1 deacetylase. EMBO 2004;23:2369–80.

Yi S-Y, Hao Y-B, Nan K-J, and Fan T-L. Cancer stem cells niche: a target for novel cancer therapeutics. Cancer Treatment Reviews 2013;39:290–6.

Yoshinaga K, Inoue H, and Utsunomiya T. N-Cadherin Is Regulated by Activin A and Associated with Tumor Aggressiveness in Esophageal Carcinoma. Clinical Cancer Research 2004;10:5702–5707.

Yoshinaga K, Mimori K, Yamashita K, Utsunomiya T, Inoue H, and Mori M. Clinical significance of the expression of activin A in esophageal carcinoma. International Journal of Oncology 2003;22:75–80.

Yoshinaga K, Yamashita K, Mimori K, Tanaka F, Inoue H, and Mori M. Activin A causes cancer cell aggressiveness in esophageal squamous cell carcinoma cells. Annals of Surgical Oncology 2008;15:96–103.

Yu Q and Stamenkovic I. Cell surface-localized matrix metalloproteinase-9 proteolytically activates TGF-beta and promotes tumor invasion and angiogenesis. Genes & Development 2000;14:163–76.

Zhang K, Zhaos J, Liu X, Yan B, Chen D, et al. Activation of NF-B upregulates Snail and consequent repression of E-cadherin in cholangiocarcinoma cell invasion. Hepato-gastroenterology 2011;58:1–7.

Zhou C, Wu Y-L, Chen G, Feng J, Liu X-Q, et al. Erlotinib versus chemotherapy as first-line treatment for patients with advanced EGFR mutation-positive non-small-cell lung cancer: a multicentre, open-label, randomised, phase 3 study. The Lancet Oncology 2011;12:735–42.

Zhu R, Snyder AH, Kharel Y, Schaffter L, Sun Q, et al. Asymmetric synthesis of conformationally constrained fingolimod analogues--discovery of an orally active sphingosine 1-phosphate receptor type-1 agonist and receptor type-3 antagonist. Journal of Medicinal Chemistry 2007;50:6428–35.

Zhuo W-L, Wang Y, Zhuo X, Zhang Y, Ao X, et al. Knockdown of Snail, a novel zinc finger transcription factor, via RNA interference increases A549 cell sensitivity to cisplatin via JNK/mitochondrial pathway. Lung Cancer 2008;62:8–14.

Zhuo W-L, Wang Y, Zhuo X-L, Zhang Y-S, and Chen Z-T. Short interfering RNA directed against TWIST, a novel zinc finger transcription factor, increases A549 cell sensitivity to cisplatin via MAPK/mitochondrial pathway. Biochemical and Biophysical Research Communications 2008;369:1098–102.

Zu X, Zhang Q, Cao R, Liu J, Zhong J, Wen G, and Cao D. Transforming growth factor-β signaling in tumor initiation, progression and therapy in breast cancer: an update. Cell and Tissue Research 2012;347:73–84.